Authors comments on Reviewer #1 “Drivers for Atlantic-origin waters abutting Greenland” by Laura C. Gillard et al.

This document will clarify point by point the adjustments made in the revised manuscript. The authors would like to thank Reviewer 1 for adding further improvements to the manuscript. Reviewer comments in **bold,** author comments will be shown following the reviewers.

RC: Page 5 line 24 ‘Until this study, this has not yet been examined’ See Jackson et al. Nat. Geosci. 7, 503–508. doi: 10.1038/ngeo2186 who report fjord velocity pulses preceded by along-shore wind events on 2-10 day time scales… “Individual events, lasting only several days, rapidly translate signals from the shelf to the upper fjord

Author Comment: Thank you for bringing this to our attention. We have updated the manuscript. We added Jackson (2014) reference as you suggested, and edited the paragraph to accurately describe previous work done and improve our research question.

Manuscript Update: Page 5 line 23 to 26
“Jackson et al. (2014) reported that synoptic events can impact water properties and heat content within two large outlet fjords. Therefore they could impact shelf exchange and the renewal of warm waters to the GrIS. This study aims to go beyond Jackson et al., (2014)’s two fjords by considering the entire coast of Greenland.”

RC: Page 7 line 20. This is a nice comparison with observations (Fig, 7), indicating model simulates interannual volume transports well.

Author Comment: We are very pleased that you are happy with our addition of model evaluation with observations.

RC: Page 11. Line 7. And page 12 line 31. The propagation of the seasonal signal in Irminger Water is analysed in observations and NEMO by Grist et al. GRL 2014, doi:10.1002/2014GL062051

Author Comment: We have added Grist et al. (2014) into the discussion regarding the propagation of Imringer Water.

Manuscript update page 11 line 13 to 19:
“Observations at Davis Strait show a temperature maximum starting around August/September through to November/December (Curry et al., 2011; Grist et al., 2014). However, the heat flux peaks in DBT occurred as early as June/July between 2004 and 2006 (Fig. 10d), suggesting a larger influence from the warm surface waters in these months. As the years progressed in the

model, the timing of the maximum heat flux delayed with strong interannual variations from September to January. This timing coincided with the peak of warmest Irminger Water observed in Davis Strait. The delay, the warmest water in Davis Strait occurred in (late) fall to (early) winter rather than summer, was due to the advection time needed by the Irminger Sea water. The peak of the seasonal cycle of warm water in the troughs north of Davis Strait was further delayed. The lag in the seasonal cycle of warm water is consistent with the Lagrangian trajectory-based study by Grist et al. (2014)..”

Manuscript update page 13 line 19 to 25:
“Grist et al. (2014) had examined the propagation of the seasonal signal for Irminger water. This study found that the peak seasonal temperatures occur on the east coast of Greenland and west coast south of Davis Strait between August and December, similar to the south-east locations in this study showed (HGT2 and KT). Grist et al. (2014) are in agreement with our study that a lagged timing of the seasonal cycle for warm waters exists north of Davis Strait. In Davis Strait the temperature maximums occur during October to December (Curry et al. 2014) this would align with the timing of the arrival of sub-surface warm waters in the troughs along the west coast of Greenland, as flow from Davis Strait can take about a month to reach DBT and five to six months to reach MVBCT according to HighRes.”

RC: Page 17. Line 5. “The study’s model experiments showed that Melville troughs experience and increased heat flux”. The authors should state when this was. Then the next sentence could read: ‘Therefore an associated increase in ocean heat presence…..’

Author Comment: Thank you for the suggestion for clarifying the period of increased heat flux. We have updated our manuscript accordingly.

Manuscript Update Page 18 line 27 to 29:
“This study showed that the presence of warm water at depth can extend far north into Baffin Bay, reaching as north as Melville Bay and its subsequent troughs. Increased heat flux through the Melville Bay section is found from 2009 to the end of 2014.”

Authors comments on Reviewer #2 “Drivers for Atlantic-origin waters abutting Greenland” by Laura C. Gillard et al.

This document will clarify point by point the adjustments made in the revised manuscript. The authors would like to thank Reviewer 2 for adding further improvements to the manuscript. Reviewer comments in *italics***,** author comments will be shown following the reviewers.

Reviewer 2 General Comments:

RC: *This is my second review of this paper. I appreciate that the authors have now included some model validation against observations, that is very helpful and it makes the results more relevant. Also it was nice to see the separation out heat flux seasonality into the volume flux vs temperature seasonality.*

However, there are a few things that have not improved, at least in my view. There are several instances where the discussion of explanation of model results is not supported by the analysis and that needs to be corrected. Further, much of the discussion of results are rather qualitative than quantitative and in my view that should be changed.

*Finally, I have some concerns about the heat flux calculations which are stated below. If these concerns are relevant a significant portion of the manuscript would have to be revised***.**

Author Comments: The authors would like to thank Reviewer 2 for taking the time to provide a thorough review of this manuscript. We hope that the updated manuscript will show an improvement in the explanation of results, including more quantitative discussion. Concerns in regards to the heat flux calculations will be discussed below.

Major:

Eddy heat flux calculation:

RC: *I am wondering what is used for T in Equation 2. I am worried the authors are using temperature in Celsius to calculate this quantity, at least Figure 9 suggests that.* At all panels the sign of the heat flux is the sign of the product of the volume flux and temperature signs, rather than the sign of the volume flux (e.g. Fig 9p).

Authors Comments:
Note that figure 9 in the previous draft is now figure 10 in this version of the manuscript. Our focus in this manuscript is the transport of heat by the ocean towards the coast of Greenland, and thus its impact on tide water glaciers. We assume the melting point of fresh glacial ice is 0^oC and thus use this as our reference temperature. This does mean that, as the reviewer stated, the sign of the heat flux is based on the product of the sign of the volume flux and the temperature. But we don't see that as a problem. We are showing when water with the potential for melting is transported towards the coast (and how much of heat is being transported). We still include the temperature panel as a previous reviewer asked about the temperature structure of the water, and we think showing separately adds value.

RC: *The temperature needs to be referenced in some meaningful way, for example to absolute zero by using Kelvin, or to the freezing point (so using Thermal driving instead of Temperature in the calculation) but as that varies with depth and properties it might be more complicated to calculate.*

Author Comments:
We would like to thank the reviewer for bringing to our attention that this equation needs further explanation to avoid confusion. We believe that our temperature is referenced in a meaningful way. The temperature is in Celsius and the reference temperature is set to 0^oC (273.15K) in the heat flux calculation. In our case, we chose 0^oC because this is the temperature glacial ice ice starts to melt at. It is the melt of the glacial ice rather than of sea ice that we are concerned about in this study. We agree that the freezing point changes with the pressure (depth) but we do not expect fundamental changes in our conclusions. We have updated the manuscript to reflect the suggestions.

Manuscript Update Page 6 Line 15 -17: "The temperature, T(t,z,x), is in Celsius implicating a reference temperature of 0^oC (273.15 K) in the heat flux calculation. In this study, a reference temperature of 0^oC is used because this is the temperature glacier ice starts to melt at."

RC: *Further, the section across which the heat flux seasonality is calculated should be marked on Fig. 8***.**

Authors Comment:

Note that figure 8 that the reviewer refers to is now figure 9 in the new draft. As suggested, we have updated Figure 9 to include a highlight of the trough which is selected for the seasonality heat flux. Figure 1 indicates the exact location of the trough, however, we hope that with this update in Figure 9 it is more clear which trough is used. We have additionally updated the Figure 9 caption.

RC: *For example in Fig. 9g the volume flux is negative all the time so the authors are showing here the seasonality of the outflow more so then the seasonality of the inflow. Either way though these two are mixed up in the way the analysis is done. I think a better way to do this would be to integrate only the inflow to the trough as that is the focus of this paper.*

Author Comments:

Note that the figure 9g that the review refers to is now figure 10g in the new draft. We think the previous figure shows the inflow and outflow distinctly and separately. Here we are looking at the net flux towards/away from the fjord. Thus we think the 2 figures work together to complement each other. That said, we agree that the text wasn't as clear as it could be, and this section has been rewritten to clarify the heat flux discussion.

Seasonality discussion:

RC: *While heat flux is integrated over the full depth for the purposes of showing seasonality, the closing discussion 3.1.7 explains this seasonality in terms of Irminger water seasonality. My problem here is that the integrated number contains both Irminger and polar water (and potentially other water masses), but the discussion only talks about Irminger water as if that was the only water included in the analysis. Either the analysis needs to be corrected to separate out the different water masses, or the discussion needs to be adjusted to what is actually shown in the paper. I think the former would be better.*

Authors Comments:

Given that we haven't isolated the fluxes by water mass elsewhere in the paper, we keep that approach here. We thus adjust our discussion to focus on warm water in general, consistent with the approach in Grist et al. (2014) for example.

In Section 3.1.7. we discuss the implications of this warm water, and compare it to the discussion in Grist et al. (2014) and Curry et al. (2014) on the seasonality of Irminger Water mass, but keep clear that there are other potential sources of warm water..

Mean flow vs fluctuation analysis:

RC: *The authors should pick a metric by which they will evaluate the importance of fluctuations. The discussion should then be formulated in a more rigorous way, e.g. this fraction of heat flux is mediated by fluctuations and this by mean flow. A follow up discussion can then compare the importance of fluctuations between the different section.*

Author Comments:

We would like to thank the reviewer for evaluating this section and asking us to include a more rigorous discussion on how the heat flux is moderated by the mean or fluctuation components of the flow. We have decided to break down each component for each trough as a percentage. This has been added as a new table, now called Table 3 in the latest draft of the manuscript.

In this table, we show the average percentage of the heat flux moderated by the fluctuation component of the flow from three configurations (HighRes, LowResControl, and LowResNoStorms) one trough per section.

We found that for all troughs other than KT, the fluctuation component of the flux does not contribute largely to the heat flux. We have added this new analysis into the manuscript, as part of a completely rewritten subsection.

RC: *There is a persistent intermingling of results and discussion and it sounds all very subjective an hand wavy. Also the comparison between low res vs high res and mean vs fluctuation should be separated as these are two different topics.*

Author Comments:

We have gone over this section (3.2) carefully. We hope that this section no longer sounds hand-wavy, as we have added an additional metric to describe how the fluctuation component vs the mean component impacts the heat flux. We decided to keep the comparison of HighRes and LowResControl together with the discussion on the mean and fluctuation components. However, with the edits we have done in the manuscript we hope that this reads better.

RC: *It doesn't appear that the fluctuation component is higher for the high res simulations, is it that the resolution change was insufficient to resolve smaller scale processes, or could a different timescale averaging choice substantially change the results? There is no clear conclusion about whether high res is better or worse than low res and so I wonder what is the point of the plots in Fig. 10 (red vs black line).*

Author Comments: In general the higher resolution simulation does a better job in representing features in and around Greenland and in the sub-polar North Atlantic (as discussed in the introduction, as well as the references given in that section of the paper). That said, for some aspects of the flow, the low resolution experiment simulates what is needed well enough. That is the purpose the comparisons given in figure 11 (fig 10 in previous version) - to show where low and high resolution are similar and different. This is made more clear in the completely rewritten sub-section. Additionally, by showing where LowResControl is similar to HighRes, we motivate that LowResControl can be used for our sensitivity simulations (which are too expensive numerically to run with HighRes - this is stated in the paper).

The averaging period makes little difference. We have tried periods around our 25 day moving window (e.g. 20 or 30 days), as well as much longer windows - 85 days (roughly 3 months) and 185 days (about 6 months). And in all cases there are only small differences (other than the really long 185 day averaging period starting to smooth out the seasonal cycle). The extreme values are also damped with a longer averaging window. We show here in the review document transports with different windows, to prove to the reviewer that our results do not depend on this choice.

We have rewritten Section 3.2 and added further clarification regarding the use of comparing the HighRes with LowResControl and the benefits of doing further sensitivity experiments with the LowRes Control.

MVBCT Mean Component of the Flow:

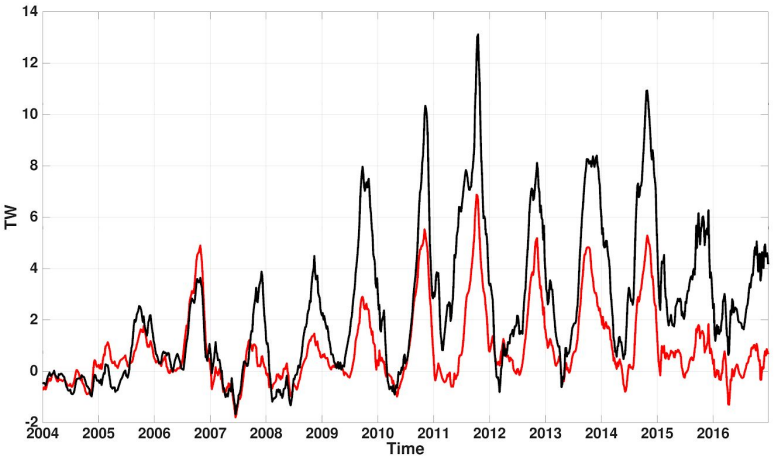

a) 25 day Window

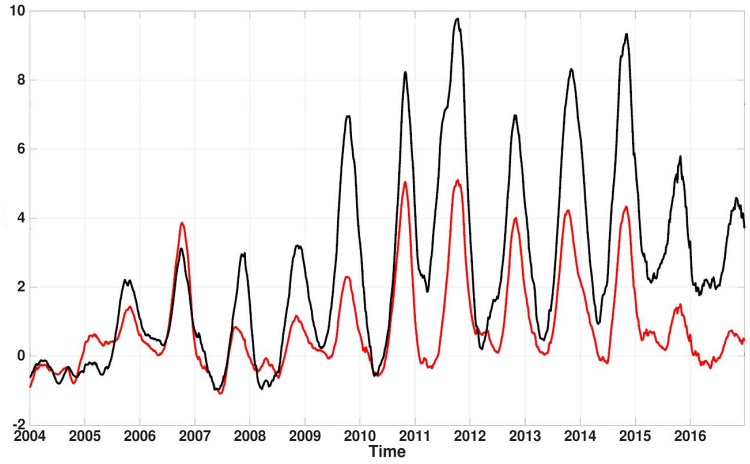

b) 85 day Window

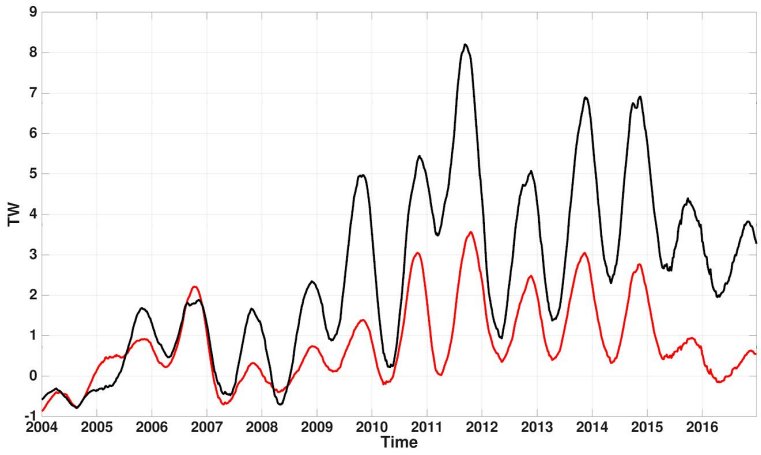

c) 185 day Window

MVBCT Fluctuation Component of the Flow:

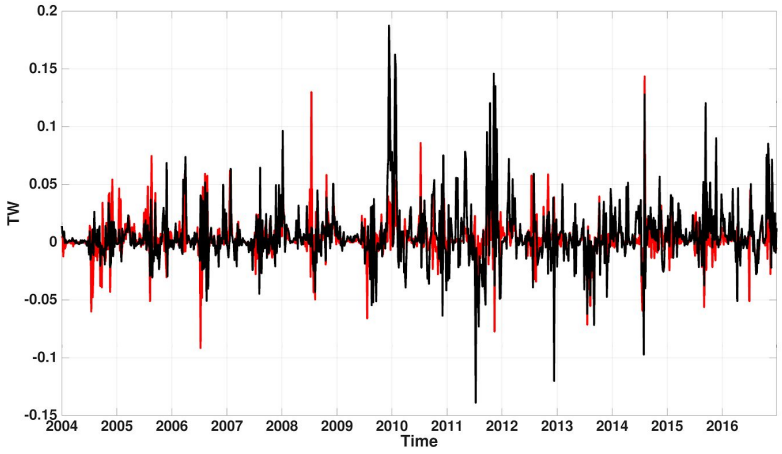

a) 25 day Window

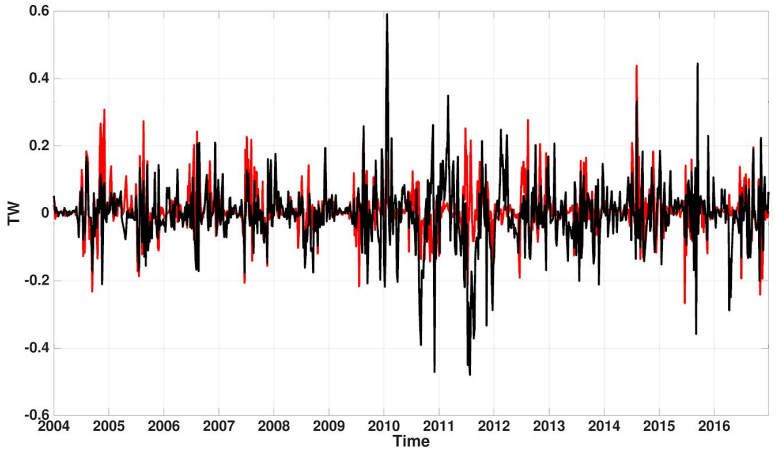

b) 85 day Window

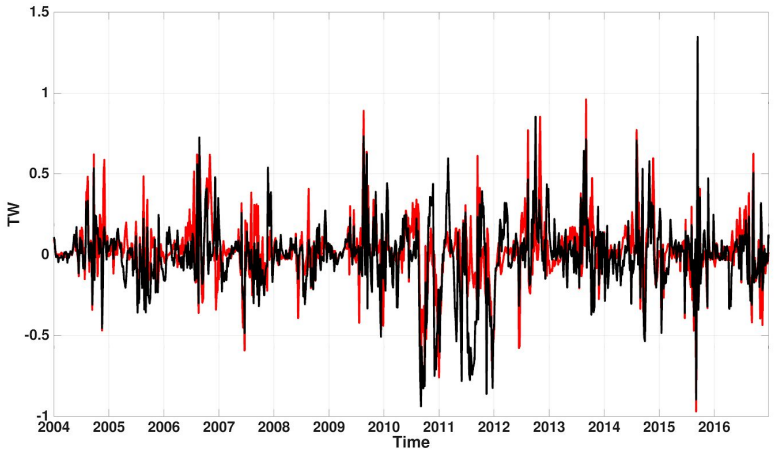

c) 185 day Window

DBT Mean Component of the Flow:

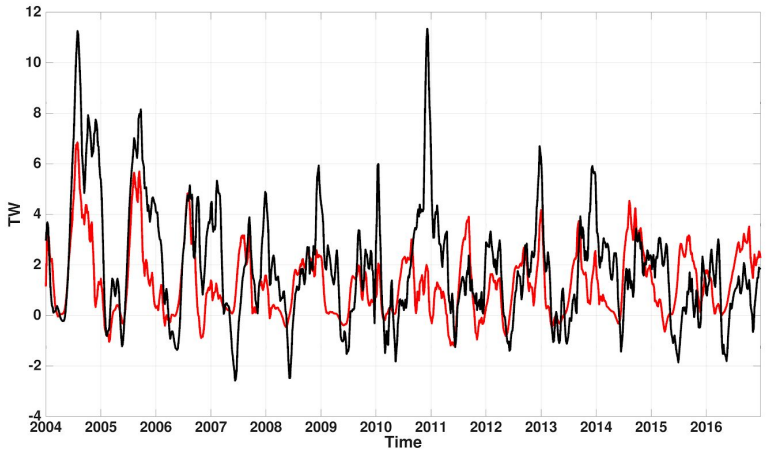

a) 25 Day Window

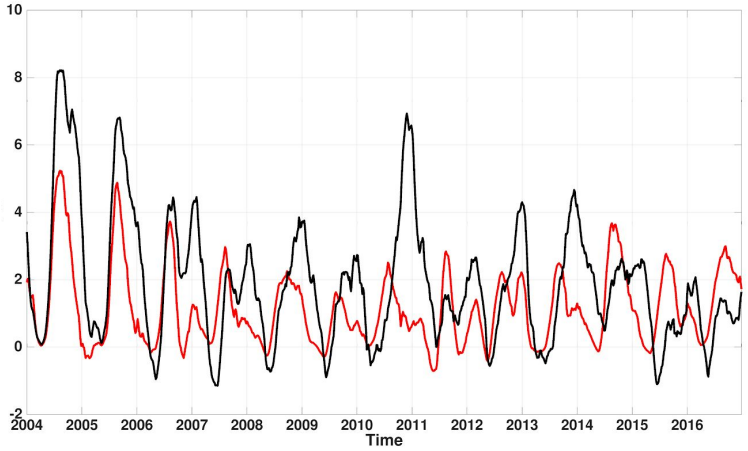

b) 85 day Window

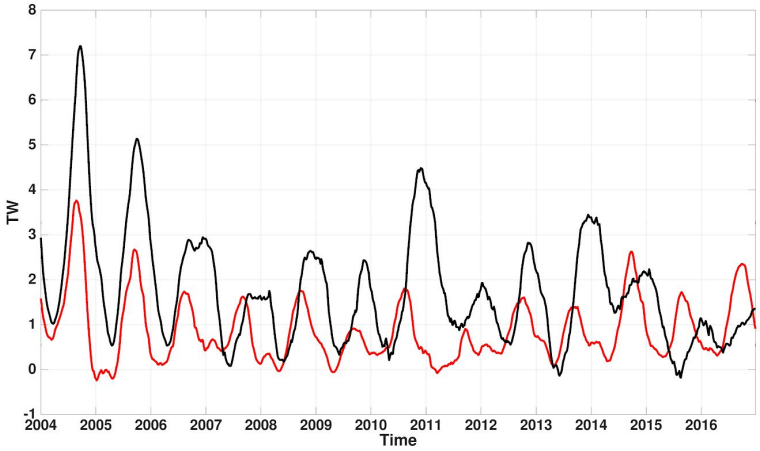

c) 185 Day Window

DBT Fluctuation Component of the Flow:

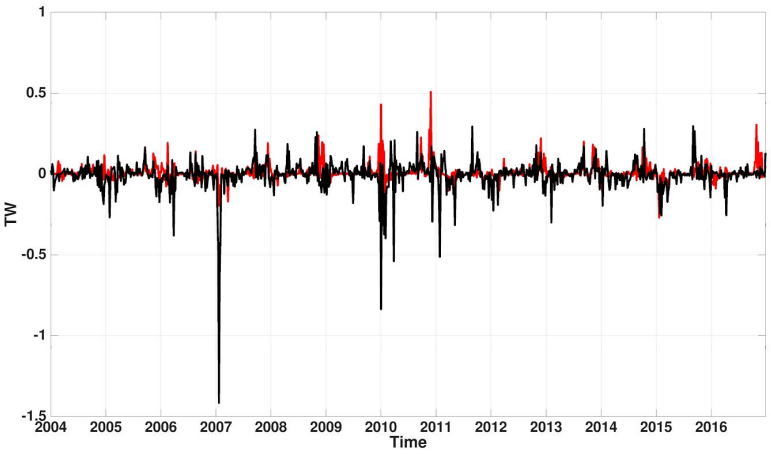

a) 25 day window

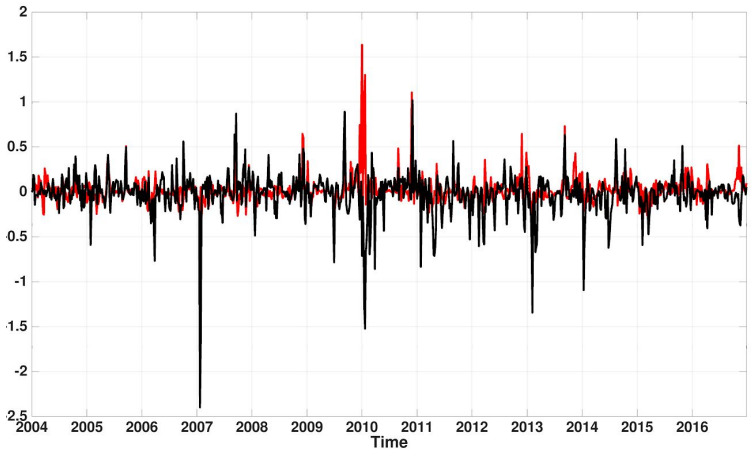

b) 85 day window

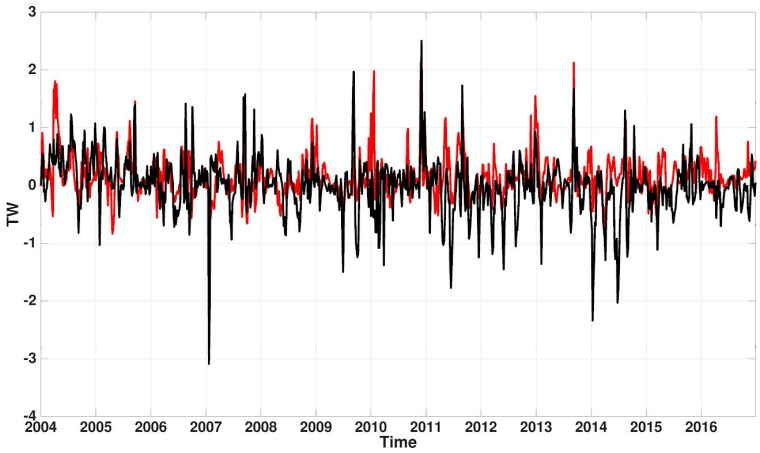

c) 185 day window

HGT2 Mean Component of the Flow:

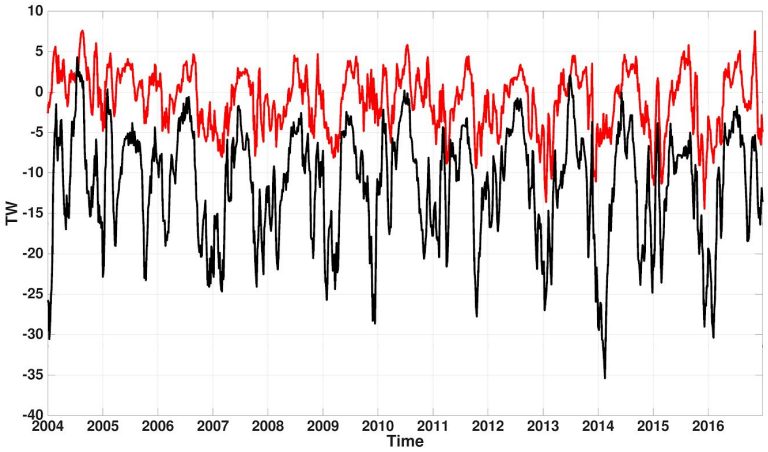

a) 25 day window

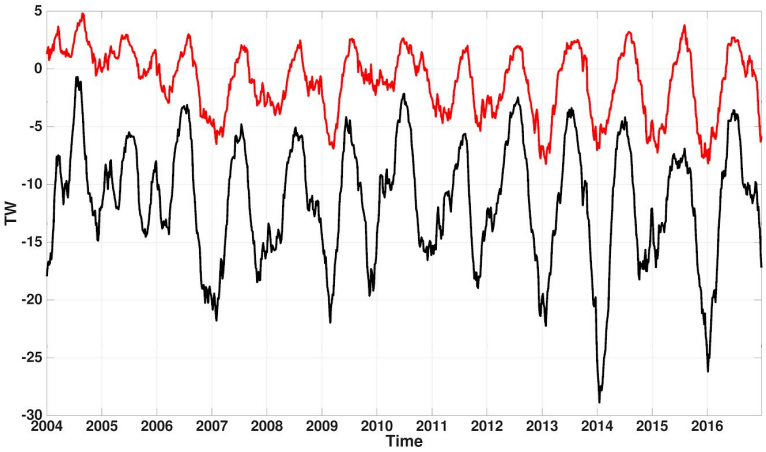

b) 85 day window

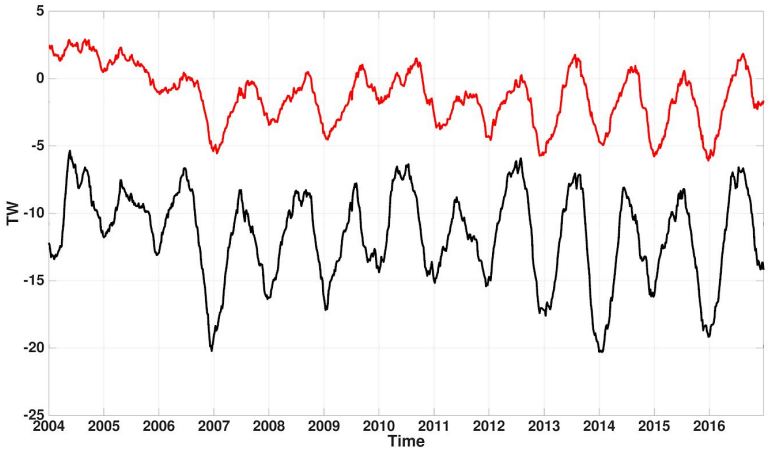

c) 185 day window

HGT2 Fluctuation Component of the Flow:

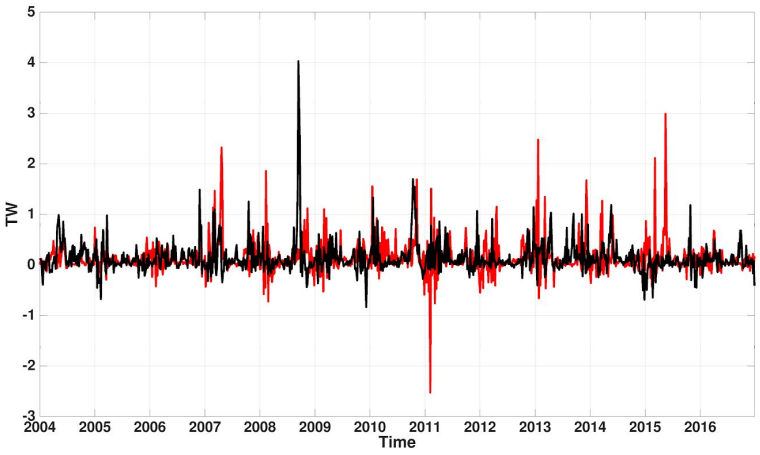

a) 25 day window

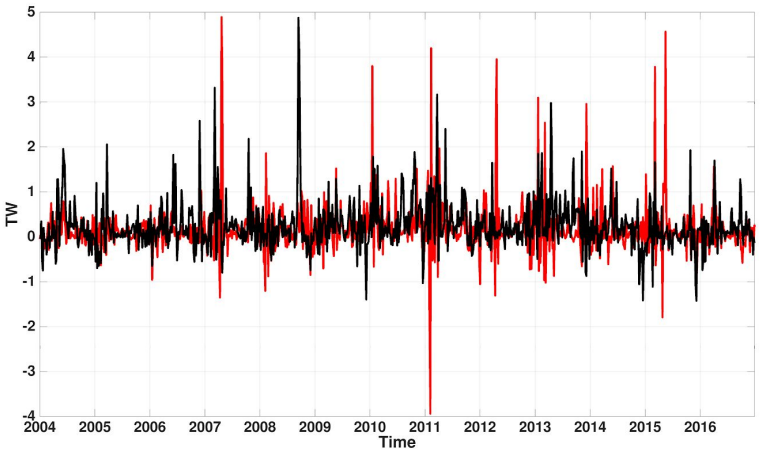

b) 85 day window

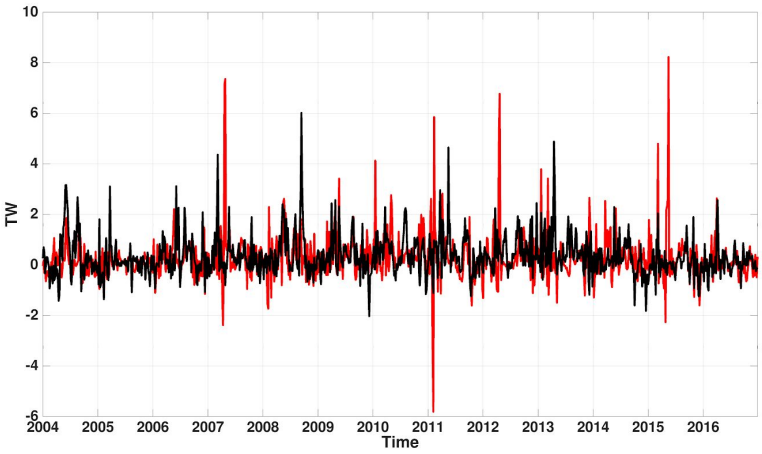

c) 185 day window

KT Mean Component of the Flow:

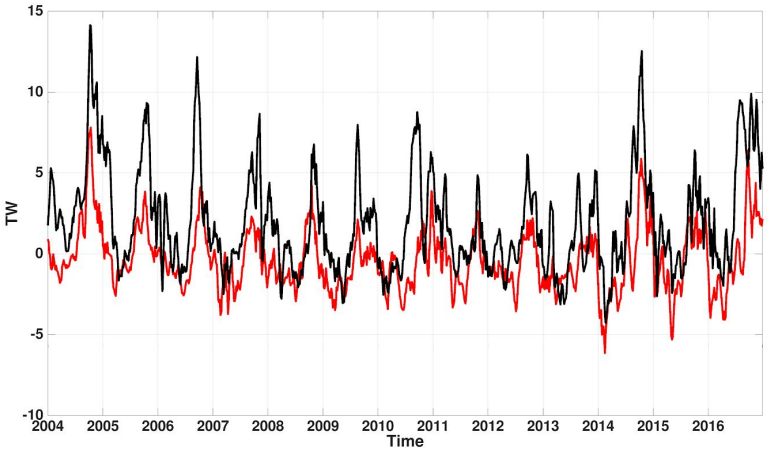

a) 25 day window

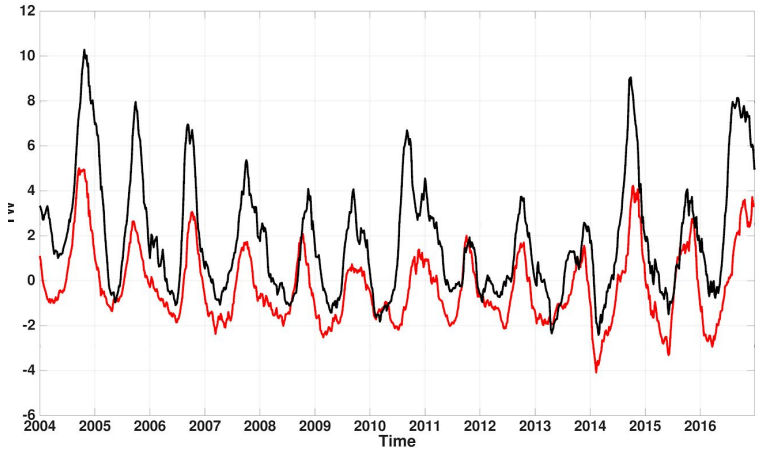

b) 85 day window

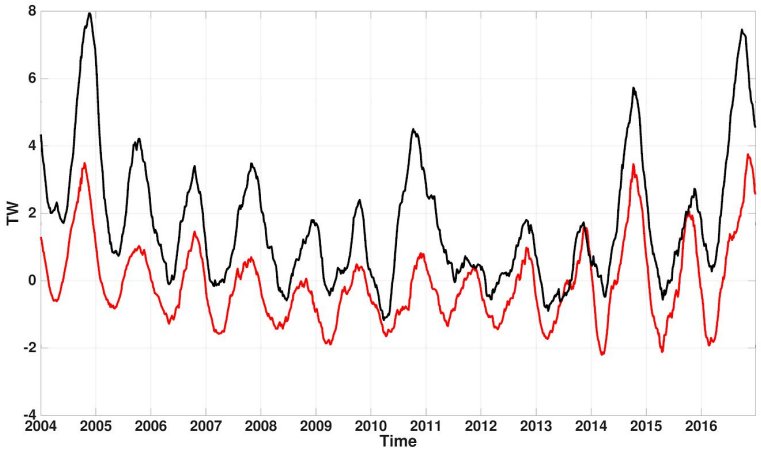

c) 185 day window

KT Fluctuation Component of the Flow:

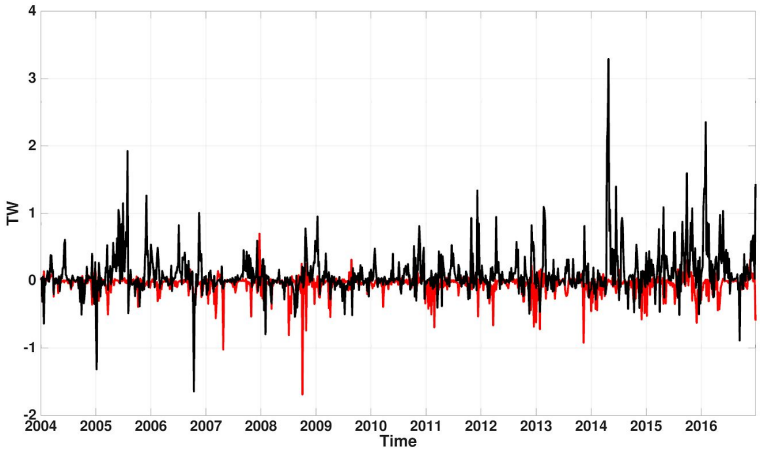

a) 25 day window

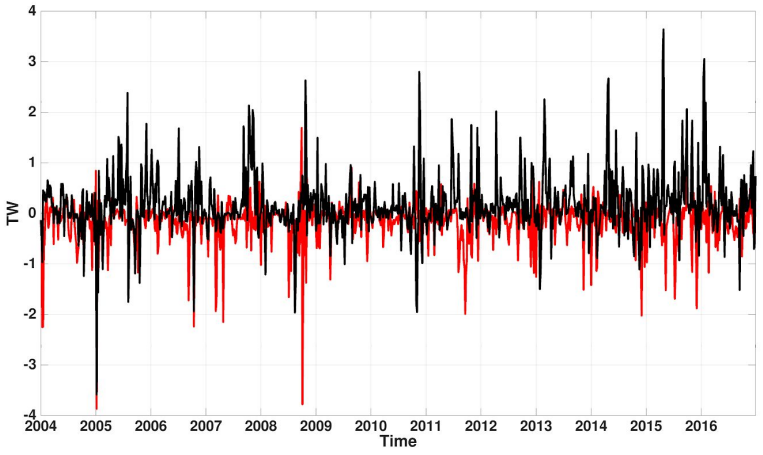

b) 85 day window

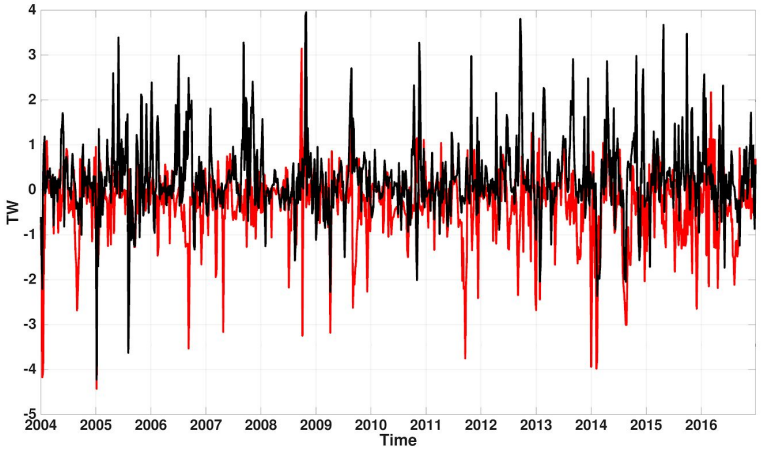

c) 185 day window

SBST Mean Component of the Flow:

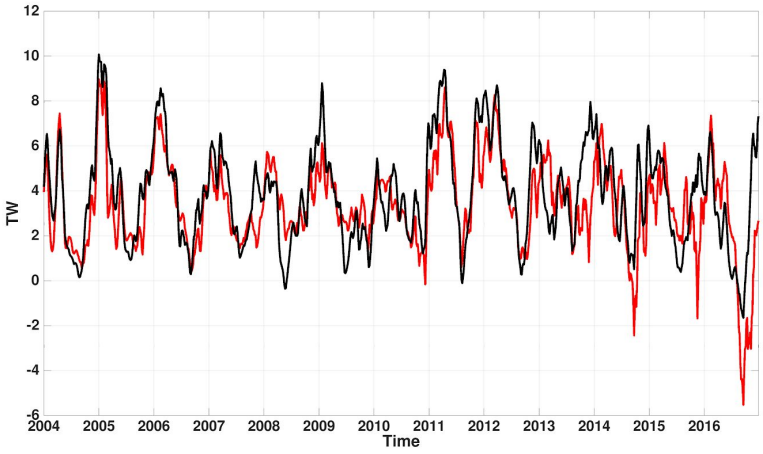

a) 25 day window

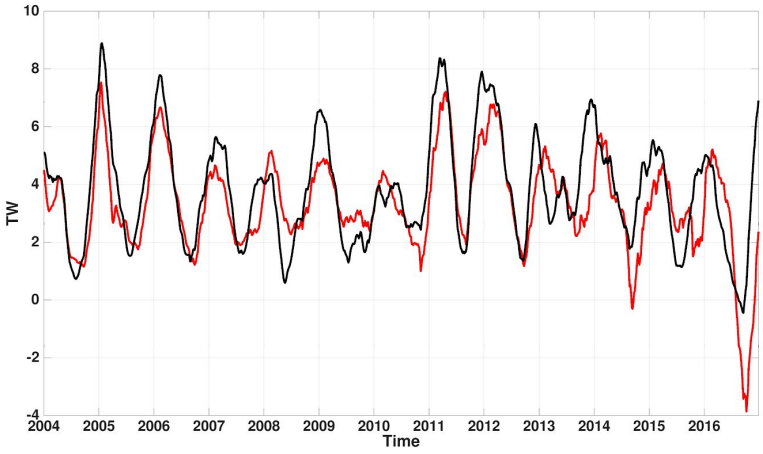

b) 85 day window

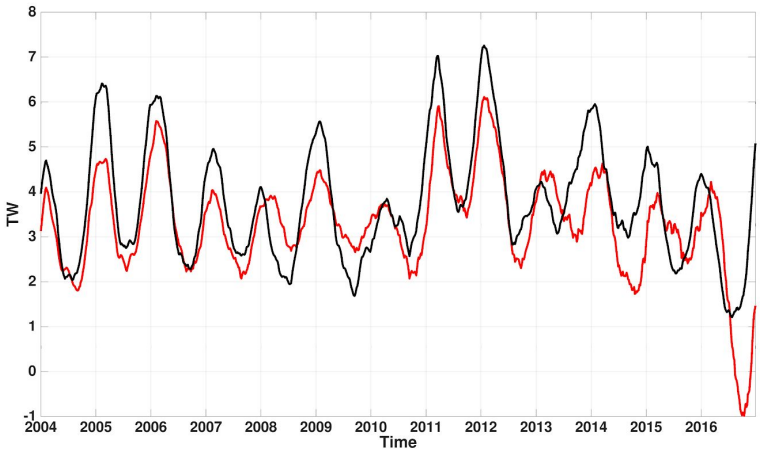

c) 185 day window

SBST Fluctuation Component of the Flow:

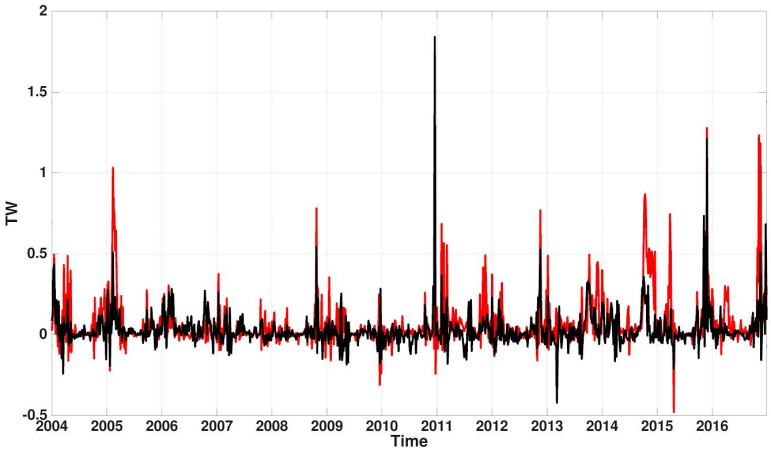

a) 25 day window

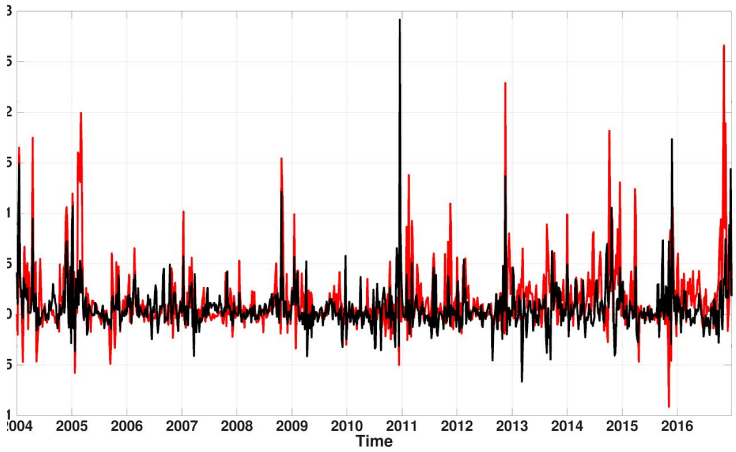

b) 85 day window

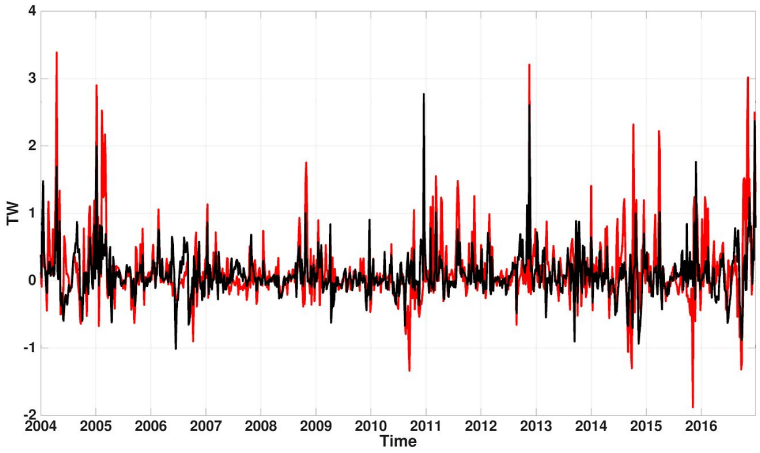

c) 185 day window

NT Mean Component of the Flow:

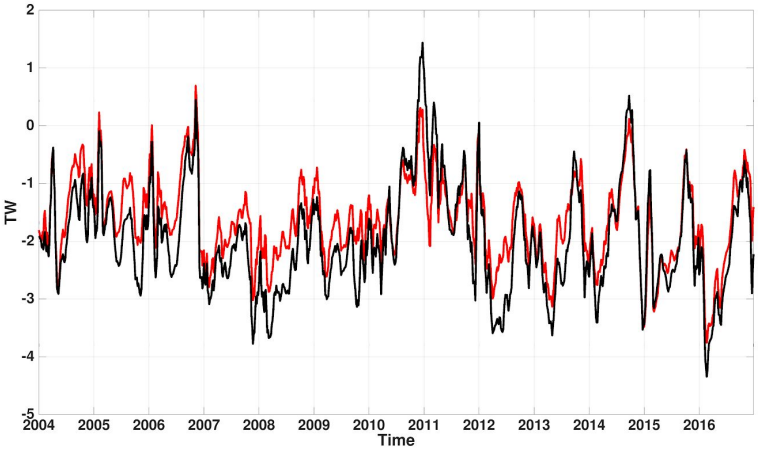

a) 25 day window

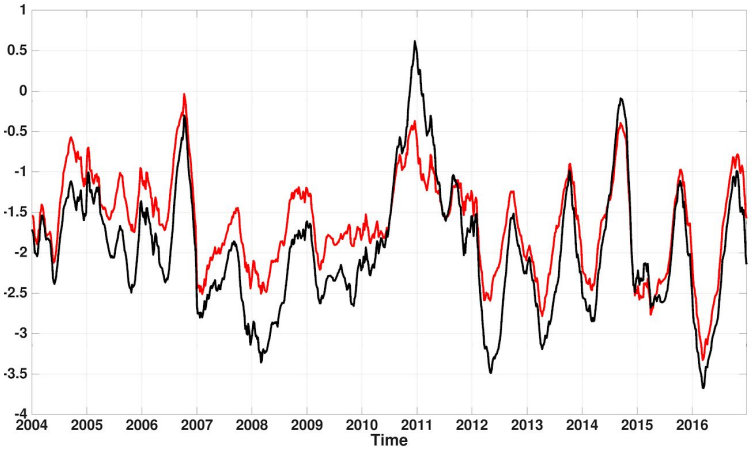

b) 85 day window

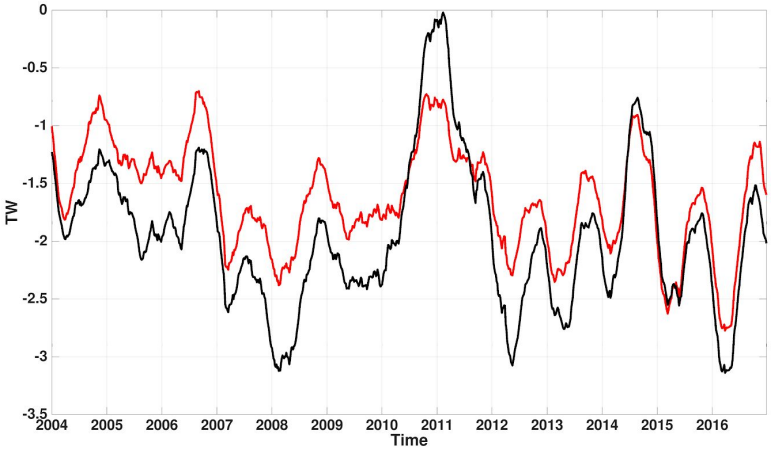

c) 185 day window

NT Fluctuation Component of the Flow:

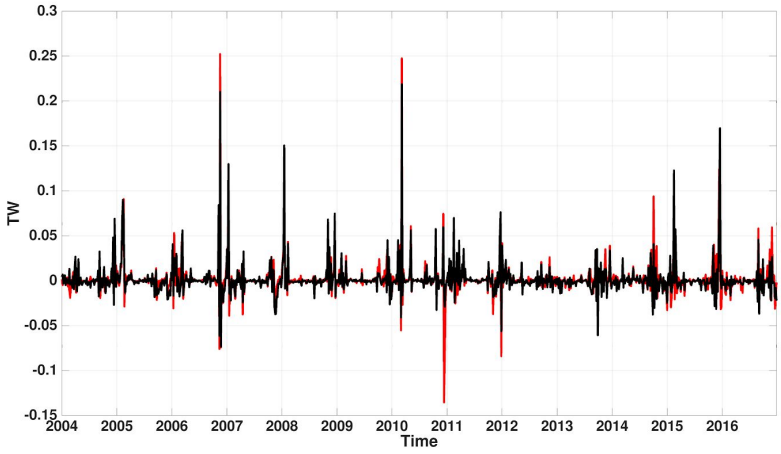

a) 25 day window

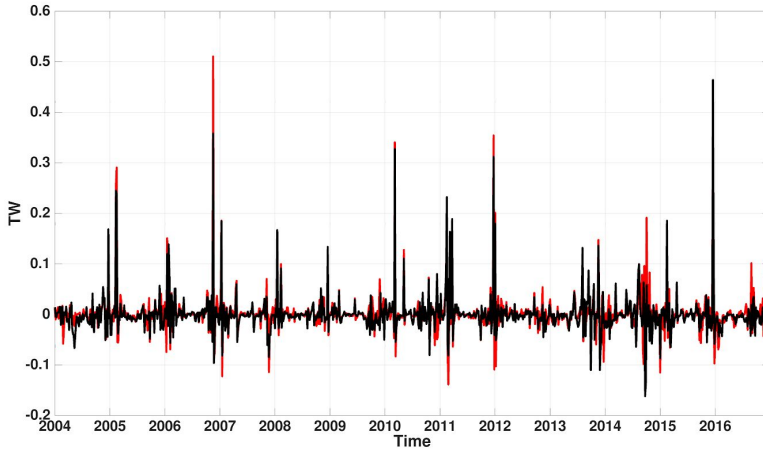

b) 85 day window

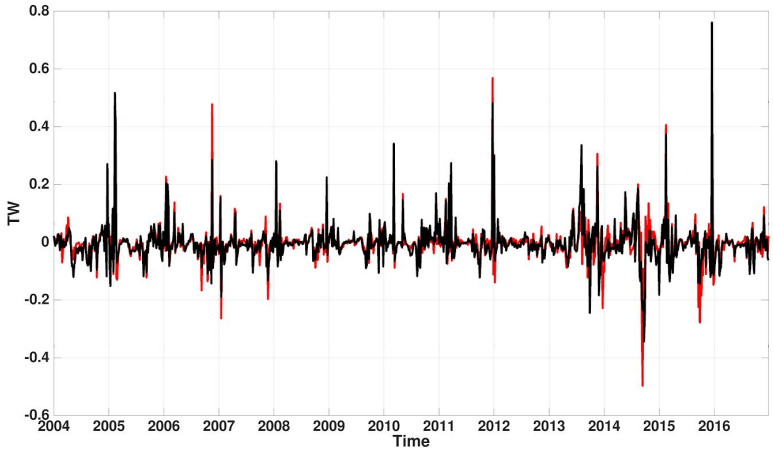

c) 185 day window

Summary:

We find that by increasing our averaging window, it does not substantially change the results. We will continue to use the 25 day window, as we find it shows much more detail.

RC:*There were lots of typos in this section, also the word order throughout the manuscript is making it difficult to read smoothly. Please have coauthors proofread.*

Author Comments: We have gone through the manuscript thoroughly and hope that this updated manuscript will read more smoothly.

Double melt experiment:

RC: *There is no analysis of the results. I agree it is interesting to see comparison of a section with melt and double melt and observe they are different. However, without understanding how this modeling results was produced (mechanisms responsible for this) I don't see much value to the publishing of this finding.*

Authors Comments:
We found that the experiment presented here with enhancing Greenland meltwater worked off Castro De La Guardia et al (2015)'s work. The processes for producing warming along the west coast, north of Davis Strait, have been discussed in great detail in Castro De La Guardia et al (2015) (See Castro De La Guardia et al., 2015 Figure 4 schematic). Enhanced meltwater runoff decreased surface salinity in the Baffin Bay. Sea surface height increased the most along with boundary current along the Greenland shelf. This strengthened Baffin Bay's cyclonic gyre. Strengthening the West Greenland Current, bringing more warm waters northward into the Baffin Bay. This also causes stronger Ekman pumping that lifts the isopycnals in the center of the Bay, causing the shallowing of the warm water layer in Baffin Bay. Results presented in this manuscript showed that the study's sectors along the West Greenland Coast (Melville Bay and Disko Bay) warm core found in LowResDoubleMelt was warmer and more shallow than for LowResControl. We have updated Section 3.3 to further explain the processes that lead to these modelling results (page 17 line 11 -18). Therefore, we find that this section adds value to our manuscript, and would like to see it in the publication.

Fluctuations:

RC: *Wrong units, this further extends to the abstract where the quantities computed in this section are reported.*

Author Comments: We would like to thank the reviewer for the catch on the incorrect units provided for the comparison of the summation of heat flux in Section 3.4. We have updated the abstract and updated the units in Section 3.4 to be in gigajoules on page 18, line 11 to 16.

“The integration of the mean component of the heat flux from 2004 to 2016 has been calculated and compared between LowResControl and LowResNoStorms. LowResNoStorms has a total of 2 GJ (1 GJ = 1 x 10^9 J), where LowResControl had a total of −2 GJ. The total energy increase of 4 GJ could have the potential to melt 12 tonnes of ice. LowResNoStorms has a 100% increase of onshore heat for this period of 4 GJ compared to LowResControl of 2 GJ. LowResNoStorms has a 50% decrease of offshore heat for this period of −2 GJ compared to LowResControl of −4 GJ. HGT2 has more energy onshore in LowResNoStorms due to filtering out offshore winds and therefore decreasing offshore heat transport.”

Minor:

RC: *For the model validation - could you provide a TS diagram with both model and observations?*
Author Comments:
Please view new Figure 7 for a new TS diagram with both model and observations. Discussion of this figure has been added to the text.

RC: *Could you include a table listing all the different water masses referred to in the manuscript and include the TS definitions of those?*
Author Comments:
Please view Table 2 for an overview on Davis Strait water masses.

ATTACHED PDF COMMENTS:

RC: *Additional comments are in the attached pdf.*
Author Comments: Thank you for attaching a pdf, we will mention all comments here point by point when required to ensure a thorough inspection of comments provided by Reviewer 2. Smaller comments strictly regarding sentence structure, English or grammar have been fixed but will not be shown here.

- **AC:** We have edited the abstract given the reviewers comments:
  "The oceanic heat available in Greenland's troughs is dependent on the geographic location of the trough, the water origin, and how the water is impacted by local processes along the pathway to the trough. This study investigates the spatial pattern and quantity of the warm water (with a temperature greater 0C) brought to the shelf and into the troughs abutting the Greenland Ice Sheet (GrIS). An increase in ocean heat in these troughs may drive a retreat of the GrIS. Warm water that is exchanged from the trough into the fjord may influence the melt on the marine-terminating glaciers. Several regional ocean model experiments were used to study regional differences in heat transport through troughs. Results showed that warm water extends north into Baffin Bay, reaching as far north as the Melville Bay troughs. Melville Bay troughs experienced warming following 2009. From 2004 to 2006, model experiments captured an increase in onshore heat flux in the Disko Bay trough, coinciding with the timing of the disintegration of Jakobshavn Isbrae's floating tongue and observed ocean heat increase in Disko Bay. The seasonality of the maximum onshore heat flux differs due to distance away from the Irminger Sea. Ocean temperatures near the north-west coast and south-east coast respond differently to changes in meltwater from Greenland and high-frequency atmospheric phenomena. With a doubling of the GrIS meltwater, Baffin Bay troughs transported ~ 40 % more heat towards the coast. Fewer storms resulted in a doubling of onshore heat (~ 100 % increase) through Helheim glacier's trough. These results demonstrate the regional variability of onshore heat transport through troughs and its potential implications to the GrIS."

- *What constitutes the ice sheet runoff? Does it include both surface melt and ocean melt?*
  AC: Yes, and have added this description on page 4 line 20 to say "The ice sheet runoff includes surface melt and melt at the front edge of a glacier."

- *Is there a reference for this breakdown?*
  AC: Yes, Bamber et al., 2012. We have added this reference on page 4 line 22.

- **AC:** Have updated Equation 1 with reviewers' comments.

- *Transient kinetic energy might be a better term. This separation includes lots more processes in the "EKE" than just eddies.*
  AC: Have updated page 6 line 17 to say " .. the transient kinetic energy (TKE)...". Therefore replaced all EKE text with TKE.

- *Could you include a TS diagram with both model and observations*
  AC: We have added a new figure for our model evaluation section. Figure 7 is a TS diagram of both the model and observations for Davis Strait. See page 7 lines 23 for a description in the manuscript.

- *Could you include a table listing all the different water masses referred to in the manuscript and include the TS definitions of those? I am unable to understand which part of the figure 5 and figure 6 this sentence refers to.*
  AC: We have included a table for water masses in Davis Strait (Table 2).

- *Are the observations and model plotted using the same output frequency (5 days), if not then for better comparison the observations should be averaged down to 5 days in the same way as the model output*
  AC: Figure 8 has been updated to have the observations and model plotted using the same output frequency of 5-day averages. We have updated the figure and associated caption and text in the manuscript.

- **AC:** We have updated the discussion on what is used for "T" in Equation 2. See major comments above.

- *What is the lag and is it the propagation speed realistic compare to the current speeds from the model?*
  AC: We have updated the sentence based on the model output on page 13 line 30 "...the timing of the arrival of sub-surface warm waters in the troughs along the west coast of Greenland, as flow from Davis Strait can take about a month to reach DBT and five to six months to reach MVBCT according to HighRes.."

- *Are you calculating this along the magenta of the tan lines?*
  AC: Figure 11 shows the mean and fluctuating component of the heat flux calculated on the tan lines of Figure 1. We have updated the manuscript to clarify this on page 14 line 7 ".Examining the mean and fluctuation components of the flow will help identify what processes drive heat through the troughs (shown as tan lines in Fig. 1)."

- *By which metric? And isnt that the case for all shown sections?*
  AC: We have added a new metric to the discussion for Section 3.2.

- *Again, what is the cutoff for contributing vs not?*
  AC: We have created a cutoff for this section and updated the manuscript on page 14 line 8 “Table 3 shows the overall percentage of the heat flux transported by the fluctuating component of the flow. In general, these percentages are less than 10%, suggesting the fluctuating component is a minor player in the heat transport through Greenland’s coastal troughs.”

- *What is the motivation to look at NToff section?*
  AC: We have removed NToff, as we have decided that it does not add much analysis to the overall manuscript.
-
- *There is no conclusion/explanation of the results*
  AC: We have edited Section 3.3 to explain more of the processes that have impacted the model.

- *There is no plume in the model so I don’t think that can explain the results here. I would think that potential shut down of convection in Labrador or Irminger sea would be good candidates for an explanation.*
  AC: We have added some explanations for the processes that may be responsible for the results. And we have added this discussion into Section 3.3

- **AC:** Unit issues on page 18 have been fixed, see major points above.

- *Is the ocean current fast enough for season peaks between HGT2 and DBT to be caused by simple advection of Irminger Water?*
  AC: We have fixed this section so that we are not just limiting our discussion to say only the Irminger water has an influence on bringing warm waters to the troughs.

- *It would be helpful if you marked on this figure the trough sections for which you calculate heat flux (the tan lines from Fig. 1)*
  AC: Done.

Drivers for Atlantic-origin waters abutting Greenland

Laura C. Gillard[1], Xianmin Hu[1,2], Paul G. Myers[1], Mads H. Ribergaard[3], and Craig M. Lee[4]

[1]Department of Earth and Atmospheric Sciences, University of Alberta, Edmonton, Alberta, Canada
[2]Bedford Institute of Oceanography, Dartmouth, Nova Scotia, Canada
[3]Danish Meterological Institute, Copenhagen, Denmark
[4]Applied Physics Laboratory, University of Washington, Seattle, Washington, United States of America

Correspondence: Laura C. Gillard (gillard2@ualberta.ca)

Abstract.

The oceanic heat available in Greenland's troughs is dependent on the geographic location of the trough, the water origin, and how the water is impacted by local processes along the pathway to the trough. This study investigates the ~~mechanisms that bring warm water~~ spatial pattern and quantity of the warm water (with a temperature greater $0\,^{\circ}C$) brought to the shelf and into the troughs abutting the Greenland Ice Sheet (GrIS). An increase in ocean heat in these troughs may drive a retreat of the GrIS. Warm water that is exchanged from the trough into the fjord may influence the melt on the ~~marine terminating glaciers. Regional~~ marine-terminating glaciers. Several regional ocean model experiments were used to study regional differences in heat transport through troughs. Results showed that warm ~~Irminger water can extend far~~ water extends north into Baffin Bay, reaching as ~~north as~~ far north as the Melville Bay troughs. Melville Bay troughs experienced warming following 2009. ~~An increase in ocean heat in these troughs may drive a retreat of the GrIS. In~~ From 2004 to 2006, model experiments captured an increase in onshore heat flux in the Disko Bay trough, coinciding with the ~~observed~~ timing of the disintegration of Jakobshavn Isbrae's floating tongue and observed ocean heat increase in Disko Bay. ~~Seasonality~~ The seasonality of the maximum onshore heat flux differs due to distance away from the Irminger Sea. Ocean temperatures near the north-west coast and south-east coast respond differently to changes in meltwater from Greenland and ~~high frequency~~ high-frequency atmospheric phenomena. With a doubling of the GrIS meltwater, Baffin Bay troughs transported ~ 40 % more heat ~~. The lack of presence of~~ towards the coast. Fewer storms resulted in ~~an increase in heat flux~~ a doubling of onshore heat ($\sim$ ~~20 %~~ 100 % increase) through Helheim glacier's trough. These results demonstrate the regional variability of onshore heat transport through troughs and its potential implications to the GrIS.

1 Introduction

The Greenland Ice Sheet (GrIS), with the second largest storage of fresh ice on earth, has a glaciated cover of 1.81 million km^2 (Rastner et al., 2012). With the volume of ice reaching 2.96 million km^3, if the entire ice sheet were to melt, the sea level

equivalent (SLE) would be ~ 7 m (Bamber et al., 2013). The GrIS recorded a maximum mass loss in 2012 with values reaching -446 ± 114 Gt yr^{-1}, a SLE of $\sim 1.2 \pm 0.3$ mm yr^{-1}, and has varied around ~ 1 mm yr^{-1} SLE since (van den Broeke et al., 2016). Analysis of the the GrIS's mass loss and equivalent sea level rise (SLR) has shown that the GrIS has recently become a major source of global mean SLR (van den Broeke et al., 2016).

Meltwater originating off the south-west coast of the GrIS has been shown to circulate into the interior of the Labrador Sea ~~(Gillard et al., 2016; ?; Luo et al., 2016; Dukhovskoy et al., 2016)~~(Gillard et al., 2016; Boning et al., 2016; Luo et al., 2016; Dukhovskoy . The Labrador Sea convection region is sensitive to changes in buoyancy, a balance between heat loss and freshwater input (Aagaard and Carmack, 1989; Straneo, 2006; Weijer et al., 2012). Thus, an increase ~~of~~ in the accumulation of meltwaters in the Labrador Sea may affect and slow down deep convection ~~(Weijer et al., 2012; ?)~~(Weijer et al., 2012; Boning et al., 2016). A weakening of the deep water formation may impact the Atlantic Meridional Overturning Circulation (AMOC), influencing how the earth distributes heat, impacting sea ice production and concentration of dissolved gases such as oxygen and carbon dioxide, and altering ecosystems ~~(Weijer et al., 2012; Swingedouw et al., 2014; ?; Arrigo et al., 2017)~~(Weijer et al., 2012; Swingedouw et al., 2014 .

Numerous studies have focused on the causation ~~for~~ of the increase in mass loss from the GrIS, such as atmospheric warming (Box et al., 2009) and synoptic wind patterns (Christoffersen et al., 2011). The annual mass balance of the GrIS has been persistently negative since the rapid retreat of ~~marine terminating~~ marine-terminating glaciers began in 1995 (van den Broeke et al., 2016).

There are approximately 900 ~~marine terminating~~ marine-terminating glaciers on the GrIS (Rastner et al., 2012) which drain ~ 88 % of the ice sheet (Rignot and Mouginot, 2012). Therefore, it is this type of glacier that has the greatest control over the fate of the ice sheet. Past studies have concluded that the influences affecting the dynamics of ~~marine terminating~~ marine-terminating glaciers include glacier surface thinning (Csatho et al., 2014), glacier fjord geometry (Porter et al., 2014; Fenty et al., 2016; Rignot et al., 2016a; Williams et al., 2017; Felikson et al., 2017), state of the ice melange (Moon et al., 2015), subglacial discharge (Jenkins, 2011; Bartholomaus et al., 2016), and ocean temperature changes (Holland et al., 2008; Myers and Ribergaard, 2013; Straneo and Heimbach, 2013; Rignot et al., 2016b; Cai et al., 2017; Wood et al., 2018). Wood et al. (2018) showed that ocean warming at intermediate depths, below 200 m, has the potential to increase ocean induced undercutting.

The fluctuation of heat content in the North Atlantic Subpolar Gyre (NASPG) may have been the cause of ocean warming in fjords of ~~marine terminating~~ marine-terminating glaciers (Holland et al., 2008; Myers and Ribergaard, 2013; Straneo and Heimbach, 2013). The NASPG contains a branch that travels northward across the North Atlantic Ocean to the West European Basins (Fig. 1). Here, a branch ~~travel~~ travels westward, forming the Irminger Current circulating along Reykjanes Ridge. The Atlantic water that remains in the Irminger Current carries relatively warm and saline waters along the south-east coast of Greenland, while Polar waters from the Arctic Ocean and Greenland meltwaters from the East Greenland Current (EGC) and East Greenland Coastal Current merge to create a (mixed and modified) relative cold and low-saline current (Bacon et al., 2014). This current forms the West Greenland Current (WGC) near Cape Farewell. The WGC separates into two branches: one travels northward along the west coast of Greenland into Baffin Bay bringing with it both less saline, cold Polar water and

relatively warm, saline, modified Atlantic water, and the second, warmer and more saline branch joins the southward flowing Baffin Island Current at Davis Strait (Fratantoni and Pickart, 2007; Myers et al., 2009). A portion of the NASPG branches off northward through the Iceland–Scotland ~~ridge~~Ridge, which separates the Norwegian Sea from the North Atlantic Ocean, as the Norwegian Atlantic Current (NwAC) (Beszczynska-Möller et al., 2012). Instead of recirculating in ~~the~~ Fram Strait, a part of the NwAC can enter the Barents Sea, south of Spitzbergen or north through Fram Strait (Beszczynska-Möller et al., 2012). A large volume of water that travels through Fram Strait may recirculate directly in the strait and return south to the Nordic Seas (Karcher et al., 2011; Beszczynska-Möller et al., 2012). Another water source in Fram Strait may have originated from the Pacific Ocean (Aksenov et al., 2010; Hu and Myers, 2013). Pacific Water in Fram Strait is mainly the water mass entering the Arctic Ocean via the Bering Strait and delivered through the Transpolar route (Hu and Myers, 2013).

Along the shelf break of Greenland ~~,~~ transverse troughs extend ~~across the coast of Greenland~~ from the coast supplying warm water through to the mouths of fjords. Then depending on the structure of the water mass at the mouth of the fjord and the height of the fjord's sills, warm waters can access ~~the marine terminating~~ marine-terminating glaciers and accelerating their mass loss (Straneo et al., 2012; Gladish et al., 2015b; Cai et al., 2017). If the warm waters from the NASPG can reach these transverse troughs, changes in the heat content of the NASPG may influence the state of ~~marine terminating~~ marine-terminating glaciers on the GrIS.

This study investigates the following questions: how is the heat flux through the troughs affected by ocean model resolution? What is the mean and variability of the heat flux through the troughs around Greenland? What are the processes that drive the variability of the flux?

2 Methods

2.1 Model description

A general circulation coupled ocean–sea ice model is utilized in this study. The fundamental modelling framework used is the Nucleus for European Modelling of the Ocean (NEMO) version 3.4 (Madec, 2008). The ocean component is based on Ocean Parallelise (OPA) and is used for ~~the~~ ocean dynamics and thermodynamics. For sea ice dynamics and thermodynamics, Louvain la Neuve Ice Model (LIM2) is used (Fichefet and Morales Maqueda, 1997). The regional domain for the coupled ocean–sea ice model covered the Arctic and Northern Hemisphere Atlantic Oceans (ANHA), with two open boundaries: one at the Bering Strait and the other at the latitude of 20°S. All simulations start from January 2002 ~~,~~ and are integrated to December 2016.

Initial and monthly open boundary conditions (temperature, salinity, horizontal velocities, and sea surface height) are derived from the $^1/_4^\circ$ Global Ocean Reanalyses and Simulations (GLORYS2V3) product (Ferry et al., 2008). The surface atmospheric forcing fields (10 m surface wind, two metre air temperature and humidity, downward shortwave and longwave radiation, and total precipitation) with a temporal resolution of one hour and spatial resolution of 33 km, are from the Canadian Meteorological Centres Global Deterministic Prediction System Reforecasts (CGRF), provided by Environment and Climate Change Canada (Smith et al., 2014). The first two years of the model output are regarded as the adjustment from the initial GLO-

RYS2V3 fields, which have already had over 10 years to evolve. Figure ~~.~~2 shows the monthly summation of total kinetic energy (~~TKE~~KE) in all layers of Baffin Bay, for ~~two configurations,~~ the two experiments that will be discussed in detail in the next section, LowResControl and HighRes (~~Fig~~Figs. 2a ~~,~~and b). The ~~TKE~~ KE is low at the model start (January 2002) and increases ~~abrupt~~ abruptly after 2004 for the LowResControl ~~configuration. For the~~ experiment. For HighRes, the ~~TKE~~ KE is fairly comparable for all ~~other yearshaving~~ years. HighRes also has more than a magnitude higher of KE values compared to ~~the~~ LowResControl. Figure 2 suggests that the ~~spin up~~ spin-up of the large scale Baffin Bay circulation from the initial conditions takes one to two years, although it would take much longer for the deep layer and the interannual variation is not considered. Thus, only five–day averaged model output from 2004 to 2016 are analyzed in this study.

2.2 Sensitivity experiment set-up

2.2.1 Control experiment

The ANHA horizontal mesh grid is extracted from a global tripolar grid, ORCA (Barnier et al., 2007), at a $^1/_4{}^\circ$ resolution (hereafter referred to as LowResControl for low resolution) with a resolution ranging from ~ 11 km to ~ 15 km around Greenland. In the vertical, the LowResControl configuration uses the geopotential or z–level coordinate with a total of 50 levels. The layer thickness increases from 1.05 m at the surface level to 453.1 m in the last level (at a depth of 5727.92 m). Vertical high resolution is applied to the upper ocean, i.e., 22 levels for the top 100 m. Partial step (Bernard et al., 2006) is also enabled to better represent the sea floor. Bathymetry in LowResControl is taken from the existing global ORCA025 bathymetry (MEOM, 2013), which is based on a global relief model (ETOPO1) (Amante and Eakins, 2009) and a gridded bathymetric data set (GEBCO1) (BODC, 2008) with modifications (Barnier et al., 2007).

This study will focus on the relatively large scale processes outside of the fjords (as fjords are not resolved in this configuration) with an assumption that meltwater will reach the ocean surface once out of the fjord (Fig. 3). This assumption defines how Greenland discharge is added in the model, injected at the surface level then mixed into a 10 m thick layer. This approach is common in the present generation of ocean models at this horizontal scale, such as in Castro de la Guardia et al. (2015) and Dukhovskoy et al. (2016). Observations (Beaird et al., 2017, 2018) have shown that freshwater may not only be at the surface but be mixed and entrained with ambient waters and find a neutral buoyancy at depth. Therefore this stratification assumption in this model may be misrepresenting plume dynamics that occur in fjords and may need to be rethought in future studies.

The LowResControl simulation uses two interannual monthly runoff sources. Greenland's freshwater flux (tundra and ~~icesheet~~ ice sheet runoff) is provided by Bamber et al. (2012) for 2002 to 2010, and the 2010 runoff is repeated for the last 6 years of this study. The ice sheet runoff includes surface melt and melt at the front edge of a glacier. Runoff in the rest of the model domain (not including Greenland) is provided by Dai et al. (2009). The model used in this study does not have an iceberg module and so only the ~~icesheet~~ ice sheet and tundra runoff ~~is~~ are included of Greenland's freshwater flux (~ 46 % of the total (Bamber et al., 2012)).

2.2.2 Changes in resolution

How is heat flux through the troughs affected by ocean model resolution? A $^1/_{12}^\circ$ horizontal mesh grid is extracted from a global tripolar grid, ORCA (Barnier et al., 2007) (hereafter referred to as HighRes for high resolution) with a resolution ranging from ~ 3.5 km to ~ 5 km around Greenland. The vertical resolution remains identical to the LowRes, however, the HighRes bathymetry is built ~~using a different approach~~based on partly different sources. The bathymetry is generated by using ETOPO1 (Amante and Eakins, 2009) for the polar region, and the Global Predicted Bathymetry (Smith and Sandwell, 1997) from satellite altimetry and ship depth soundings for the rest of the domain. Therefore, given the ~~different approach of the generated bathymetry , downscalling~~ difference in the sources of bathymetry data, downscaling HighRes will not reduce to LowRes. The HighRes configuration provides model fields at a finer scale that is not always visible in LowRes. This provides the potential for a better simulation of warm ocean currents travelling towards the GrIS via ~~a~~ better representation of deep troughs. In addition, the model resolution also plays a role in simulating ocean mixing and mesoscale features ~~,~~such as eddies ~~, that~~ which bring warm water towards the GrIS shelf through the ~~trough along the GrIS~~troughs. Note that, even ~~in~~ at the $^1/_{12}^\circ$ resolution referred to as HighRes in this study, the majority of the fjords are still not resolved. HighRes has the same runoff and Greenland's freshwater flux setup as LowResControl. Given the numerical cost of ~~the~~ HighRes, LowResControl is utilized for the sensitivity experiments.

2.2.3 Enhanced Greenland discharge experiment

How can changing Greenland's freshwater flux impact the heat flux through the troughs around Greenland? As Castro de la Guardia et al. (2015) showed, enhanced Greenland melt can change nearby ocean circulation, e.g., spinning up the circulation in Baffin Bay. Here we ~~conduct~~ compare a pair of ~~sensitivity~~ experiments (LowResControl and LowResDoubleMelt) with the more realistic spatial distribution and temporal varying Greenland freshwater flux to quantify the impact on warm waters flowing towards the ~~marine terminating~~ marine-terminating glaciers through troughs.

LowResControl under-represents the total of Greenland's freshwater flux. Therefore, LowResDoubleMelt ~~,~~takes into account the solid mass discharge. LowResDoubleMelt has the identical setup as LowResControl, ~~expect~~ except for Greenland's freshwater flux. It is important to note that the entire solid discharge in LowResDoubleMelt is transformed into the liquid component (i.e., treated the same as the runoff). In addition, the ocean does not affect GrIS melting as the melting is prescribed and non-interactive. This results in roughly twice as much freshwater flux (hereafter called meltwater) (100 % Greenland's freshwater flux, broken down by ~ 46 % runoff and total iceberg discharge ~ 54 %) in LowResDoubleMelt compared to LowResControl (roughly 46 % of Greenland's freshwater flux, only including runoff). Therefore, the total meltwater added to LowResDoubleMelt had been ~~rouglhy doubled ,~~ roughly doubled and actually has a more realistic amount of meltwater than LowResControl. For this study, a comparison of the GrIS meltwater is made to demonstrate the ocean model's sensitivity to increased GrIS melt. How will ocean temperatures in troughs that terminate into Baffin Bay be impacted by an increase in GrIS melt?

2.2.4 ~~High frequency~~ High-frequency atmospheric event experiment

Previous studies (Holdsworth and Myers, 2015; Garcia-Quintana et al., 2019), have shown that ~~high frequency~~ high-frequency atmospheric phenomena, such as storms, barrier winds, fronts, and topographic jets, play an important role in ~~the~~ ocean processes (e.g., deep convection in the Labrador Sea) in the study area. ~~Do they also influence warm water brought towards the GrIS? Until this study , this has not yet been examined~~Jackson et al. (2014) reported that synoptic events can impact water properties and heat content within two large outlet fjords. Therefore they could impact shelf exchange and the renewal of warm waters to the GrIS. This study aims to go beyond Jackson et al. (2014)'s two fjords by considering the entire coast of Greenland.

We use the Kolmogorov–Zurbenko (KZ) filter method (Zurbenko et al., 1996) as Eskridge et al. (1997) has shown that this filter has the same level of accuracy as the wavelet transformation method, however, is much easier to use. The KZ filter is based on an iterative moving average that removes ~~high frequency~~ high-frequency variations. We apply the moving average over a length of 10 days with one iteration as Garcia-Quintana et al. (2019) has done. Therefore, the removal of atmospheric variability ~~(such as temperature and wind speeds)~~ that persisted for ~~a length of~~ 10 days or less from the atmospheric forcing was done to drive a sensitivity simulation, called LowResNoStorms. LowResNoStorms has ~~the~~ an identical setup as LowResControl, except for the KZ filter applied in the wind and air temperature fields~~(Zurbenko et al., 1996; Eskridge et al., 1997)~~. For more information regarding the methodology of the KZ filtering, please see ~~Zurbenko et al. (1996); Eskridge et al. (1997)~~ Zurbenko et al. (1996) and Eskridge et al. (1997). A complete list of simulations used in this study is given in Table 1.

2.3 Mean flow and its fluctuation

To evaluate the ocean's heat that reaches onto the shelf and into the troughs, heat fluxes are calculated at six sections along the coast of Greenland (across one trough per section, as shown in purple and tan, respectively, in Fig. 1). Section names and their associated trough names are seen in Fig. 1. To calculate the fluctuation of the heat flux, the ~~five day~~ five-day average model output of both temperature (T) and velocity (U) normal to the section are treated as the full current. A moving ~~averaged Eq. (~~average (Eq. 1) was applied by ~~taking the average of~~ averaging five model outputs (25 days) centered on a particular output (n) by taking outputs from two previous ($(n-2)$ and $(n-1)$), the centered (n), and two future ($(n+1)$ and $(n+2)$). ~~The~~ A test had been previously done (not shown) for different timescale averaging of 85 days (roughly three months) and 185 days (roughly six months) and found that the different timescale averaging did not significantly change the results. Therefore, the mean of the temperature and velocity ~~normal to the section~~ ($\overline{T}$, $\overline{U}$) ~~can be taken over a longer period (~~have been taken over 25 days~~)~~. The mean values were then subtracted from the full current to get the fluctuation component of the heat flux in Eq. (2). Given Eq. (2), ρ_0 is the reference density, Cp is the specific heat capacity of ~~sea water, x~~ seawater, L is the length ~~of the section~~ along the section direction x, $H(z,x)$ is the water depth along the section, ~~$T(t,z,x)$ is the temperature,~~ and $U(t,z,x)$ is the velocity normal to the section. The temperature, $T(t,z,x)$, is in Celsius implicating a reference temperature of 0^oC (273.15

K) in the heat flux calculation. In this study, a reference temperature of 0^oC is used because this is the temperature glacier ice starts to melt at.

$$(\overline{U},\overline{T})_n = \frac{1}{5}\sum_{j=n-2}^{n+2}(U,T)_{nj} \tag{1}$$

$$HeatFlux_{eddy}(t) = \rho_0 Cp \int_0^{xL}\int_0^{H(x)} U(t,z,x)T(t,z,x) - \overline{U}(t,z,x)\overline{T}(t,z,x)dzdx \tag{2}$$

To see the importance of the fluctuation component of the flow around Greenland, the ~~eddy~~ transient kinetic energy (~~EKE~~TKE) was calculated using ~~the five day~~ Eq. (3). u and u are the five-day averaged model outputs of ~~velocity in the zonal (u)~~ the zonal and the meridional ~~(v) components. The EKE was calculated using Eq. (3). Then the annual EKE average over the period of 2004 to 2016 were calculated~~velocity and $\overline{u}$ and $\overline{v}$ denotes the monthly mean averages.

$$EKETKE = \frac{(\overline{u^2} - \overline{u}^2) + (\overline{v^2} - \overline{v}^2)}{2} \tag{3}$$

2.4 Model evaluation

~~In order to~~ To continue with this study, a comparison was done to make sure that the model behaves similar to observations ~~. A comparison of the model behavior against observations was done~~ for West Greenland. The water mass structure at Fylla Bank is compared to observations from Ribergaard (2014). This section is chosen, as the WGC branches shortly after ~~it has passed~~ passing Fylla Bank, with a portion moving westward and joining the Labrador Current while the other portion continues north through Davis Strait. The Fylla Bank section is shown with ~~magenta~~ a magenta line in Fig. 1 (red in Fig. 1 in Ribergaard (2014)). The observed temperature and salinity for June 14th, 2013 (Fig. 31 in Ribergaard (2014)) ~~is~~ are compared to the modeled averages for June 2013 (Fig. 4). LowResControl (Fig. 4a.) ~~has~~ had a similar water mass structure as ~~observations. There is~~ the observations. In both observations and LowResControl, there was cooler water at the surface with a thickness of 50 m offshore and about 100 m thick, just off the west side of the bank (kilometre marker 45 in Fig. 4a), with warmer water (greater than $3\,^\circ C$) below 100 m depth. The cold water layer in the LowResControl ~~is~~ was slightly saltier with the depth of the modelled 34.2 isohaline similar to that of the observed 34 isohaline (Fig. 31 in Ribergaard (2014)). For ~~the~~ HighRes, the cold surface layer ~~is~~ was thicker (Fig. 4b~~.~~) than in observations, where the $2\,^\circ C$ layer (contour in magenta) ~~extends~~ extended to about 100 m depth off the west side of Fylla Bank at kilometre marker 45. Similar to observations the $4\,^\circ C$ and warmer water mass starts below 200 m and slopes upwards towards the west. At a depth of ~ 400 m ~~the~~ HighRes is warmer than observations by $\sim 1\,^\circ C$. Overall, the modelled water mass structure ~~compares~~ compared well with the observations but with minor offsets in temperature and salinity. The model ~~has~~ had a shallow fresh and colder surface layer in the west portion of the section ~~, and deepens~~ that deepened towards Fylla Bank. Finally, the HighRes configuration ~~has a much stronger and better represented~~ had a much sharper and better-represented thermocline compared to the LowResControl configuration

Moving northward to Davis Strait, ~~a~~ the primary gateway for meltwater and heat exchange between Baffin Bay and the North Atlantic Ocean, to look at the model and the observations. A comparison was done with LowResControl and HighRes to the Curry et al. (2014) moored array data (see Fig. 2 in Curry et al. (2014)). The monthly modelled temperature averaged over 2004 – 2010 at Davis Strait (Fig. 5 and Fig. 6) ~~is~~ was compared to the mooring observations (~~Curry et al. 2014~~Curry et al. (2014), their Fig. 3(c)). July through to September LowResControl (Fig. 5) ~~captures~~ captured the same structure of the West Greenland ~~Slow~~ Slope Water (WGSW) and West Greenland Irminger Water (WGIW) as in the Curry et al. (2014) study. See Table 2 for water mass characteristics in Davis Strait. From March to June LowResControl ~~shows~~ showed WGIW and WGSW cooler ($\sim 3°C$) by about a degree than that of the observations ($\sim 4°C$). LowResControl also ~~has~~ had a tongue of relatively warm water from the WGIW protruding into the interior of Davis Strait at $\sim 200\ km$ and $\sim 200\ m$ depth. For ~~the~~ HighRes (Fig. 6), the structure ~~is~~ was similar to that of LowResControl, with the protruding tongue at $\sim 200\ km$ and $\sim 200\ m$ depth. HighRes also ~~has~~ had a similar structure to the observations for the WGSW from July to October. Note that compared to observation, the WGSW and WGIW ~~seems~~ seem to be about $1°C$ warmer.

Curry et al. (2011) plotted a TS diagram (their Fig. 3) showing the main water masses (Table 2) at Davis Strait, based on September 2004 and 2005 data along the mooring line. Curry et al. (2011)'s plot is repeated using all September and October observational data collected within ~ 30 km of the Davis Strait sill, as part of the Davis Strait program, from 2004 to 2010 (Fig. 7). Although the result is denser, the same general structure as in Curry et al. (2011) can be seen. HighRes and LowResControl are plotted similarly (September and October fields, for the same region as the observations, from 2004 to 2010). HighRes shows a similar structure for the WGIW and WGSW, while LowResControl's WGSW is warmer and its WGIW doesn't show the same tail-off to lower salinities with its transitional water between $2°C$ and $0°C$. Both runs show Polar Water with a constant temperature between 32.5 and 33.5, albeit about a degree warmer than the observations, with then warming to $1°C$ to $2°C$ as the salinity drops to 31.

The LowResControl and HighRes volume transport from September 2004 to September 2013 ~~is able to~~ (Fig. 8) can satisfactorily represent the observations from ~~a~~ the mooring array at Davis Strait (e.g. Curry et al. (2011, 2014))~~(Fig. 8). Positive values indicates~~ . Positive values indicate southward volume fluxes through Davis Strait, and negative values ~~indicates the waters move northward . However, the simulations underestimate the high frequency~~ indicate northward transport. All model and observation output are plotted as the same 5-day average. The simulations underestimated the high-frequency peaks of transport from the observations (values ~~surpassing~~ approaching 6 Sv in some cases). ~~Lack of tides in the model may explain why there is less fluctuation of transport compared to observations.~~ The mean volume flux based on the Davis Strait moorings (Curry et al., 2011, 2014), calculated over the ~~time~~ period of Sept 21, 2004, to Sept 30, 2013, is 1.6 Sv. Over the same ~~time~~ period, the model transports are 1.2 Sv for LowResControl ~~,~~ with a correlation of 0.54, ~~and 1.0~~ significant at the 99 % level, and 1.2 Sv for HighRes with a correlation of 0.49. Yet many features, such ~~a~~ as the reduction in transport at the end of 2010, are well simulated.

2.5 Study area

This study focuses on six sections around Greenland (Fig. 1) with ~~marine terminating~~ marine-terminating glaciers and deep bathymetric features. In Fig. 9, the six sections are drawn (seen in light purple on the map inset 1). HighRes model bathymetry is in grey and each section runs north to south on the x–axis starting at the ~~left hand~~ left-hand side of the figure indicated by the zero kilometre marker. The rest of this section will compare the six sections and discuss how observed bathymetry from other studies compares to the HighRes model bathymetry (Fig. 9).

In north-west Greenland, Kong Oscar is the fastest ~~marine terminating~~ marine-terminating glacier, terminating into Melville Bay (Rignot and Kanagaratnam, 2006; Rignot and Mouginot, 2012). Twenty percent of the GrIS drainage volume is directed along glaciers that feed into Melville Bay, amounting to a discharge of $\sim 80\ \mathrm{km^3\ yr^{-1}}$ (Rignot and Kanagaratnam, 2006). Located in north-east Baffin Bay (Fig. 1), Melville Bay holds the widest and deepest Greenland cross shelf troughs. This system consists of three troughs: the North, Centre, and South Melville Bay Troughs (MVBTs: MVBNT, MVBCT, and MVBST). The MVBTs are 170 to $320\ \mathrm{km}$ long, 45 to $120\ \mathrm{km}$ wide and reach depths between $740\ \mathrm{m}$ to $1100\ \mathrm{m}$ with shallow banks (around $100\ \mathrm{m}$ below sea level) called inter–trough banks (Slabon et al., 2016; Morlighem et al., 2017). The HighRes bathymetry (seen in Fig. 9a) is relatively shallow compared to the observations discussed. MVBNT is located at the kilometre markers $10\ \mathrm{km}$ to $120\ \mathrm{km}$, MVBCT at $320\ \mathrm{km}$ to $450\ \mathrm{km}$, and MVBST at $480\ \mathrm{km}$ to $580\ \mathrm{km}$. The depths in the HighRes are about $400\ \mathrm{m}$ for MVBNT, ~~and~~ reaching almost $700\ \mathrm{m}$ depth for MVBCT and MVBST.

Further south, on the west coast of Greenland, Jakobshavn Isbrae (JI) terminates into Disko Bay. The rapid retreat and disintegration of JI's floating ice tongue ~~has~~ have been attributed to an increase in heat content, deep bathymetry, and NASPG warming (Holland et al., 2008; Myers and Ribergaard, 2013; Gladish et al., 2015a; An et al., 2017). Recent slowing down of JI's acceleration has been attributed to the glacier reaching a higher bed, high amounts of freshwater from the Canadian Arctic, a weak WGC, or a cold Baffin Bay current flooding the West Greenland Shelf and cooling in the Labrador and Irminger Seas (Joughin et al., 2012; Gladish et al., 2015a; An et al., 2017; Khazendar et al., 2019). In HighRes, the section drawn for Disko Bay (Fig. 9b) shows two deep bathymetric features: the first trough, located at $100\ \mathrm{km}$ to $200\ \mathrm{km}$, and the second trough at $380\ \mathrm{km}$ to $500\ \mathrm{km}$, now called UT (Uummannaq Trough) and DBT (Disko Bay Trough), respectively. UT connects to Uummannaq Fjord and DBT connects into Disko Bay. Both UT and DBT reach depths of around $500\ \mathrm{m}$, similar to observations found in ~~(Hogan et al., 2016)~~Hogan et al. (2016). In a more recent data set provided by BedMachineV3, UT similarly reaches approximately $500\ \mathrm{m}$ but DBT is much deeper, reaching depths of $900\ \mathrm{m}$ (Morlighem et al., 2017).

In the south-east region, there are two major glaciers of interest: Helheim Glacier (HG) and Kangerlussuaq Glacier (KG). HG terminates at a depth of $700\ \mathrm{m}$ in Sermilik Fjord, which is approximately $900\ \mathrm{m}$ deep at the U shape mouth with the adjacent continental shelf, reaching depths of $350\ \mathrm{m}$ (Straneo et al., 2010; Morlighem et al., 2017). Temperature variability in Sermilik Fjord cannot be explained by local heating or surface fluxes. The temperature variability in the fjord is instead a result of the advection of warmer waters into the fjord, as warm waters are present on the shelf ~~year round~~year-round, peaking from July to September (Straneo et al., 2010). In HighRes, the section ~~drawn~~ for HG (Fig. 9c) shows four unique features. The first one at kilometre marker $25\ \mathrm{km}$ to about $100\ \mathrm{km}$ shows a slumping of bathymetry reaching about $250\ \mathrm{m}$ in depth. Moving

further south there are three deep troughs. The first trough is located at 120 km to 180 km, reaching depths surpassing 500 m, and the second and third troughs, located at 190 km to 260 km and 350 km to 375 km, respectively, reach depths closer to 700 m. Features will be referred to as Slump, HGT1, HGT2, and HGT3.

In the BedMachineV3 data set, Kangerdlussuaq trough (KT) reaches depths closer to 800 m (Morlighem et al., 2017). Atlantic water occupies the deep waters of the KT and Kangerlussuaq Fjord (KF) (Azetsu-Scott and Tan, 1997). KF, similar to Sermilik Fjord has a deep open mouth, which could influence the Atlantic water transport that is observed there (Azetsu-Scott and Tan, 1997; Christoffersen et al., 2011; Inall et al., 2014). In HighRes, the section drawn for KT (Fig. 9d) is drawn over an area with the maximum depth in the middle of the section, deeper than 600 m, at kilometre marker 175 km. The KT extends from 125 km to about 200 km.

In the north-east, Daugaard-Jensen Glacier terminates into Scoresby Sund and Nioghalvfjerdsbrae (79NG) terminates into the sound of Jøkelbugten. The BedMachineV3 shows depths of around 600 m (Morlighem et al., 2017). The HighRes section drawn for Scoresby Sund (Fig. 9e) is outside of the opening of the coastline, from north to south, connecting fjord waters to the open ocean. The bathymetry here is smoother with fewer carved features. Instead, it shows a skewed U shape in this section. The maximum depth is reached at kilometre marker 120 km with a depth slightly greater than 500 m.

79NG has a floating ice tongue that abuts Hovgaard Ø, which divides the tongue into two sections (Wilson and Straneo, 2015). The most rapid melting occurs at the grounded (pinned) front, south of Hovgaard Ø, where the ice tongue is thickest and is exposed to deeper and warmer waters (Mayer et al., 2000; Seroussi et al., 2011; Wilson and Straneo, 2015). Schaffer et al. (2017) study showed that Atlantic Intermediate Water flows via bathymetric channels to the south of Hovgaard Ø at a pinned ice front, where there is a shorter pathway between the shelf and cavity, exposing the cavity to more shelf driven processes such as intermediary flows. The warm water is supplied from the warm water that resides in Norske Trough (NT) east of Hovgaard Ø (Fig. 1) (Wilson and Straneo, 2015). Some of the relatively fresh glacially modified water is exported to the continental shelf via Dijmphna Sund, north of the glacier (Wilson and Straneo, 2015). In the BedMachineV3, NT reaches depths close to 600 m (Morlighem et al., 2017). The HighRes section drawn for 79NG (Fig. 9f) is drawn from north to south. The HighRes bathymetry shows the deepest region exceeding depths of 300 m, though the majority of this section lies around 200 m.

3 Results and discussion

3.1 Onshore heat flux through coastal troughs

What is the significance of the deep troughs along Greenland's shelf to the supply of warm water to the fjords with ~~marine terminating~~ marine-terminating glaciers? A look at the onshore heat flux through these troughs will be shown using High-Res, as the benefits of a higher horizontal resolution have been shown. However, given the numerical costs of the HighRes, LowResControl is utilized for the sensitivity experiments that will be discussed later in this paper.

3.1.1 West coast: mean state

~~The section~~ A section was drawn for Melville Bay (Fig. 9a), located on the north-west coast of Greenland, which shows three deep bathymetric troughs: the MVBNT, MVBCT, and MVBST (all troughs described in Sect. 2.5). At the north edge of all three troughs (kilometre marker 15 km, 330 km, and 500 km, for MVBNT, MVBCT, and MVBST, respectively) there is an offshore heat flux. At the south edge of all three troughs (kilometre marker 110 km, 450 km, and 560 km, for MVBNT, MVBCT, and MVBST, respectively) there is an onshore heat flux. ~~However,~~ MVBNT, the shallowest of ~~them, has~~ the troughs, had the weakest onshore heat flux ~~,~~ ($0\ \mathrm{TW\,km^{-1}}$) except for short periods during 2010, 2012 and 2014. This ~~identifies~~ identified that the northward warm waters travelling along the west ~~Greenland coast~~ coast of Greenland are influenced by bathymetry and are steered eastward along the trough towards the coast.

MVBNT, MVBCT, and MVBST transport increased between 2009 and 2010 and persisted in an anomalously high state for five years. For MVBNT there was little heat transfer before 2010 when the heat transport through to 2015 increased to $0.05\ \mathrm{TW\,km^{-1}}$. At MVBCT ~~,~~an increase of heat flux started at the end of 2009 ~~,~~and reached a relatively stable value of $0.1\ \mathrm{TW\,km^{-1}}$ through to the end of 2016. For ~~the~~ MVBST there was a more persistent interannual heat flux throughout the entire period, increasing from $0.1\ \mathrm{TW\,km^{-1}}$ to $0.2\ \mathrm{TW\,km^{-1}}$ starting at the end of 2009. An increase in ~~warm water~~ heat flux through troughs in northern regions of the Greenland shelf starting in 2009 for MVBCT and 2010 for MVBNT and MVBST was also identified. A change from $0.1\ \mathrm{TW\,km^{-1}}$ is significant, as that increase in heat can potentially melt 300 tons of ice per second. Thus, an increase in ocean heat presence in these troughs may have driven more melt from the glaciers that terminate in Melville Bay.

~~The~~ A section drawn for Disko Bay (Fig. 9b), located on the west coast of Greenland, shows two deep troughs: UT and DBT. Both troughs ~~experience~~ showed an onshore heat flux at the south edge (kilometre marker about 180 km and 480 km, for UT and DBT, respectively) and an offshore heat flux at the north edge (kilometre marker 100 km to 120 km and 400 km to 420 km, for UT and DBT, respectively). ~~In addition to modified Atlantic water travelling northward via the WGC, along the coast, this study shows~~ This section, as well as the Melville Bay section showed that the ocean currents are influenced by the bathymetry and are steered eastward into the trough towards the coast.

HighRes was able to capture a ~~relatively higher~~ longer duration in onshore heat flux in ~~UT and~~ DBT in the early 2000s (~~2005 for UT and~~ 2004 to 2007~~for DBT). For UT there are specific events when the heat flux peaked up to ~ 0.3 , and at the end of 2005 there was a peak heat flux of about 0.1 and then through 2010 to 2012 there are variable pulses (0.1) with maximum in the winter of 2010–2011 with a value of 0.2 . There is a~~). There was a consistent heat flux onshore in DBT from 2004 to the end of 2007, and an increase in the heat flux (values showing ~~0.4~~ $0.4\ \mathrm{TW\,km^{-1}}$) reaching a maximum in 2010 and then ~~decreasing back towards 0.35~~ decreased back towards $0.35\ \mathrm{TW\,km^{-1}}$ ~~afterwards~~ afterward. The increased heat flux in years of 2004 to 2006 ~~coincide~~ coincided with the disintegration of the JI floating tongue ~~, and~~ and was within the period of observed oceanic heat increase in Disko Bay (from 1997 to 2007) (Holland et al., 2008).

For UT there are pulses of onshore heat flux of about 0.1 $\mathrm{TW\,km^{-1}}$ throughout the period. Through 2010 to 2012 there are variable pulses (0.1 $\mathrm{TW\,km^{-1}}$) with maximum in the winter of 2010–2011 with a value of 0.2 $\mathrm{TW\,km^{-1}}$.

3.1.2 West coast: seasonal and interannual variation

The seasonality of the ~~average~~ averaged onshore heat flux is shown in MVBCT (Fig. 10a). Late fall and early winter ~~shows~~ showed the maximum onshore heat flux with a peak in November. Through late winter to spring the onshore heat flux is weakest ~~,~~ with the minimum in April. Years of 2004–2007, as indicated in a variety of blues in Fig. 10, overall have less onshore heat flux. As time ~~progresses,~~ progressed the onshore heat flux ~~increases~~increased. 2011 and 2014 (as indicated in colours of pale green and orange) ~~show~~ showed the highest values of onshore heat flux ~~,~~ reaching maximums of about 13 TW and 11 TW respectively. ~~Again this~~ This increase of heat flux indicates that more heat has been ~~received~~ brought into MVBCT in more recent years. The lack of a summer peak at MVBCT, suggests seasonality is dominated by the subsurface warm layer. MVBCT heat flux seasonality seems to be dependent on both the seasonality of the volume flux and temperature (Fig. 10b and Fig. 10c), respectively, with a correlation of 0.92 and 0.93, respectively (shown in Table ~~??~~3).

Further south in DBT (Fig. 10d), the fall and winter seasons have ~~higher~~ stronger onshore heat flux. However, earlier years (2004 to 2005) show ~~above average~~ above-average onshore heat flux in the summer. ~~A maximum~~ Maximum onshore heat flux was identified in July and August of 2004 and 2005 (reaching values around 7 TW to 10 TW). However, in other years, June and July have lower values of heat flux (hovering close to 0 TW). This ~~peak in~~ warming event from 2004 to 2006 is ~~shown in DBT (~~also seen in DBT in Fig. 9b~~)~~. In 2011 there is a spike of onshore heat flux in December, reaching over 10 TW, then decreased in January (Fig. 10d). ~~For UT,~~ The enhanced heat flux in 2011 ~~, there was also a peak~~ is also seen in UT and MVBST (Figs. 9a and b), indicating that the warming event is a large scale rather than a localized process. The timing of the onshore heat flux peak also undergoes large interannual variation (Fig. ~~9b).~~ 10d), which is likely driven by the volume flux of the inflow (Fig. 10e)

Observations at Davis Strait ~~see~~ show a temperature maximum ~~in August~~starting around August/September through to November~~(Curry et al., 2011). The results here show DBT received onshore heat flux earlier in the season in the period of~~ /December (Curry et al., 2011; Grist et al., 2014). However, the heat flux peaks in DBT occurred as early as June/July between 2004 ~~to~~ and 2006 ~~, around June and July, coinciding with warmer surface waters~~ (Fig. 10d), suggesting a larger influence from the warm surface waters in these months. As the years progressed in the model, the timing of the maximum heat flux ~~becomes later in the season,~~ delayed with strong interannual variations from September to January~~, coinciding~~ . This timing coincided with the peak ~~in the Irminger Water (Fig. 10d). The August–December lag corresponds to~~ of warmest Irminger Water observed in Davis Strait. The delay, the warmest water in Davis Strait occurred in (late) fall to (early) winter rather than summer, was due to the advection time ~~from when the water was last near the surface in Irminger Sea. These results show~~ needed by the Irminger Sea water. The peak of the seasonal cycle of warm water in the troughs north of Davis Strait was further delayed. The lag in the seasonal cycle of warm water is consistent with the Lagrangian trajectory-based study by Grist et al. (2014).

The results (Fig. 10d) showed an early arrival ~~in warm waters~~ of warm waters (June in 2004) occurred at the time when JI started to melted rapidly (Holland et al., 2008). This may~~therefore~~ , therefore, have been due to not only an increase in ocean

heat flux but perhaps an arrival of warm waters earlier in the melt season ~~and stayed~~ impacting JI for a longer ~~time~~duration. DBT heat flux seasonality is dependent on the seasonality of the temperature of the water mass and not the seasonality of the volume flux (Fig. 10f and Fig. 10e), with a correlation of 0.93 and 0.43 (shown in Table ~~??~~3).

3.1.3 South-east coast: mean state

The section drawn for Helheim (Fig. 9c) located off the south-east coast of Greenland, shows four unique features, Slump, HGT1, HGT2, and HGT3. ~~For~~ At the north edge of the troughs in this section, HGT1 through to HGT3, ~~at the north edge of the troughs~~ (kilometre marker 100 km, 200 km, and 350 km) there is an onshore heat flux, and an offshore heat flux at the south edge (kilometre marker 175 km, 225 km, and 355 km). This identifies that there must be southward flowing warm water travelling along the south-east coast of Greenland, potentially drawn in from the Irminger Current, and the warm waters are again being bathymetrically steered westward along the trough towards the coast. Slump ~~shows an off shelf~~ showed an offshore heat flux, oscillating from 0 TW~~to ~~-0.5TW~~~~ km^{-1} to $\sim -0.5\ \mathrm{TW\,km^{-1}}$, potentially associated with ~~lots of~~ transient mixing and eddies.

The section that is drawn for KT (Fig. 9d) ~~,~~ highlights the extent of this trough. ~~On~~ In the north portion of the section, from about 25 km to 100 km there is evidence of mixing of signals of ~~on and off shelf~~onshore and offshore heat fluxes. At the 150 km mark, throughout the years, there is a consistent onshore heat flux of greater than $0.1\ \mathrm{TW\,km^{-1}}$ and similar in magnitude is an offshore heat flux on the south edge of the trough. ~~This trough appears to have the strongest onshore signal of the section. At the~~ In the south portion of the section (from 225 km to 325 km) there is a lot of variability of on and offshore in space and time.

3.1.4 South-east coast: seasonal and interannual variation

For HGT2 (Fig. 10g) ~~, the~~ the sign of the heat flux is always negative (offshore), with the highest magnitude occurring between the period of August through to May~~has the weakest onshore heat flux. However, offshore heat flux occurs~~ . Offshore heat flux occurred all year round making this location unique compared to all other regions examined. Observations from a fjord in south-east Greenland (Sermilik Fjord) showed that water properties and heat content vary significantly on synoptic timescales throughout non-summer months (Jackson et al., 2014). Looking at HGT2 (Fig. 10g), from October to March, there was large variability in the magnitude ~~and direction~~ of the heat flux ~~, a period with~~ and also an increase in average temperature (Fig. 10i).

~~Seasonality~~ The seasonality of HGT2 heat flux is ~~related similarly to the seasonality~~ dominated by that of the volume flux (correlation of 0.91) (Fig. 10h), ~~rather than the temperature~~ while the seasonality of the averaged temperature is out of phase (correlation of ~~−0.25~~− 0.25) (Fig. 10i)~~as shown in Table ??~~. At KT (Fig. 10j), ~~a peak of onshore heat flux occurs after August for most years. Summer onshore heat peaks occur in 2004, 2005, 2015, and 2016. KT heat flux seasonality~~ the seasonality of heat flux seems to be dependent on both the seasonality of the volume flux and temperature (Fig. 10k and Fig. 10l), with a correlation of 0.83 and 0.89~~(shown in Table ??).~~ , respectively (Table 3). At KT, the peak of onshore heat flux occurred after August for most years with significant interannual variation. The stronger warming events were found in 2004, 2005, 2015, and 2016.

3.1.5 North-east coast: mean state

The section drawn for Scoresby Sund (Fig. 9e), shows Scoresby Sund Trough (SBST). ~~It is again on the north edge of~~ On the trough's north edge near the maximum depth, at kilometre marker 110 km ~~that~~ there is a consistent signal for the onshore heat flux of more than 0.025 TW~~. On the north edge of the~~ km^{-1}. For the section, on the north edge at kilometre marker 20 km to 30 km, there is variability in the offshore heat flux. ~~The~~ Therefore, the middle of the section (at kilometre marker 110 km) is where the heat is ~~coming~~ being transported towards the coast.

The section ~~drawn~~ for 79NG (Fig. 9f), located in the north-east of Greenland, is drawn from north to south. On the north side of the trough, at around 400 km there is a pattern for onshore heat flux at different periods within the time series, and also similar for 1000 km and 1100 km. This area's bathymetry is quite complex and the deeper regions such as near the kilometre marker, 40 km, and from 1000 km to 1100 km, has heat flux onshore. The onshore heat flux has a ~~much smaller magnitude than any of the other sections,~~ small magnitude reaching its maximum value at about 0.04 TW km^{-1}.

3.1.6 North-east coast: seasonal and interannual variation

At SBST (Fig. 10m) ~~,~~ the onshore heat flux ~~begins~~ began to increase in October and ~~declines~~ declined in April. Peak years include early 2005, then 2010 and 2011, with 2016 having a weaker onshore heat flux. A maximum of 10 TW ~~is~~ was reached in 2005. ~~SBST heat flux seasonality seems to not be solely dependent on either the seasonality of the volume flux or temperature flux alone (Fig. 10n and~~ It is worth noting that the "onshore" heat flux is caused by the offshore outflow of cold (below $0\,^{\circ}C$) waters (Figs. 10m to Fig. 10o). ~~The heat flux shows a negative correlation of -0.73 for~~ SBST's heat flux seasonality is a function of both the volume flux and ~~-0.76 for the average temperature(shown in Table ??).~~ temperature, with a correlation of -0.73 and -0.76, respectively (Table 3). The above $0\,^{\circ}C$ mean temperature is only seen in September/October in 2016, suggesting that transport of warm water into the trough would not be a common phenomenon.

At NT~~(Fig. 10p)the seasonality is not clear. A consistent growth in onshoreheat flux occurs in August , with a minimum of heat flux in June. There is a lot of variability from 2004 to 2016, with maximum flux in 2004, 2005, and 2010 and strongest offshore heat flux occurring in January through May of 2015. From August to December, maximum onshore heat occurred in~~ , opposite to that in SBST, the heat flux was mainly controlled by the inflow of cold water (Figs. 10p-10r). The "onshore" heat flux generally started a consistent growth in August till October due to a steady decrease of inflow of cold waters, while the first half of each year the cold water (close to freezing temperatures) (Fig. 10r) commonly flowed into the fjord with a significant variation on both sub-seasonal and interannual scales (Fig. 10p). Positive onshore heat flux was seen only in very few cases due to the outflow of cold waters, e.g., 2006, 2010, 2011, and ~~2014, with a maximum offshore heat flux in 2004, 2009 and 2007. From 2012 to 2016 there is a peak in February with a decline in March and April. The heat flux then increases steadily to a maximum in September and October, where it then declines again. Therefore, for this region, the seasonality has changed throughout the time of the study. NT heat flux seasonality is dependent on both the seasonality of the~~ 2014. As the volume flux explained almost 100% (with a correlation coefficient of -0.99) of the heat flux variation, the "warm" (still below $0\,^{\circ}C$) peak

in the averaged temperature (Fig. 10r) ~~an the volume flux (Fig.10q), with a correlation of 0.81 and −−0.99 (shown in Table ??~~is very likely the result of less incoming cold water to compensate the local source of warming (i.e., from the surface).

3.1.7 Summary of onshore heat flux through coastal troughs

Of these six regions ~~,~~ the region closest to the Irminger Sea, HGT2, ~~receive~~ received the highest heat flux ~~in~~ earliest in the year, from June to September. The results presented here showed heat flux of waters with temperatures greater than $0\,°C$. There appears to be a pattern that the two regions farther away from the NASPG on the west coast of Greenland (MVBCT and DBT), have ~~warm water transported later~~a warm water peak later, potentially due to the ~~arrival of warm Irminger Water from the subduction area in the~~ later arrival of modified warm water from the Irminger Sea. DBT ~~has~~ had the largest onshore ocean heat flux from July to December. Further north, a later arrival occurs at MVBCT (September through December). On the north-east coast of Greenland, warm water is received from the NwAC. The ~~transport~~ onshore heat flux through the three troughs ~~peak in onshore heat flux~~ peaked thusly: KT from August to November, followed by SBST from November to April and the NT peaked from September to January. Therefore, HGT2 could receive warm water first from the Irminger Sea, then the WGC reaches DBT then MVBCT and the NwAC ~~reaches~~ reached KT, followed by SBST and NT. ~~For the WGC branch, ? identified the warmest and saltiest Irminger waterin Davis Strait during summer months,~~

Grist et al. (2014) had examined the propagation of the seasonal signal for Irminger water. This study found that the peak seasonal temperatures occur on the east coast of Greenland and west coast south of Davis Strait between August and December, similar to the south-east locations in this study showed (HGT2 and KT). Grist et al. (2014)are in agreement with our study that a lagged timing of the seasonal cycle for warm waters exists north of Davis Strait. In Davis Strait the temperature maximums occur during October to December (Curry et al., 2014) this would align with the timing of the arrival of sub-surface warm waters in the troughs along the west coast of Greenland, as ~~their is a lagged time when the warm water is shown in these troughs, in summer or fall.~~ flow from Davis Strait can take about a month to reach DBT and five to six months to reach MVBCT according to HighRes.

The seasonality of heat flux through these troughs seems to correspond with the volume flux (HGT2) or average temperature (DBT and NT), and even both components in some cases (MVBCT, KT). SBST had a negative correlation with both the volume flux and the average temperature, where there ~~is~~ was less onshore heat flux in the summer months (July to October) there ~~is~~ were more onshore volume flux and warmer ocean temperatures. Where in the winter months, there is more onshore heat flux, but more offshore volume flux and cooler ocean temperatures.

3.2 Contribution of the mean flow and its fluctuation

~~An ocean current can be broken down into two components, mean and fluctuation. Sect. 2.3 defines how the mean and fluctuation components are calculated (using Eq. (2)).~~

Examining the mean and fluctuation components of the ~~current~~ flow will help identify what processes ~~drives the heat flux~~ drive heat through the troughs (~~Fig. 11). This section will compare LowResControl and HighRes.~~ shown as tan lines in Fig. 1). Table 3 shows the overall percentage of the heat flux transported by the fluctuating component of the flow. In general, these

percentages are less than 10%, suggesting the fluctuating component is a minor player in the heat transport through Greenland's coastal troughs.

~~For the west coast of Greenland, MVBCT and DBT show that the mean flow is crucial for bringing heat on the shelf (Fig. 11a and Fig. 11c). For MVBCT (Fig. 11b) the fluctuation component is negligible, approximately 0 with the mean component reaching a maximum of ~ 13 in the HighRes. LowResControl total (mean and fluctuation) onshore heat flux correlates well with the HighRes with a value of 0.84 (Table **??**). LowResControl transport is lower and reaches it's peak of approximately 7 at the end of 2012. From the end of 2005 the arrival of the heat flux occurs at the end of the year , consistent with Fig. 10a.~~

~~With~~ In Baffin Bay, consistent with the overall big picture view, the heat flux transported by the mean component peaks later in the year at $4-12$ TW, based on HighRes. The general behaviour is similar in LowResControl, albeit with smaller peak fluxes. This may be related to HighRes being better able to represent the bathymetry and coastal flows, although the northward-flowing Atlantic Water at Davis Strait is also around $1\,^{\circ}C$ warmer in HighRes. DBT (Fig. 11~~d~~)c. and Fig. 11d) sees peak fluxes over
6 TW in 2004, 2005, ~~the fluctuation component is less than the mean component. The maximum absolute value of the fluctuation heat flux is 1.3 and the maximum absolute value of the mean heat flux is 11 . Mean peaks occurred throughout the period with interannual variability, with amaximum in July and August in 2004 to 2007 and at the end of the year (November) in 2007 to~~ 2010 ~~, 2013~~ and ~~2014 (in October). LowResControl total (mean and fluctuation) onshore heat flux does not have a strong correlation with the HighRes with a value of 0.54 (Table **??**~~2012. The peak heat fluxes for MVBCT (Fig. 11a. and Fig. 11b) were concentrated in the early 2010s, between the end of 2009 and 2014. For both of these locations, the fluctuation component rarely exceeds $0.1-0.2$ TW.

Warm water exchange into the troughs is very different in southeast Greenland as compared to Baffin Bay. At HGT2, the mean heat transport in HighRes is offshore, with peak transport of -20 to -25 TW (Fig. 11e). The ~~maximum onshore heat flux in HighRes, in 2004~~ behaviour of the mean component in LowResControl is very different, with onshore heat transport reaching 5 TW in summer/autumn, balanced by offshore transport the rest of the year. Significant differences in cross-shelf transport between 1/4 and ~~2011 is 11 and 7 for LowResControl in 2004. The summation of yearly heat flux of MBVCT and DBT is 96 % higher in the HighRes than the LowResControl (Table 4). This maybe as seen in Section 2.4 (Fig. 6), that the HighRes resolves about a $1\,^{\circ}C$ warmer water mass at Davis Strait than compared to observations (Curry et al., 2014).~~

~~The south-east Greenland trough,~~ 1/12 degree simulations were also seen by Pennelly et al. (2019). At HGT2, ~~shows that~~ the fluctuation component ~~has transports between 0 to ~ 4 in HighRes (~ 2.5 in LowResControl) of onshore heat flux~~ of the heat fluxes was smaller than the mean, reaching only $1-2$ TW at peaks, but is generally directed onshore (Fig. 11f). ~~The fluctuation~~ Thus, here at HGT2, even though the fluctuation component is relatively small compared to the mean (Table 3), the difference in directions means it plays a key role in transporting heat towards this glacier fjord. This is ~~crucial for bringing heat onto the shelf especially for HighRes, as there is a large mean offshore heat flux through the study period (Fig. 11e). LowResControl total (mean and fluctuation) onshore heat flux correlates well with the HighRes with a value of 0.77 (Table **??**). For LowResControl the offshore heat flux ranges from -15 to 5 , where HighRes ranges from -30 to 0 . It is due to the mean velocity, normal to the section, that is driving the offshore heat exchange. The fluctuation component of the flow~~

having an impact on the control of the oceanic heat is consistent with studies that have looked at Christoffersen et al. (2011), who showed strong wind events in this region were important in bringing warm waters to the coast(Christoffersen et al., 2011) . How winds may impact the ocean heat flux will be discussed later in this section.

For KT, both the mean component and fluctuation component contribute to the onshore heat flux similarly in LowResControl and HighRes (Fig. 11g and Fig. 11h). There was variability with on and offshore pulses with the mean and fluctuation components, though the fluctuation is larger for HighRes than LowResControl. LowResControl onshore heat flux correlates well with the HighRes with a value of 0.71 (Table **??**). For HighRes, the mean onshore heat flux reaches a maximum at the end of 2004 and 2014 with values of approximately 14 , whereas LowResControl reaches about 7 in those years.

It is interesting to note the differences between HGT2 and KT, in HighRes , since they are located in close proximity to each other. The summation of yearly heat flux of HGT2 and KT is 4 % higher in the HighRes than the LowResControl (Table 4). Therefore, overall there is not a large change in HighRes vs LowResControl.

In the north-east at SBST Meanwhile, KT stood out with the fluctuating component of the flow transporting about 50% of the heat flux at this location (Table 3). The mean flow still transports the most heat, mainly in summer/autumn with peak transports reaching $8 - 15$ TW in HighRes (substantially smaller in LowResControl) (Fig. 11i)varying the resolution does not impact the mean onshore heat flux. LowResControl total (mean and fluctuation) onshore heat flux correlates well with the HighRes with a value of 0.74 (Table **??**).The fluctuation of the heat flux (Fig. 11j) has little contribution onshore for most of the study period, though there is an increase from $\sim \pm 2$ at the end of 2010 in HighRes. However, the mean onshore heat flux component is consistently higher for all simulations throughout the study period with peaks of ~ 10 in 2005. Peaks in the mean onshore heat flux occurs at the end of each year following into the beginning of the next year, consistent with the seasonality shown in Fig. 10m.

Further north at NT g). However, in the winter the mean transport reverses, transporting heat offshore. Meanwhile, although intermittent, the transient component of the heat flux is generally onshore in HighRes, regularly exceeding 0.5 TW (Fig. 11k), LowResControl total (mean and fluctuation) correlations strongly with the HighRes with a value of 0.92 (Table **??**). The mean component dominates over the fluctuation component for onshore heat flux. The mean component carries heat offshore as well with values reaching over -3 compared to ~ 0.5 onshore. The fluctuation component also contributes to carrying heat towards the shelf, with values reaching ~ 0.2 (Fig. 11l). The annual summation of h). This would be consistent with low-pressure systems propagating along the coast past KT, potentially linked to the Lofoten Low as suggested by Moore et al. (2014).

Moving to north-east Greenland, SBST has a significant onshore heat fluxfor the north-east coast (SBST and NT) is 9 % higher in the HighRes than the LowResControl(Table 4).

To see what is happening further off shelf, a section was drawn called NToff (Fig. 1). LowResControl total (mean and fluctuation) correlates strongly with the HighRes with a value of 0.92 (Table **??**). There exists stronger onshore pulses of the mean heat flux (values reach 2 or up to as high at 4) (, peaking at $6 - 10$ TW in HighRes (and little different in LowResControl), associated with the mean flow (Fig. 11m). Most onshore mean heat flux pulses occur at the end of each year though maximums of 4 occurred at the beginning of 2005, and end of 2011 into 2012. Like in NT, the mean heat flux still contributes to the offshore component. There is not much different between the fluctuation of the heat flux between NT and NToff i). Although

there are occasionally strong peaks in the fluctuating component, exceeding 0.2 TW, in general, this term is small (Fig. 11~~n).~~ j). There are more peaks in the fluctuating component in recent years (2011 onwards) and this might be related to the reductions in sea ice in this region. The mean component, which generally contributes to net offshore heat transport, dominates at NT as well (Fig. 11k and Fig. 11l).

~~The percent difference of the annual summation of the onshore heat through NToff verus NT is 5.3 % and 6.5 % for HighRes an LowResControl, respectively. Therefore, NToff has more heat travelling through the section than NT. This may be to do the deepening off shelf allowing for warm waters to enter this region, and not closer to the shelf where the bathymetry shallows.~~

The correlation of the heat flux between the HighRes and LowResControl for most ~~troughs is~~ of the troughs was high (NT ~~and NToff greater than 0.9~~greater than 0.9, MVBCT greater than ~~0.8~~0.8, and HGT, KT, and SBST greater than ~~0.7~~0.7, see Table ~~??~~3). The LowResControl and HighRes compared well with observations (see Section 2.4). ~~As running several high resolution experiments are computational expensive (such as HighRes)~~ However, since running several high-resolution experiments are computationally expensive compared to lower resolution configurations~~(such as LowResControl)~~, the LowResControl ~~has~~ had been used for the sensitivity experiments which will be discussed later in this paper (Section 3.3 and Section 3.4).

3.3 Impact of enhanced Greenland meltwater

~~Through each section, the annual average onshore heat flux and the total onshore heat flux was calculated for the study period (2004 to 2016). A comparison between the experiments were made for each sector (west includes Melville Bay, Disko Bay, south-east includes Helheim and Kangerdlussuaq, north-east includes Scoresby Sund, 79NG sections) (Table 4). With double the meltwater, the west sector had a 37 % increase in onshore heat flux. It appears that this mechanism (increase of heat flux with an increase in meltwater) is not as strong or reproduced in any other sector (~5 % and 9 % for south-east and north-east sectors)~~

Previous studies, from a variety of scales of modelling, have shown that enhanced freshwater discharge from the GrIS could increase the presence of heat near the ice sheet. For example, if GrIS melt increases it may add more energetic plume dynamics along a glacier face and increase the strength of the thermohaline circulation in fjords. Cai et al. (2017) showed in a 2–D model ran for one year, with ice shelf melt derived from observed melt rates for Petermann Glacier, that an increase in thermohaline circulation in the fjord could bring more heat and salt towards the ice sheet. Note that such fjord scale processes are not resolved by the model simulations presented in this paper. Outside of the fjord, Castro de la Guardia et al. (2015) and Grivault et al. (2017) had found enhanced meltwater from the GrIS could increase the heat content within the Baffin Bay. Enhanced runoff decreased surface salinity in Baffin Bay, particularly along the coast. Due to the halosteric effect, it led to a lift of the sea surface height on the shelf, and then an enhanced boundary current. This strengthened Baffin Bay's cyclonic gyre in the upper layer, which resulted in a stronger Ekman pumping that lifted the isopycnals and caused the shallowing of the warm water layer in Baffin Bay. Strengthening the WGC also brought more warm waters northward into Baffin Bay. The warming and lifting of the intermediate warm layer are clearly evident in the temperature field along the west Greenland coast (Fig. 12) in LowResDoubleMelt. This study provides more realistic experiments and analysis on specific locations concerning

troughs which connect to fjords with large marine-terminating glaciers. With an increase in GrIS melt, Baffin Bay's ocean heat content may increase. Thus increasing the potential for glaciers to continue to melt, impacting climate, SLR, and ecosystems.

For Melville Bay in LowResControl (Fig. 12a), a warm core of water ~~exists~~ existed at depths 100 m to 400 m, with a maximum (kilometre marker 500 km) in MVBST reaching almost $2°C$. In LowResDoubleMelt (Fig. 12b), the warm water core temperature increased and MVBST ~~reaches~~ reached temperatures closer to $3°C$. The cold water layer in LowResDoubleMelt thinned more than in the LowResControl. For Disko Bay, both deep troughs (UT and DBT) ~~hold~~ held warmer water in LowResDoubleMelt ($3°C$, Fig. 12d) than in LowResControl ($\sim 2°C$, Fig. 12c). The maximum increase occurred in a warm core in both troughs, UT and DBT (at kilometre marker 150 km and 400 km), ~~with~~ of a depth of 150 m to 350 m. The cooler water layer at the surface ~~again~~ thinned in LowResDoubleMelt (Fig. 12c). However, when examining average velocities normal to the section, for the entire period there was no clear trend that increasing the meltwater strengthens the velocities.

~~Previous studies, from a variety of scales of modelling, have shown that additional freshwater can increase the presence of heat to a region. In the ocean, if GrIS melt increases, it may add more energetic plume dynamics along a glacier face and increase the strength of the thermohaline circulation in fjords. Cai et al. (2017) showed in a 2–D model, ran for one year, with ice shelf melt derived from observed melt rates for Petermann Glacier, that~~ This study found that Baffin Bay was a very unique system. Other regions around Greenland did not respond to an increase in ~~thermohaline circulation in the fjord can bring more heat and salt towards the ice sheet. Castro de la Guardia et al. (2015) used a regional ocean model to set up eight sensitivity experiments, adjusting melt rates from the GrIS and ran for a period of 10 years. Grivault et al. (2017) also used a regional ocean model, and had interannual runoff and had experiments run for a 40 year period. With an increase in the GrIS melt, the heat content increases in Baffin Bay (Castro de la Guardia et al., 2015; Grivault et al., 2017).~~

~~Of all the regions around Greenland, Baffin Bay is a unique system, as it responds to an~~ the GrIS melt in the same way. With a doubling of the meltwater, the west sector had a 37 % increase in onshore heat flux (Table 4) but only resulted in a 9 % increase in the ~~GrIS melt in a different way than the two other regions around Greenland considered in this study. Identifying that ocean temperatures in troughs in Baffin Bay are indeed warming with increasing the GrIS melt provides further support to the work by Castro de la Guardia et al. (2015). This study, however, provides more realistic experiments and analysis on specific locations concerning troughs which connect to fjords with large marine terminating glaciers. Therefore, with an increase in GrIS melt, Baffin Bay's ocean heat content may increase. Thus increasing the potential for glaciers to continue to melt, impacting climate, SLR, and ecosystems.~~ north-east region and a 5 % decrease in the south-east region.

3.4 Impact of ~~high frequency~~ high-frequency atmospheric events

A question of how the atmospheric variability may impact the region of HG for renewing heat from the shelf has been discussed in previous observational studies (Straneo et al., 2010; Christoffersen et al., 2011). How does filtering out storms, where winds and the associated temperatures are impacted, affect the high frequency variability in the south-east Greenland? A comparison of LowResControl and LowResNoStorms will be shown ~~.~~ to examine this question.

Figure 13 ~~a shows the EKE~~ shows the average TKE integrated over the entire depth for the south-east region ~~using LowResControl and Fig. 13b~~ with LowResControl and LowResNoStorms. A comparison was done for the north-west and north-east regions ~~,~~

however as well. However, the south-east region has the highest EKE had the highest TKE as well as stronger sensitivity with the strongest sensitivity to changes in atmospheric conditionsthan all other regions. . Therefore only the south-east region will be shown for further analysis. LowResControl (Fig. 13a) had EKE values reaching TKE values reaching 4×10^{-3} m^2 s^{-2}. However, LowResNoStorms EKE peaks in magnitudes of TKE peaked at 2.5×10^{-3} m^2 s^{-2}, i.e.turbulent energy , TKE is reduced by about half. It is clear that the EKE decreases closer Significant TKE decrease close to HGT2 where the bathymetry reaches depths of is seen on the shelf at depths less than 500 m in the LowResControl (Fig. 13a). It appears that By filtering out storms, decreases the EKE strength the TKE strength decreased in the south-east region (Fig. 13b).

Figure 13c and Fig. 13d show the trend of mean heat flux and fluctuation time series of the mean and fluctuation components of the heat flux on or off shelf component for HGT2 with the LowResControl and LowResNoStorms. The mean heat flux appears to be smaller in LowResNoStorms than LowResControl component has less onshore heat flux in the LowResControl than LowResNoStorms. The LowResNoStorms mean component of the onshore heat flux reached values closer to 10 TW in 2004 to the end of 2007. LowResControl had onshore heat flux values greater than 5 TW in 2004, 2010, 2015 and 2016. The fluctuation component of After 2011, both experiment's mean component shows a direction change in the heat fluxis smaller with the LowResNoStorms. Therefore storms decreases the fluctuation component of the heat flux and increases the mean . The time series show more negative (offshore direction) heat flux values. LowResControl mean component shows more prominent offshore heat flux in 2013, 2015 and 2016, reaching maximums close to -15 TW , where LowResNoStorms has a weaker offshore mean heat flux, though similar values with LowResControl in 2014 (~ -10 TW). The fluctuation component of the heat flux . There is less mean winds from the north towards south and therefore less upper water Ekman transport towards the shelf and fjords. With less Ekman transport of deeper waters away from the fjords, the warm waters present within the deeper layers, therefore they can stay more easily within the fjord. As a result, less storms may increase the overall onshore heat flux into HGT2, as the changes in mean values exceed the changes fluctuation values (~ 5 vs ~ 1)is smaller with the LowResNoStorms. The fluctuation component moderated the heat flux more with storms (24% for the LowResControl vs 19% with LowResNoStorms, Table 3). Therefore, filtering storms decreased the fluctuation component of the heat flux as well as it's control over the total heat flux.

The summation of the onshore integration of the mean component of the heat flux from 2004 to 2016 has been calculated and compared between LowResControl and LowResNoStorms. LowResNoStorms has a total of 2260.2 , and the LowResControl is ~ 18 % less, with energy accumulation of 2 GJ (1 GJ $= 1 \times 10^9$ J), where LowResControl had a total of 1914.5 . This extra 345.7 -2 GJ. The total energy increase of 4 GJ could have the potential to melt 1037.1 kilotons of iceper second. Therefore this increase in total onshore heat flux might be due to less heat being transferred off the shelf due to high variability atmospheric forcing. 12 tonnes of ice. LowResNoStorms has a 100 % increase of onshore component of the heat for this period of 4 GJ compared to LowResControl of 2 GJ. LowResNoStorms has a 50% decrease of offshore component of the heat for this period of -2 GJ compared to LowResControl of -4 GJ. HGT2 has more energy in the onshore direction in LowResNoStorms due to filtering out offshore winds and therefore decreasing offshore heat transport. A decrease in storms decreased the offshore winds (southward) and therefore less Ekman transport (upwelling) along the shelf. Less upwelling and

offshore winds may decrease the offshore exchange of heat flux. As a result, fewer storms in this region may increase the overall onshore heat flux into HGT2.

4 Conclusions

The oceanic heat available in Greenland's troughs is dependent on both the location of the trough, ~~variability~~ source of the warm water origin, how the water is transformed as it travels to the troughs, as well as local processes~~occurring~~, such as heat loss to the atmosphere. It is important to understand the processes that bring this warm water to the shelf and into the troughs, as this water can be then exchanged into the fjords. Warm water ~~that exists in fjords creates an~~ present in fjords provides oceanic heat forcing on ~~the marine terminating~~ marine-terminating glaciers (Rignot et al., 2016b; Cai et al., 2017; Wood et al., 2018). To our knowledge, this is the first ~~look at~~ study looking at seasonal changes in heat flux in troughs that are connected to fjords with ~~marine terminating~~ marine-terminating glaciers.

This study showed that the presence of warm water at depth can extend far north into Baffin Bay, reaching as north as Melville Bay and its subsequent troughs. ~~The study's model experiments showed that Melville Bay troughs experienced an increased heat flux . Therefore an~~ Increased heat flux through the Melville Bay section is found from 2009 to the end of 2014. Therefore an associated increase in ocean heat presence in these troughs may have driven more heat to glaciers that terminate ~~here. In~~ there. From 2004 to 2006, model experiments captured an increase in onshore heat flux in DBT, coinciding with the timing of the disintegration of JI floating ~~tounge~~ tongue and within the period of observed oceanic heat increase in Disko Bay (from 1997 to 2007) (Holland et al., 2008).

~~Seasonality~~ The seasonality of the maximum onshore heat flux through ~~troughs around the GrIS differs due to distance away from the the Irminger Sea~~all six regions was presented. This study looked at warm water with temperatures greater than $0\,^{\circ}C$, therefore, it is not just simply modified Irminger water that may be present in the troughs. The seasonality of the maximum onshore heat flux through ~~all six regions were presented. For the Irminger Current influence the peaks begin~~troughs around the GrIS differs as the distance between the Irminger Sea increases. Therefore, the influence of the Irminger Current may still present itself in these troughs as well as other warm waters. The seasonal peak of warm waters began in: June for HGT2, July for DBT and September for MVBCT. Then for the areas receiving warm water from the NwAC: August for KT, November for SBS, and September to January for NT.

The south-east region ~~has the highest EKE~~ had the highest TKE as well as ~~stronger sensitivity with~~ the strongest sensitivity to changes in atmospheric conditions~~than all other regions~~. The south-east coast of Greenland is impacted the most by the atmospheric filter (i.e. no storms). No storms resulted in a reduction of ~~EKE~~ TKE ($\sim$ 50 %) and less offshore heat transport and therefore more onshore heat flux ($\sim$ 20 %) through the Helheim ~~glacier trough~~ Glacier Trough 2 (HGT2).

It is imperative to try to understand how sensitive the ocean is to additional meltwater from Greenland. Baffin Bay is a unique system, as it ~~responds~~ responded to an increase in the GrIS melt in a different way than any other region around Greenland ~~. Baffin Bay troughs will bring~~ in this study. Troughs off the west coast of Greenland in Baffin Bay brought more heat ($\sim$ 40 %) towards the GrIS ~~if~~ when the GrIS freshwater flux ~~doubles~~doubled. This study ~~shows~~ showed that a doubling of the GrIS melt

may cause ~~a~~ warming in Baffin Bay and an increase in heat flux through troughs, potentially escalating the melt of the GrIS, consistent with Castro de la Guardia et al. (2015) but now in a more realistic set–up with Greenland meltwater temporally and spatially distributed.

Since the model used in this study ~~does not have the capability to~~ cannot resolve small scale processes such as fjord circulation, the exchange between fjords and troughs cannot be looked into. Instead, there is an assumption in place ~~,~~ that the water characteristics that exist in the troughs will match those in the fjords due to ~~dynamics of cross shelf~~ the dynamics of cross-shelf exchanges (Jackson et al., 2014; Sutherland et al., 2014). ~~A warming of ocean heat~~ Warming of ocean water in troughs may lead to a warming of ocean ~~heat to~~ waters in fjords. Due to the model bathymetry ~~under representing~~ under-representing the depth of these troughs, this study may be underestimating the amount of ocean heat available to enter these troughs. The study only looked at the impact ~~from~~ of the freshwater flux ~~of~~ from the GrIS. The inclusion of an iceberg model coupled with an ocean model (Marson et al., 2018) may give further insight ~~to~~ into the heat and freshwater budget in regions of high GrIS discharge~~, such as explained in Marson et al. (2018)~~.

Author contributions. L.G. and P.M. designed the study and L.G. carried it out. X.H. developed the model configuration and performed the simulations. L.G. prepared the manuscript with contributions from all co-authors. M.R. and C.L. provided comments on the manuscript, with C.L. also providing Davis Strait data.

Competing interests. No competing interest are present.

Disclaimer. TEXT

Acknowledgements. We would like to thank Yarisbel ~~Garcia Quintana~~ Garcia-Quintana for carrying out the LowResNoStorm experiment. We are grateful to the NEMO development team and the Drakkar project for providing the model and continuous guidance, and to Westgrid and Compute Canada for computational resources, where all model experiments were performed and archived (http://www.computecanada.ca). We gratefully acknowledge the financial and logistic support of grants from the Natural Sciences and Engineering Research Council (NSERC) of Canada. These include Discovery Grant (rgpin227438) awarded to Dr. P.G. Myers, Climate Change and Atmospheric Research Grant (VITALS - RGPCC 433898), and an International Create (ArcTrain - 432295). The author would like to thank the anonymous reviewers for their insightful comments and suggestions that have contributed to improving this paper.

References

Aagaard, K. and Carmack, E. C.: The role of sea ice and other fresh water in the Arctic circulation, Journal of Geophysical Research: Oceans, 94, 14 485–14 498, https://doi.org/10.1029/JC094iC10p14485, 1989.

Aksenov, Y., Bacon, S., Coward, A. C., and Holliday, N. P.: Polar outflow from the Arctic Ocean: A high resolution model study, Journal of Marine Systems, 83, 14 – 37, https://doi.org/http://dx.doi.org/10.1016/j.jmarsys.2010.06.007, 2010.

Amante, C. and Eakins, B.: ETOPO1 1 Arc-Minute Global Relief Model: Procedures, Data Sources and Analysis, NOAA Technical Memorandum NESDIS NGDC-24, https://doi.org/10.7289/V5C8276M, 2009.

An, L., Rignot, E., Elieff, S., Morlighem, M., Millan, R., Mouginot, J., Holland, D. M., Holland, D., and Paden, J.: Bed elevation of Jakobshavn Isbrae, West Greenland, from high-resolution airborne gravity and other data, Geophysical Research Letters, 44, 3728–3736, https://doi.org/10.1002/2017GL073245, http://dx.doi.org/10.1002/2017GL073245, 2017GL073245, 2017.

Arrigo, K. R., van Dijken, G. L., Castelao, R. M., Luo, H., Rennermalm, s. K., Tedesco, M., Mote, T. L., Oliver, H., and Yager, P. L.: Melting glaciers stimulate large summer phytoplankton blooms in southwest Greenland waters, Geophysical Research Letters, 44, 6278–6285, https://doi.org/10.1002/2017GL073583, https://agupubs.onlinelibrary.wiley.com/doi/abs/10.1002/2017GL073583, 2017.

Azetsu-Scott, K. and Tan, F. C.: Oxygen isotope studies from Iceland to an East Greenland Fjord: behaviour of glacial meltwater plume, Marine Chemistry, 56, 239 – 251, https://doi.org/http://dx.doi.org/10.1016/S0304-4203(96)00078-3, http://www.sciencedirect.com/science/article/pii/S0304420396000783, modern Chemical and Biological Oceanography: The Influence of Peter J. Wangersky, 1997.

Bacon, S., Marshall, A., Holliday, N. P., Aksenov, Y., and Dye, S. R.: Seasonal variability of the East Greenland Coastal Current, Journal of Geophysical Research: Oceans, 119, 3967–3987, https://doi.org/10.1002/2013JC009279, 2014.

Bamber, J., Van Den Broeke, M., Ettema, J., Lenaerts, J., and Rignot, E.: Recent large increases in freshwater fluxes from Greenland into the North Atlantic, Geophysical Research Letters, 39, 2012.

Bamber, J. L., Griggs, J. A., Hurkmans, R. T. W. L., Dowdeswell, J. A., Gogineni, S. P., Howat, I., Mouginot, J., Paden, J., Palmer, S., Rignot, E., and Steinhage, D.: A new bed elevation dataset for Greenland, The Cryosphere, 7, 499–510, https://doi.org/10.5194/tc-7-499-2013, 2013.

Barnier, B., Brodeau, L., Le Sommer, J., Molines, J., Penduff, T., Theetten, S., Treguier, A. M., Madec, G., Biastoch, A., Bőning, C., Dengg, J., Gulev, S., Bourdallé, B. R., Chanut, J., Garric, G., Alderson, S., Coward, A., de Cuevas, B., New, A., Haines, K., Smith, G., Drijfhout, S., Hazeleger, W., Severijns, C., and Myers, P.: Eddy-permitting ocean circulation hindcasts of past decades, CLIVAR Exchanges, 12, 8–10, 2007.

Bartholomaus, T. C., Stearns, L. A., Sutherland, D. A., Shroyer, E. L., Nash, J. D., Walker, R. T., Catania, G., Felikson, D., Carroll, D., Fried, M. J., and et al.: Contrasts in the response of adjacent fjords and glaciers to ice-sheet surface melt in West Greenland, Annals of Glaciology, 57, 25–38, https://doi.org/10.1017/aog.2016.19, 2016.

Beaird, N., Straneo, F., and Jenkins, W.: Characteristics of meltwater export from Jakobshavn Isbræ and Ilulissat Icefjord, Annals of Glaciology, 58, 107–117, https://doi.org/10.1017/aog.2017.19, 2017.

Beaird, N. L., Straneo, F., and Jenkins, W.: Export of Strongly Diluted Greenland Meltwater From a Major Glacial Fjord, Geophysical Research Letters, 45, 4163–4170, https://doi.org/10.1029/2018GL077000, https://agupubs.onlinelibrary.wiley.com/doi/abs/10.1029/2018GL077000, 2018.

Bernard, B., Madec, G., Penduff, T., Molines, J.-M., Treguier, A.-M., Le Sommer, J., Beckmann, A., Biastoch, A., Böning, C., Dengg, J., Derval, C., Durand, E., Gulev, S., Remy, E., Talandier, C., Theetten, S., Maltrud, M., McClean, J., and De Cuevas, B.: Impact of partial

steps and momentum advection schemes in a global ocean circulation model at eddy-permitting resolution, Ocean Dynamics, 56, 543–567, https://doi.org/10.1007/s10236-006-0082-1, https://doi.org/10.1007/s10236-006-0082-1, 2006.

Beszczynska-Möller, A., Fahrbach, E., Schauer, U., and Hansen, E.: Variability in Atlantic water temperature and transport at the entrance to the Arctic Ocean, 1997–2010, ICES Journal of Marine Science: Journal du Conseil, https://doi.org/10.1093/icesjms/fss056, 2012.

BODC: British Oceanographic Data Center's General Bathymetric Chart of the Oceans, 2008.

Boning, C. W., Behrens, E., Biastoch, A., Getzlaff, K., and Bamber, J. L.: Emerging impact of Greenland meltwater on deepwater formation in the North Atlantic Ocean, Nature Geosci, 9, 523–527, https://doi.org/10.1038/ngeo2740, 2016.

Box, J. E.and Yang, L., Bromwich, D. H., and Bai, L.: Greenland Ice Sheet Surface Air Temperature Variability: 1840–2007, Journal of Climate, 22, 4029–4049, https://doi.org/10.1175/2009JCLI2816.1, 2009.

Cai, C., Rignot, E., Menemenlis, D., and Nakayama, Y.: Observations and modeling of ocean-induced melt beneath Petermann Glacier Ice Shelf in northwestern Greenland, Geophysical Research Letters, https://doi.org/10.1002/2017GL073711, http://dx.doi.org/10.1002/2017GL073711, 2017.

~~Carroll, D., Sutherland, D. A., Curry, B., Nash, J. D., Shroyer, E. L., Catania, G. A., Stearns, L. A., Grist, J. P., Lee, C. M., and de Steur, L.: Subannual and Seasonal Variability of Atlantic-Origin Waters in Two Adjacent West Greenland Fjords, Journal of Geophysical Research: Oceans, 123, 6670–6687, , , 2018.~~

Castro de la Guardia, L., Hu, X., and Myers, P. G.: Potential positive feedback between Greenland Ice Sheet melt and Baffin Bay heat content on the west Greenland shelf, Geophysical Research Letters, 42, 4922–4930, https://doi.org/10.1002/2015GL064626, 2015.

Christoffersen, P., Mugford, R. I., Heywood, K. J., Joughin, I., Dowdeswell, J. A., Syvitski, J. P. M., Luckman, A., and Benham, T. J.: Warming of waters in an East Greenland fjord prior to glacier retreat: Mechanisms and connection to large-scale atmospheric conditions, Cryosphere, 5, 701–714, 2011.

Csatho, B. M., Schenk, A. F., van der Veen, C. J., Babonis, G., Duncan, K., Rezvanbehbahani, S., van den Broeke, M. R., Simonsen, S. B., Nagarajan, S., and van Angelen, J. H.: Laser altimetry reveals complex pattern of Greenland Ice Sheet dynamics, Proceedings of the National Academy of Sciences, 111, 18 478–18 483, https://doi.org/10.1073/pnas.1411680112, http://www.pnas.org/content/111/52/18478, 2014.

Curry, B., Lee, C. M., and Petrie, B.: Volume, Freshwater, and Heat Fluxes through Davis Strait, 2004–05, Journal of Physical Oceanography, 41, 429–436, https://doi.org/10.1175/2010JPO4536.1, https://doi.org/10.1175/2010JPO4536.1, 2011.

Curry, B., Lee, C., Petrie, B., Moritz, R., and Kwok, R.: Multiyear volume, liquid freshwater, and sea ice transports through Davis Strait, 2004-10, Journal of Physical Oceanography, 44, 1244–1266, https://doi.org/10.1175/JPO-D-13-0177.1, 2014.

Dai, A., Qian, T., Trenberth, K. E., and Milliman, J. D.: Changes in continental freshwater discharge from 1948 to 2004, Journal of Climate, 22, 2773–2792, 2009.

Dukhovskoy, D. S., Myers, P. G., Platov, G., Timmermans, M.-L., Curry, B., Proshutinsky, A., Bamber, J. L., Chassignet, E., Hu, X., Lee, C. M., and Somavilla, R.: Greenland freshwater pathways in the sub-Arctic Seas from model experiments with passive tracers, Journal of Geophysical Research: Oceans, https://doi.org/10.1002/2015JC011290, 2016.

Eskridge, R. E., Ku, J. Y., Rao, S. T., Porter, P. S., and Zurbenko, I. G.: Separating Different Scales of Motion in Time Series of Meteorological Variables, Bulletin of the American Meteorological Society, 78, 1473–1484, https://doi.org/10.1175/1520-0477(1997)078<1473:SDSOMI>2.0.CO;2, https://doi.org/10.1175/1520-0477(1997)078<1473:SDSOMI>2.0.CO;2, 1997.

Felikson, D., Bartholomaus, T. C., Catania, G. A., Korsgaard, N. J., Kjær, K. H., Morlighem, M., Noël, B., van den Broeke, M., Stearns, L. A., Shroyer, E. L., Sutherland, D. A., and Nash, J. D.: Inland thinning on the Greenland Ice Sheet controlled by outlet glacier geometry, Nature Geoscience, 10, 366–369, https://doi.org/10.1038/ngeo2934, 2017.

Fenty, I., Willis, J. K., Khazendar, A., Dinardo, S., Forsberg, R., Fukumori, I., Holland, D., Jakobsson, M., Moller, D., Münchow, J. M. A., Rignot, E., Schodlok, M., Thompson, A. F., Tinto, K., Rutherford, M., and Trenholm, N.: Oceans Melting Greenland: Early Results from NASA's Ocean-Ice Mission in Greenland , Oceanography, 29, https://doi.org/10.5670/oceanog.2016.100, 2016.

Ferry, N., Greiner, E., Garric, G., Penduff, T., Treiguier, A.-M., and Reverdin, G.: GLORYS-1 Reference Manual for Stream 1 (2002-2007), GLORYS project report, 2008.

Fichefet, T. and Morales Maqueda, M.: Sensitivity of a global sea ice model to the treatment of ice thermodynamics and dynamics, Journal of Geophysical Research, 102, 12 609–12 646, 1997.

Fratantoni, P. S. and Pickart, R. S.: The western North Atlantic shelfbreak current system in summer, Journal of Physical Oceanography, 37, 2509–2533, 2007.

Garcia-Quintana, Y., Courtois, P., Hu, X., Pennelly, C., Kieke, D., and Myers, P. G.: Sensitivity of Labrador Sea Water ~~formation to changes in model resolution, atmospheric forcing and freshwater input~~Formation to Changes in Model Resolution, Atmospheric Forcing, and Freshwater Input, Journal of Geophysical Research: Oceans, ~~0,~~ 124, 2126–2152, https://doi.org/10.1029/2018JC014459, https://agupubs.onlinelibrary.wiley.com/doi/abs/10.1029/2018JC014459, 2019.

Gillard, L. C., Hu, X., Myers, P. G., and Bamber, J. L.: Meltwater pathways from marine terminating glaciers of the Greenland Ice Sheet, Geophysical Research Letters, 43, 10,873–10,882, https://doi.org/10.1002/2016GL070969, http://dx.doi.org/10.1002/2016GL070969, 2016.

Gladish, C., Holland, D., and Lee, C.: Oceanic boundary conditions for Jakobshavn Glacier. Part II: Provenance and sources of variability of disko bay and Ilulissat Icefjord waters, 1990-2011, Journal of Physical Oceanography, 45, 33–63, https://doi.org/10.1175/JPO-D-14-0045.1, 2015a.

Gladish, C., Holland, D., Rosing-Asvid, A., Behrens, J., and Boje, J.: Oceanic boundary conditions for Jakobshavn Glacier. Part I: Variability and renewal of Ilulissat Icefjord waters, 2001-14, Journal of Physical Oceanography, 45, 3–32, https://doi.org/10.1175/JPO-D-14-0044.1, 2015b.

Grist, J. P., Josey, S. A., Boehme, L., Meredith, M. P., Laidre, K. L., Heide-Jørgensen, M. P., Kovacs, K. M., Lydersen, C., Davidson, F. J. M., Stenson, G. B., Hammill, M. O., Marsh, R., and Coward, A. C.: Seasonal variability of the warm Atlantic water layer in the vicinity of the Greenland shelf break, Geophysical Research Letters, 41, 8530–8537, https://doi.org/10.1002/2014GL062051, 2014.

Grivault, N., Hu, X., and Myers, P. G.: Evolution of Baffin Bay Water Masses and Transports in a Numerical Sensitivity Experiment under Enhanced Greenland Melt, Atmosphere-Ocean, 55, 169–194, https://doi.org/10.1080/07055900.2017.1333950, http://dx.doi.org/10.1080/07055900.2017.1333950, 2017.

Hogan, K. A., Cofaigh, C. ., Jennings, A. E., Dowdeswell, J. A., and Hiemstra, J. F.: Deglaciation of a major palaeo-ice stream in Disko Trough, West Greenland, Quaternary Science Reviews, 147, 5 – 26, https://doi.org/https://doi.org/10.1016/j.quascirev.2016.01.018, http://www.sciencedirect.com/science/article/pii/S0277379116300208, special Issue: PAST Gateways (Palaeo-Arctic Spatial and Temporal Gateways), 2016.

Holdsworth, A. M. and Myers, P. G.: The Influence of High-Frequency Atmospheric Forcing on the Circulation and Deep Convection of the Labrador Sea, Journal of Climate, 28, 4980–4996, https://doi.org/10.1175/JCLI-D-14-00564.1, https://doi.org/10.1175/JCLI-D-14-00564.1, 2015.

Holland, D. M., Thomas, R. H., De Young, B., Ribergaard, M. H., and Lyberth, B.: Acceleration of Jakobshavn Isbrae triggered by warm subsurface ocean waters, Nature Geoscience, 1, 659–664, 2008.

Hu, X. and Myers, P. G.: A Lagrangian view of Pacific water inflow pathways in the Arctic Ocean during model spin-up, Ocean Modelling, 71, 66 – 80, https://doi.org/http://dx.doi.org/10.1016/j.ocemod.2013.06.007, 2013.

Inall, M. E., Murray, T., Cottier, F. R., Scharrer, K., Boyd, T. J., Heywood, K. J., and Bevan, S. L.: Oceanic heat delivery via Kangerdlugssuaq Fjord to the south-east Greenland Ice Sheet, Journal of Geophysical Research: Oceans, 119, 631–645, https://doi.org/10.1002/2013JC009295, 2014.

Jackson, R. H., Straneo, F., and Sutherland, D. A.: Externally forced fluctuations in ocean temperature at Greenland glaciers in non-summer months, Nature Geoscience, 7, 503–508, 2014.

Jenkins, A.: Convection-driven melting near the grounding lines of ice shelves and tidewater glaciers, Journal of Physical Oceanography, 41, 2279–2294, 2011.

Joughin, I., Alley, R. B., and Holland, D. M.: Ice-Sheet Response to Oceanic Forcing, Science, 338, 1172–1176, https://doi.org/10.1126/science.1226481, 2012.

Karcher, M., Beszczynska-Möller, A., Kauker, F., Gerdes, R., Heyen, S., Rudels, B., and Schauer, U.: Arctic Ocean warming and its consequences for the Denmark Strait overflow, Journal of Geophysical Research: Oceans, 116, https://doi.org/10.1029/2010JC006265, 2011.

Khazendar, A., Fenty, I. G., Carroll, D., Gardner, A. an Lee, C. M., Fukumori, I., Wang, O., Zhang, H., Seroussi, H., Moller, D., Noël, B. P. Y., van den Broeke, M. R., Dinardo, S., and Willis, J.: Interruption of two decades of Jakobshavn Isbrae acceleration and thinning as regional ocean cools, Nature Geoscience, 12, https://doi.org/10.1038/s41561-019-0329-3, https://doi.org/10.1038/s41561-019-0329-3, 2019.

Luo, H., Castelao, R. M., Rennermalm, A. K., Tedesco, M., Bracco, A., Yager, P. L., and Mote, T. L.: Oceanic transport of surface meltwater from the southern Greenland Ice Sheet, Nature Geoscience, https://doi.org/10.1038/ngeo2708, 2016.

Madec, G.: NEMO ocean engine, Note du Pole de modélisation, 2008.

Marson, J. M., Myers, P. G., Hu, X., and Le Sommer, J.: Using Vertically Integrated Ocean Fields to Characterize Greenland Icebergs' Distribution and Lifetime, Geophysical Research Letters, 45, 4208–4217, https://doi.org/10.1029/2018GL077676, https://agupubs.onlinelibrary.wiley.com/doi/abs/10.1029/2018GL077676, 2018.

Mayer, C., Reeh, N., Jung-Rothenhäusler, F., Huybrechts, P., and Oerter, H.: The subglacial cavity and implied dynamics under Nioghalvfjerdsfjorden Glacier, NE-Greenland, Geophysical Research Letters, 27, 2289–2292, https://doi.org/10.1029/2000GL011514, https://agupubs.onlinelibrary.wiley.com/doi/abs/10.1029/2000GL011514, 2000.

MEOM: Bathymetry ORCA0.25, http://servdap.legi.grenoble-inp.fr/meom/ORCA025-I/, 2013.

Moon, T., Joughin, I., and Smith, B.: Seasonal to multiyear variability of glacier surface velocity, terminus position, and sea ice/ice mélange in northwest Greenland, Journal of Geophysical Research: Earth Surface, 120, 818–833, https://doi.org/10.1002/2015JF003494, https://agupubs.onlinelibrary.wiley.com/doi/abs/10.1002/2015JF003494, 2015.

Moore, G. W. K., Straneo, F., and Oltmanns, M.: Trend and interannual variability in southeast Greenland Sea Ice: Impacts on coastal Greenland climate variability, Geophysical Research Letters, 41, 8619–8626, https://doi.org/10.1002/2014GL062107, 2014.

Morlighem, M., Williams, C. N., Rignot, E., An, L., Arndt, J. E., Bamber, J. L., Catania, G., Chauché, N., Dowdeswell, J. A., Dorschel, B., Fenty, I., Hogan, K., Howat, I., Hubbard, A., Jakobsson, M., Jordan, T. M., Kjeldsen, K. K., Millan, R., Mayer, L., Mouginot, J., Noël, B. P. Y., O'Cofaigh, C., Palmer, S., Rysgaard, S., Seroussi, H., Siegert, M. J., Slabon, P., Straneo, F., van den Broeke, M. R., Weinrebe, W., Wood, M., and Zinglersen, K. B.: BedMachine v3: Complete Bed Topography and Ocean Bathymetry Mapping of

Greenland From Multibeam Echo Sounding Combined With Mass Conservation, Geophysical Research Letters, 44, 11,051–11,061, https://doi.org/10.1002/2017GL074954, https://agupubs.onlinelibrary.wiley.com/doi/abs/10.1002/2017GL074954, 2017.

Myers, P. G. and Ribergaard, M. H.: Warming of the polar water layer in Disko Bay and potential impact on Jakobshavn Isbrae, Journal of Physical Oceanography, 43, 2629–2640, 2013.

Myers, P. G., Donnelly, C., and Ribergaard, M. H.: Structure and variability of the West Greenland Current in Summer derived from 6 repeat standard sections, Progress in Oceanography, 80, 93–112, 2009.

Pennelly, C., Hu, X., and Myers, P. G.: Cross-Isobath Freshwater Exchange Within the North Atlantic Subpolar Gyre, Journal of Geophysical Research: Oceans, 124, 6831–6853, https://doi.org/10.1029/2019JC015144, https://agupubs.onlinelibrary.wiley.com/doi/abs/10.1029/2019JC015144, 2019.

Porter, D. F., Tinto, K. J., Boghosian, A., Cochran, J. R., Bell, R. E., Manizade, S. S., and Sonntag, J. G.: Bathymetric control of tidewater glacier mass loss in northwest Greenland, Earth and Planetary Science Letters, 401, 40 – 46, https://doi.org/https://doi.org/10.1016/j.epsl.2014.05.058, http://www.sciencedirect.com/science/article/pii/S0012821X14003744, 2014.

Rastner, P., Bolch, T., Mölg, N., Machguth, H., Le Bris, R., and Paul, F.: The first complete inventory of the local glaciers and ice caps on Greenland, The Cryosphere, 6, 1483–1495, https://doi.org/10.5194/tc-6-1483-2012, https://www.the-cryosphere.net/6/1483/2012/, 2012.

Ribergaard, M. ~~H.~~: Oceanographic Investigations off West Greenland 2013, NAFO Scientific Council Documents, ~~14/001,~~ 2014.

Rignot, E. and Kanagaratnam, P.: Changes in the velocity structure of the Greenland Ice Sheet, Science, 311, 986–990, 2006.

Rignot, E. and Mouginot, J.: Ice flow in Greenland for the International Polar Year 2008-2009, Geophysical Research Letters, 39, 2012.

Rignot, E., Fenty, I., Xu, Y., Cai, C., Velicogna, I., Cofaigh, C. ., Dowdeswell, J. A., Weinrebe, W., Catania, G., and Duncan, D.: Bathymetry data reveal glaciers vulnerable to ice-ocean interaction in Uummannaq and Vaigat glacial fjords, west Greenland, Geophysical Research Letters, 43, 2667–2674, https://doi.org/10.1002/2016GL067832, http://dx.doi.org/10.1002/2016GL067832, 2016GL067832, 2016a.

Rignot, E., Xu, Y., Menemenlis, D., Mouginot, J., Scheuchl, B., Li, X., Morlighem, M., Seroussi, H., den Broeke, M. v., Fenty, I., Cai, C., An, L., and Fleurian, B. d.: Modeling of ocean-induced ice melt rates of five west Greenland glaciers over the past two decades, Geophysical Research Letters, 43, 6374–6382, https://doi.org/10.1002/2016GL068784, https://agupubs.onlinelibrary.wiley.com/doi/abs/10.1002/2016GL068784, 2016b.

Schaffer, J., von Appen, W.-J., Dodd, P. A., Hofstede, C., Mayer, C., de Steur, L., and Kanzow, T.: Warm water pathways toward Nioghalvfjerdsfjorden Glacier, Northeast Greenland, Journal of Geophysical Research: Oceans, 122, 4004–4020, https://doi.org/10.1002/2016JC012462, https://agupubs.onlinelibrary.wiley.com/doi/abs/10.1002/2016JC012462, 2017.

Seroussi, H., Morlighem, M., Rignot, E., Larour, E., Aubry, D., Ben Dhia, H., and Kristensen, S. S.: Ice flux divergence anomalies on 79north Glacier, Greenland, Geophysical Research Letters, 38, https://doi.org/10.1029/2011GL047338, http://dx.doi.org/10.1029/2011GL047338, l09501, 2011.

Slabon, P., Dorschel, B., Jokat, W., Myklebust, R., Hebbeln, D., and Gebhardt, C.: Greenland ice sheet retreat history in the northeast Baffin Bay based on high-resolution bathymetry, Quaternary Science Reviews, 154, 182 – 198, https://doi.org/http://dx.doi.org/10.1016/j.quascirev.2016.10.022, http://www.sciencedirect.com/science/article/pii/S0277379116304930, 2016.

Smith, G. C., Roy, F., Mann, P., Dupont, F., Brasnett, B., Lemieux, J.-F., Laroche, S., and Bélair, S.: A new atmospheric dataset for forcing ice-ocean models: Evaluation of reforecasts using the Canadian global deterministic prediction system, Quarterly Journal of the Royal Meteorological Society, 140, 881–894, 2014.

Smith, W. H. F. and Sandwell, D. T.: Global seafloor topography from satellite altimetry and ship depth soundings, Science, 277, 1957–1962, 1997.

Straneo, F.: Heat and freshwater transport through the central Labrador Sea, Journal of Physical Oceanography, 36, 606–628, 2006.

Straneo, F. and Heimbach, P.: North Atlantic warming and the retreat of Greenland's outlet glaciers, Nature, 504, 36–43, 2013.

Straneo, F., Hamilton, G., Sutherland, D., Stearns, L. A., Davidson, F., Hammill, M., Stenson, G. B., and A., R.: Rapid circulation of warm subtropical waters in a major glacial fjord in East Greenland, Nature Geosci, 3, 182–186),, 2010.

Straneo, F., Sutherland, D. A., Holland, D., Gladish, C., Hamilton, G. S., Johnson, H. L., Rignot, E., Xu, Y., and Koppes, M.: Characteristics of ocean waters reaching Greenland's glaciers, Annals of Glaciology, 53, 202–210, 2012.

Sutherland, D. A., Straneo, F., and Pickart, R. S.: Characteristics and dynamics of two major Greenland glacial fjords, Journal of Geophysical Research: Oceans, 119, 3767–3791, 2014.

Swingedouw, D., Rodehacke, C. B., Olsen, S. M., Menary, M., Gao, Y., Mikolajewicz, U., and Mignot, J.: On the reduced sensitivity of the Atlantic overturning to Greenland Ice Sheet melting in projections: a multi-model assessment, Climate Dynamics, 2014.

van den Broeke, M. R., Enderlin, E. M., Howat, I. M., Kuipers Munneke, P., Noël, B. P. Y., van de Berg, W. J., van Meijgaard, E., and Wouters, B.: On the recent contribution of the Greenland Ice Sheet to sea level change, The Cryosphere, 10, 1933–1946, https://doi.org/10.5194/tc-10-1933-2016, https://www.the-cryosphere.net/10/1933/2016/, 2016.

Weijer, W., Maltrud, M. E., Hecht, M. W., Dijkstra, H. A., and Kliphuis, M. A.: Response of the Atlantic Ocean circulation to Greenland Ice Sheet melting in a strongly-eddying ocean model, Geophysical Research Letters, 39, 2012.

Williams, C. N., Cornford, S. L., Jordan, T. M., Dowdeswell, J. A., Siegert, M. J., Clark, C. D., Swift, D. A., Sole, A., Fenty, I., and Bamber, J. L.: Generating synthetic fjord bathymetry for coastal Greenland, The Cryosphere, 11, 363–380, https://doi.org/10.5194/tc-11-363-2017, https://www.the-cryosphere.net/11/363/2017/, 2017.

Wilson, N. J. and Straneo, F.: Water exchange between the continental shelf and the cavity beneath Nioghalvfjerdsbrae (79 North Glacier), Geophysical Research Letters, 42, 7648–7654, https://doi.org/10.1002/2015GL064944, 2015.

Wood, M., Rignot, E., Fenty, I., Menemenlis, D., Millan, R., Morlighem, M., Mouginot, J., and Seroussi, H.: Ocean-Induced Melt Triggers Glacier Retreat in Northwest Greenland, Geophysical Research Letters, 45, 8334–8342, https://doi.org/10.1029/2018GL078024, https://agupubs.onlinelibrary.wiley.com/doi/abs/10.1029/2018GL078024, 2018.

Zurbenko, I., Porter, P. S., Gui, R., Rao, S. T., Ku, J. Y., and Eskridge, R. E.: Detecting Discontinuities in Time Series of Upper-Air Data: Development and Demonstration of an Adaptive Filter Technique, Journal of Climate, 9, 3548–3560, https://doi.org/10.1175/1520-0442(1996)009<3548:DDITSO>2.0.CO;2, https://doi.org/10.1175/1520-0442(1996)009<3548:DDITSO>2.0.CO;2, 1996.

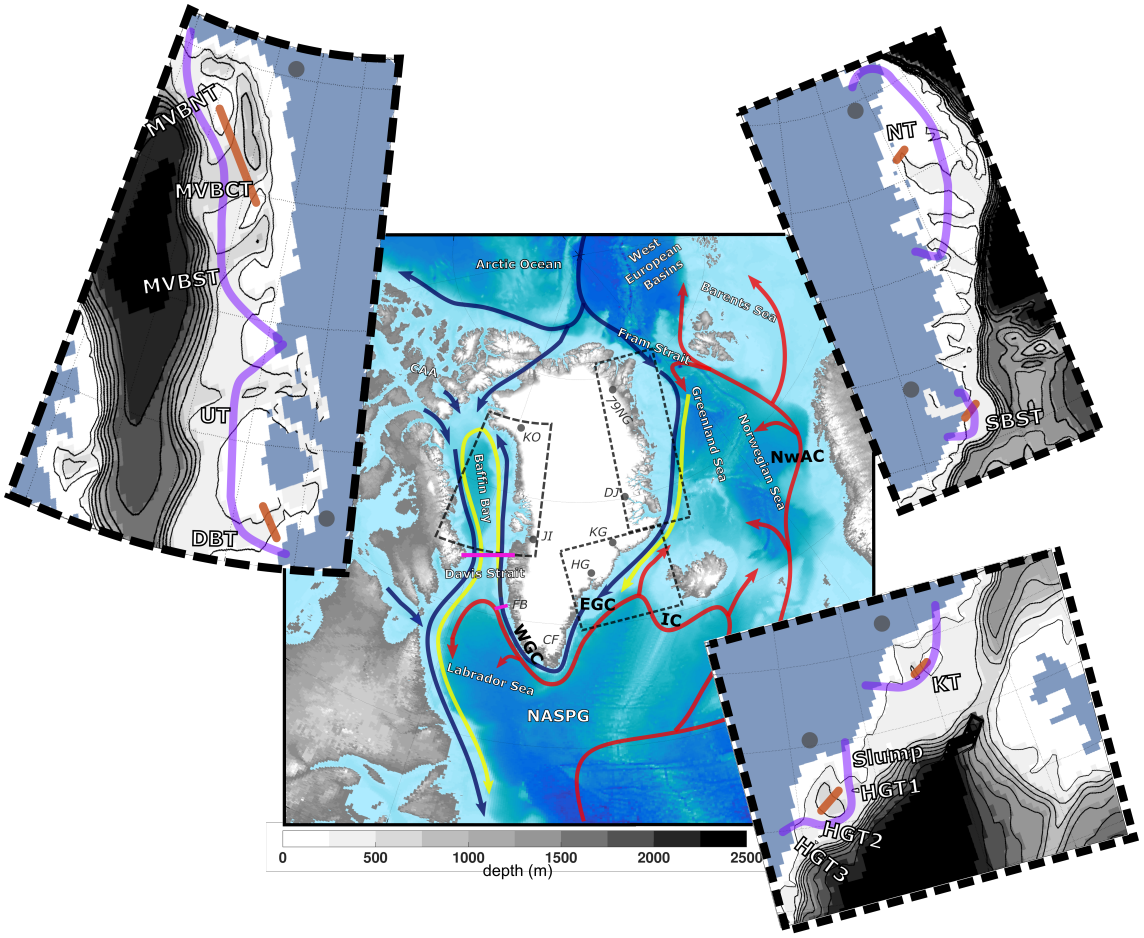

Figure 1. Ocean circulation around Greenland ~~,~~ with relatively warm Atlantic waters are ~~seen~~ shown in red, modified Atlantic waters in yellow and the Arctic and freshwater pathways in blue lines. The large map shows areas that will be discussed throughout this study such as the North Atlantic Subpolar Gyre (NASPG), Labrador Sea, Davis Strait (section drawn in magenta), Baffin Bay, Canadian Arctic Archipelago (CAA), Arctic Ocean, West European Basins, Norwegian Sea, Greenland Sea, Fram Strait, Cape Farwell (CF), and Fylla Bank (FB) (section drawn in magenta). Ocean currents (adapted from Straneo et al. (2012); Hu and Myers (2013)) that will be discussed are shown here, Irminger Current (IC), Norwegian Atlantic Current (NwAC), East Greenland Current (EGC), and West Greenland Current (WGC). The light grey circles show the locations of six ~~marine terminating~~ marine-terminating glaciers. Kong Oscar (KO) that terminates into Melville Bay (MVB), Jakobshavn Isbrae (JI) that terminates into Disko Bay (DB), Helheim Glacier (HG), Kangerlussuaq Glacier (KG), Daugaard-Jensen Glacier that terminates into Scoresby Sund (SBS) and Nioghalvfjerdsbrae (79NG). The insets show a closer view of ~~this studies~~ specific regions around Greenland. Starting from the top left, the west, south-east, and north-east coast. The insets show the model coastline, model bathymetry in metres (in grey shading and black contours), six sections of our analysis along the shelf in light purple, and sections of troughs (tan lines).

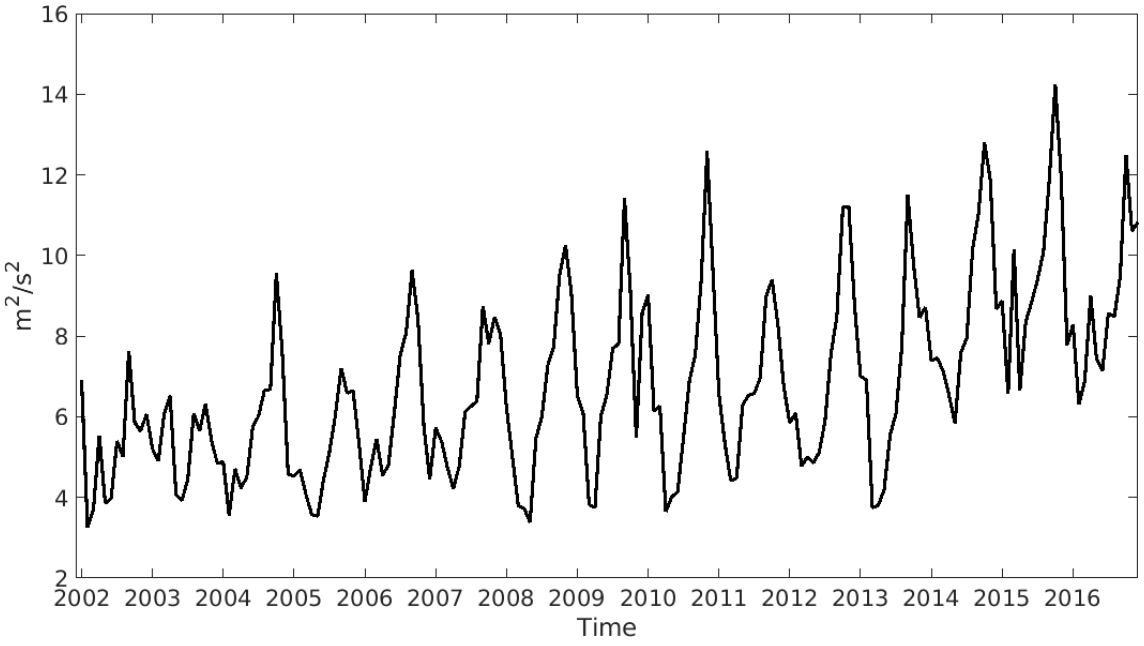

LowResControl (a)

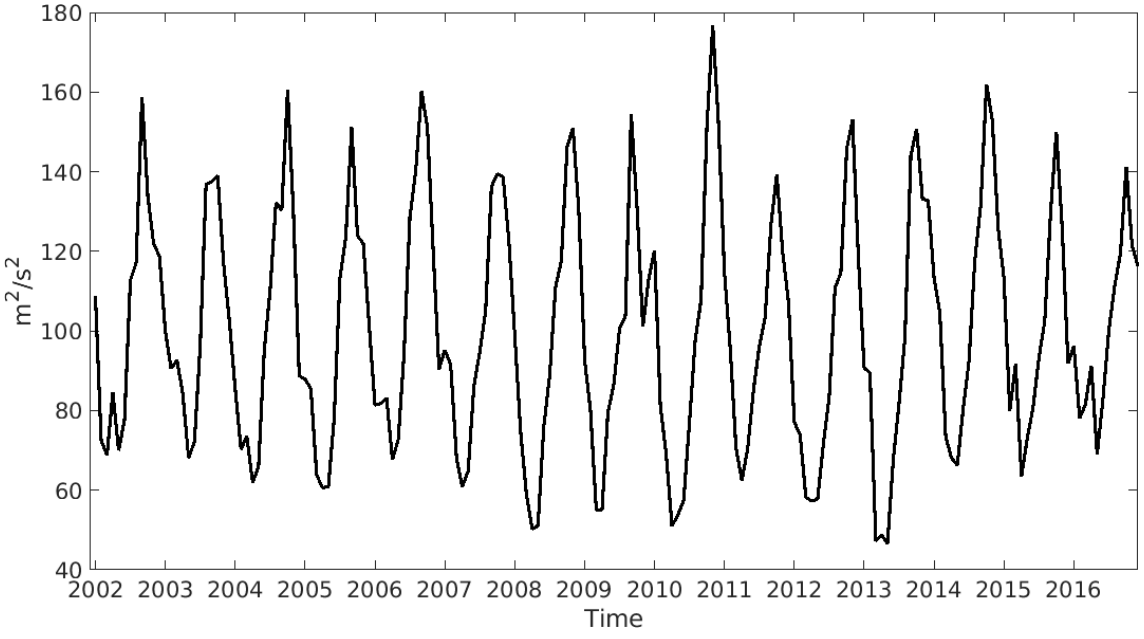

HighRes (b)

Figure 2. Monthly summation of total kinetic energy in Baffin Bay for two ~~configurations~~experiments, LowResControl and HighRes.

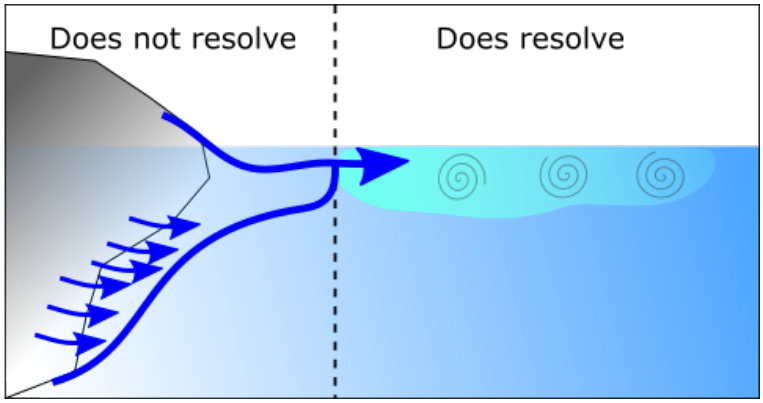

Figure 3. The schematic shows how the model injects meltwater. The left side of the figure shows what the model cannot resolve. This includes a glacier, small scale melting from the glacier, and the plume dynamics that ~~occurs~~ occur along the face of the glacier. ~~Our~~ Instead, the model resolves ~~larger scale~~ larger-scale processes that occur along the coastline, and therefore, injects the meltwater from the GrIS at the first ocean model layer at the surface, ~~and~~ which then is mixed ~~to~~ over a thickness of 10 m.

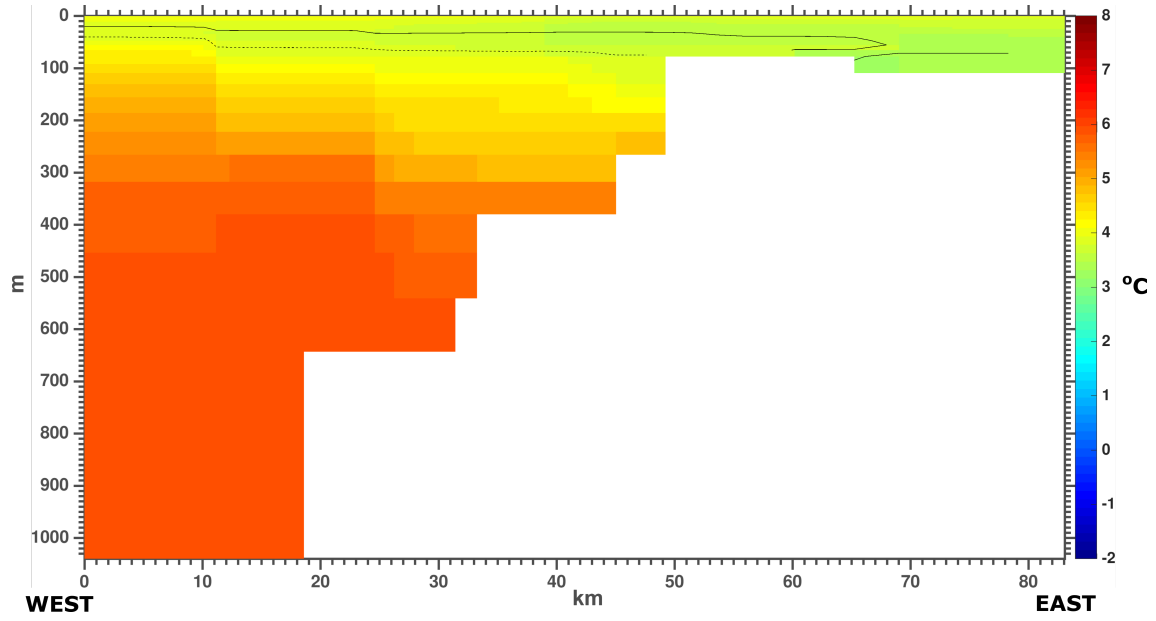

(a) LowResControl

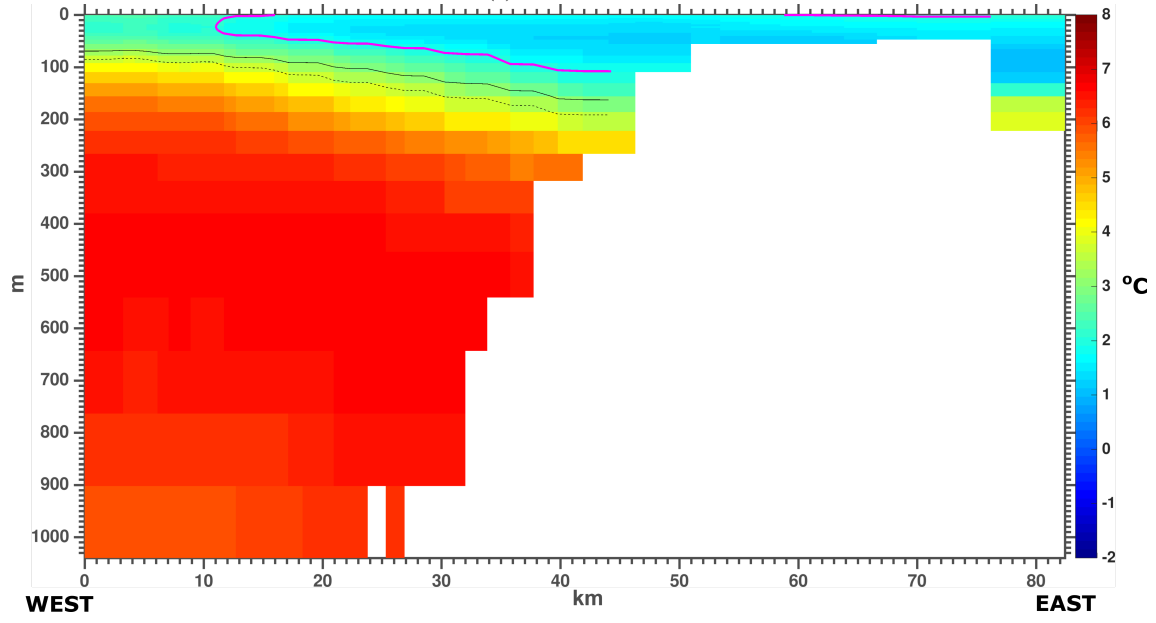

(b) HighRes

Figure 4. Average Fylla Bank temperature ~~average~~ for June 2013 for (a) LowResControl and (b) HighRes. ~~Magenta~~ The magenta line shows ~~temperature of~~ the $2^{\circ}C$ isotherm, the black line ~~indicates a contour of Salinity of 34~~is the 34.0 salinity isohaline, and the blacked dashed line ~~indicates a contour of salinity of~~ is the 34.2 salinity isohaline.

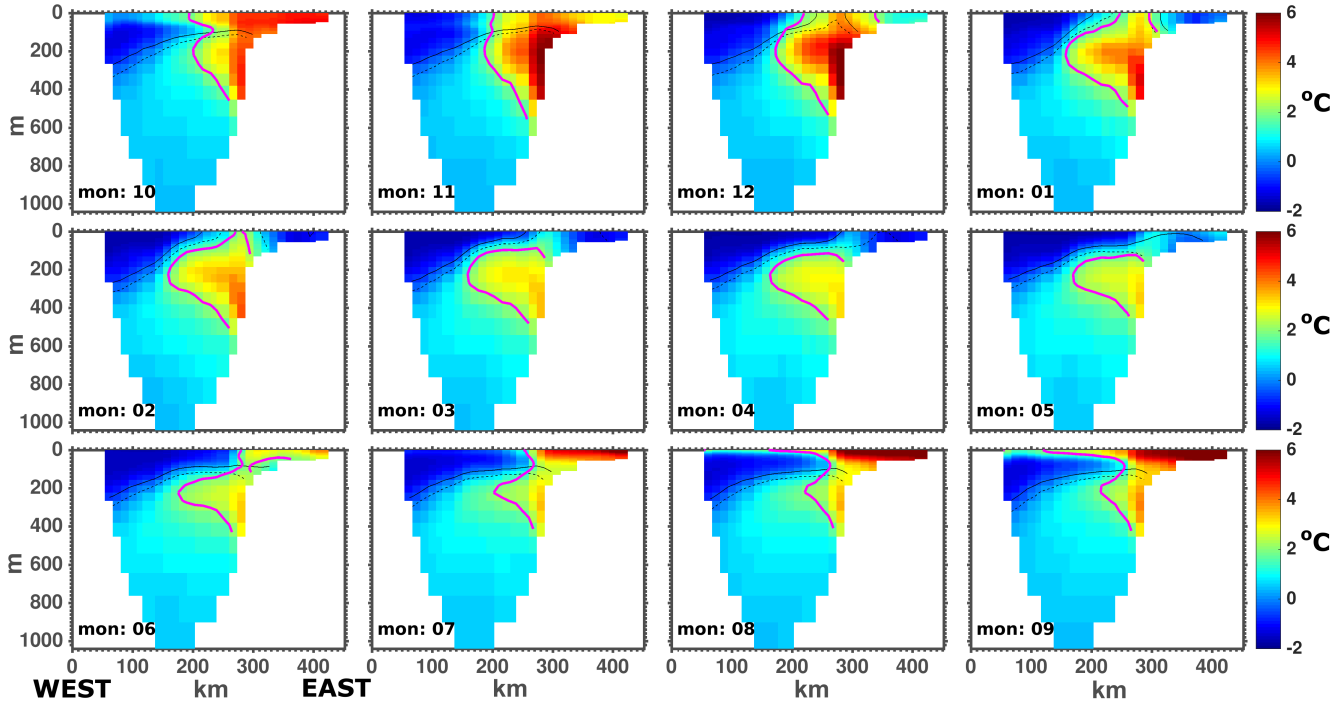

Figure 5. ~~LowResControl~~ The monthly average temperature ~~of Davis Strait~~ through the period of 2004 to 2010 at Davis Strait from LowResControl. ~~Magenta shows temperature of~~ The magenta line represents the $2^{\circ}C$ isotherm, the black line ~~indicates a contour of Salinity of 34~~is the 34.0 salinity isohaline, and the blacked dashed line ~~indicates a contour of salinity of~~ is the 34.2 salinity isohaline.

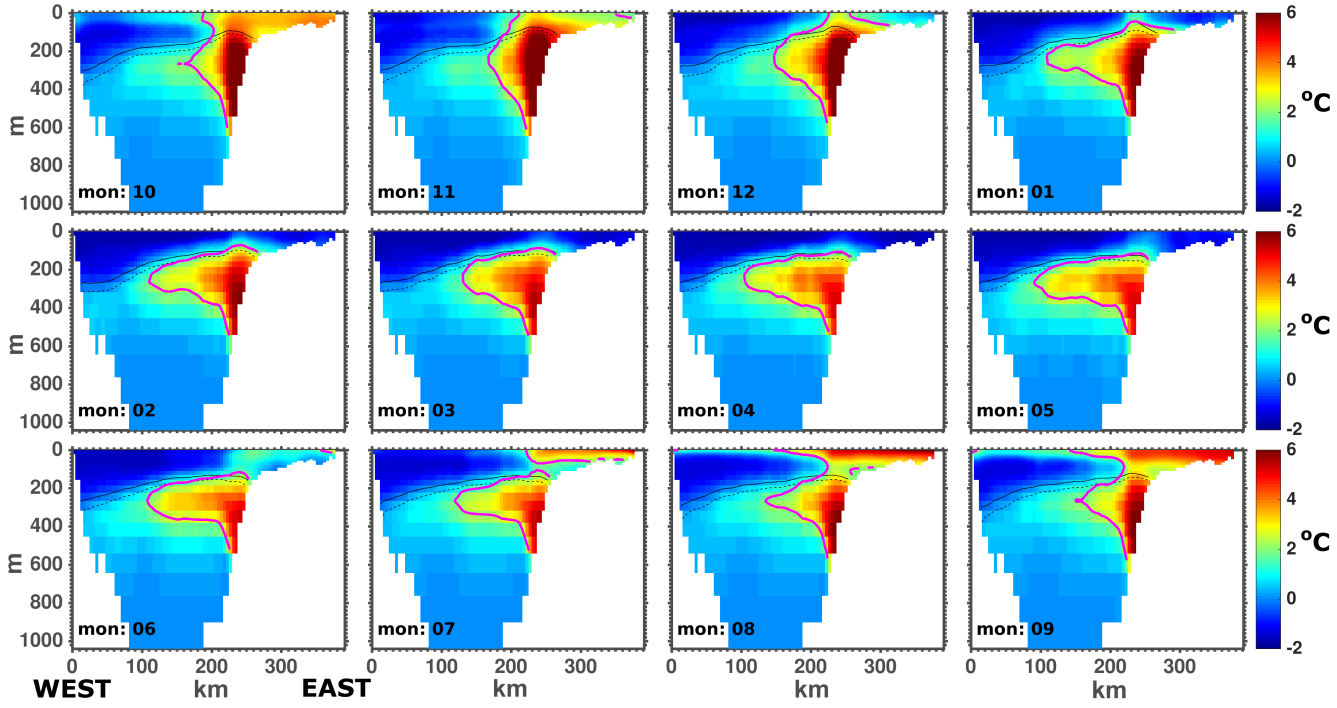

Figure 6. ~~HighRes~~ The monthly average temperature ~~of Davis Strait~~ through the period of 2004 to 2010 at Davis Strait from HighRes. ~~Magenta shows temperature of~~ The magenta line represents the $2\,^{\circ}C$ isotherm, the black line ~~indicates a contour of Salinity of 34~~is the 34.0 salinity isohaline, and the blacked dashed line ~~indicates a contour of salinity of~~ is the 34.2 salinity isohaline.

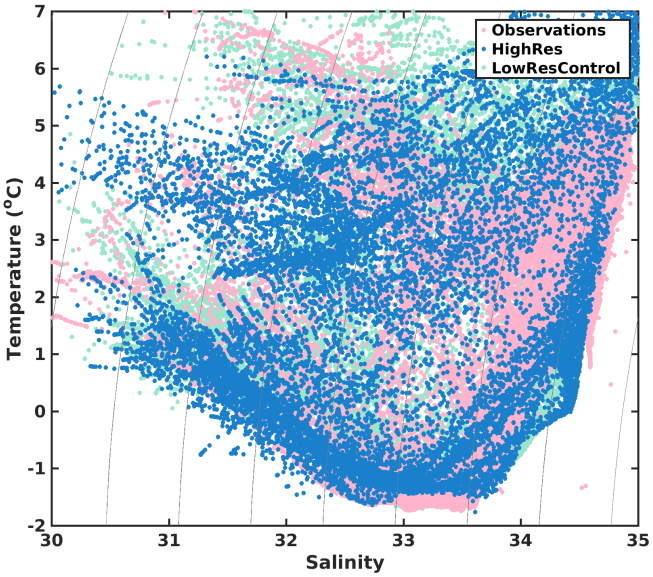

Figure 7. Temperature and salinity plot for the region around the Davis Strait sill ($\sim 30\text{km}$). Observations contain data collected by the Davis Strait program's fall mooring cruises. Observations are taken in fall months, late August to October, for years 2004 to 2010. Model fields are plotted the same for HighRes and LowRes Control (mid-September and mid-October fields, within $\sim 30\text{km}$ of the Davis Strait sill, from 2004 to 2010). Model fields are subsampled to a 1/2 degree grid to reduce the number of points plotted. Points with a salinity of less than 30 or more than 35, or warmer than $7^{\circ}C$ are excluded. Contour lines are density in kg/m^3.

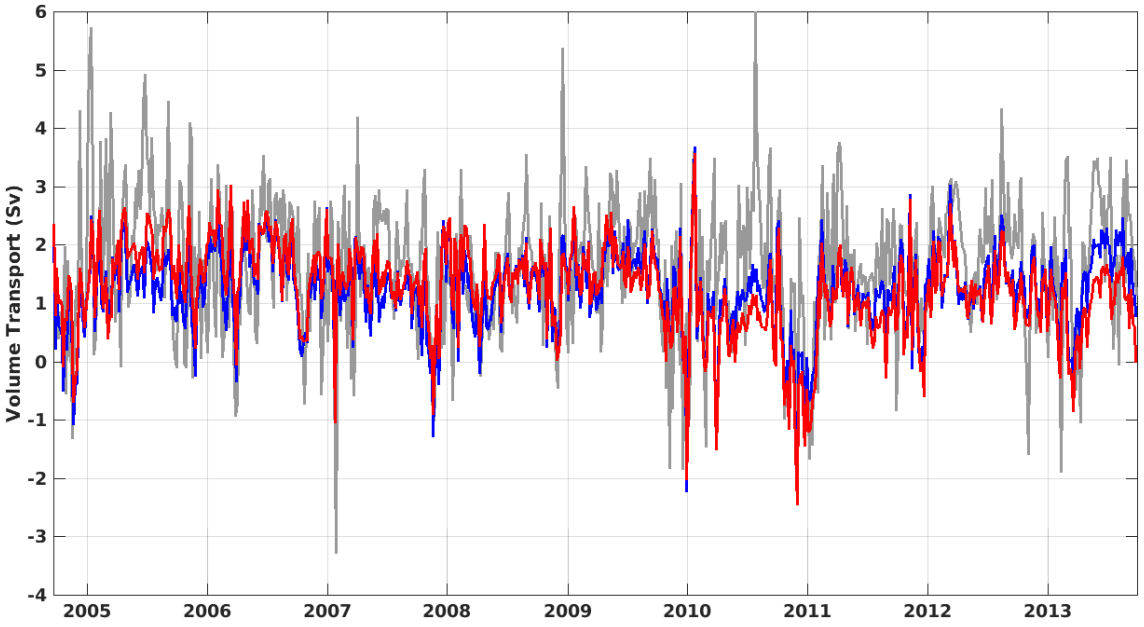

Figure 8. Volume flux through Davis Strait with HighRes (in red), LowResControl (in blue), and Davis Strait observations replotted from the mooring record discussed in Curry et al. (2014) (in grey). Positive values indicate southward volume fluxes through Davis Strait and negative values indicate the waters move northward. All fields, model and observation, are plotted as 5-day averages.

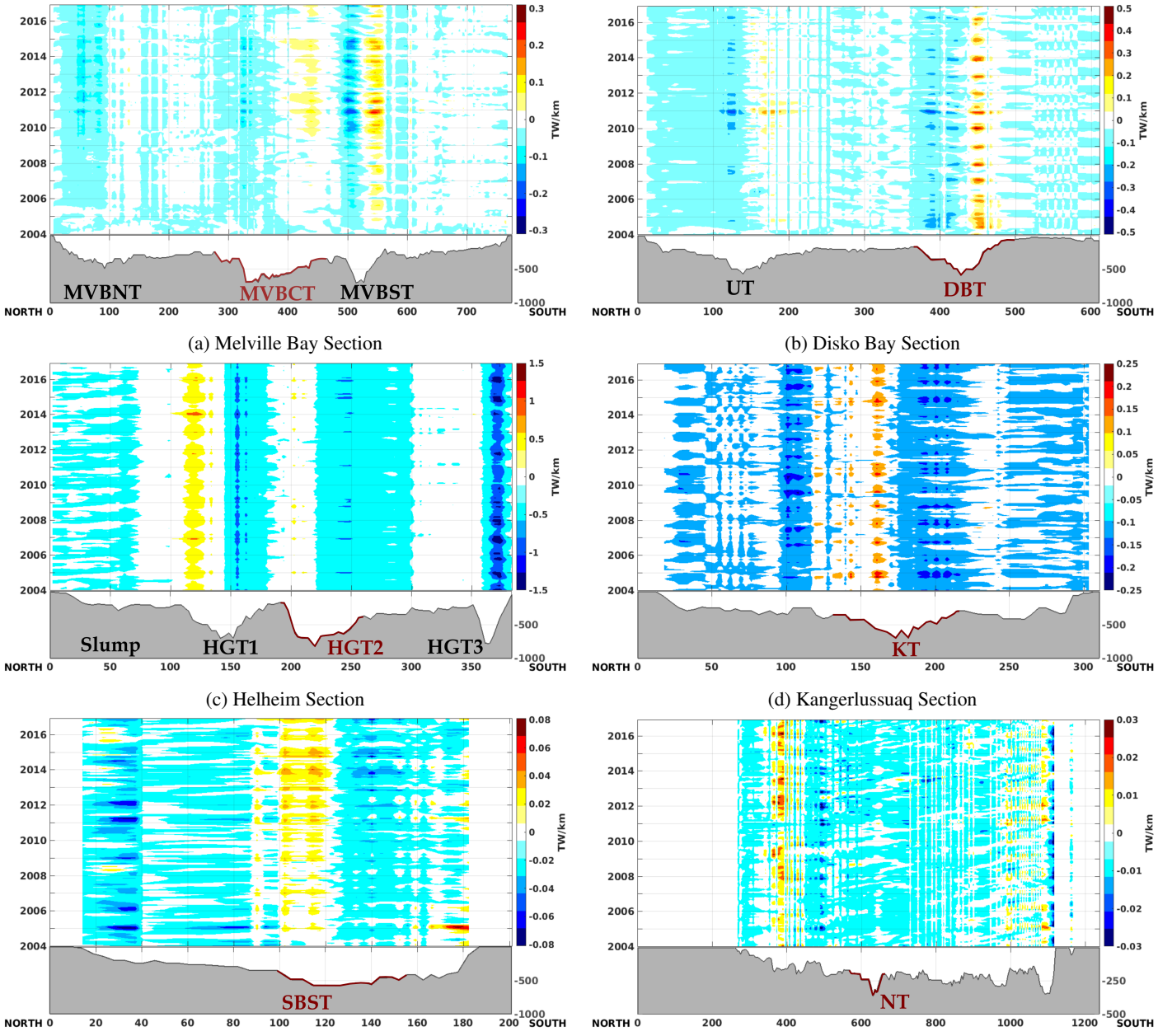

(a) Melville Bay Section

(b) Disko Bay Section

(c) Helheim Section

(d) Kangerlussuaq Section

(e) Scoresby Sund Section

(f) 79NG Section

Figure 9. This figure shows the entire ocean heat exchange (total flux) with respect to topography (in grey) within the time series of 2004 to the end of 2016 with the HighRes model output. These hovmoller plots show the monthly average heat flux coming on or off the shelf in ~~TW~~TW km^{-1}, (into or out of the page respectively), through a section (sections drawn in light purple on the map inset Fig. 1). Model bathymetry is in grey and the section runs north to south on the x-axis starting at the ~~left hand~~ left-hand side of the figure indicated by the zero kilometre marker. Along the y-axis is the depth for the bathymetry and then time for the 2004 to 2016 period. Colours indicate direction and magnitude of the ~~on~~ onshore or ~~off shelf~~ offshore heat flux. Positive numbers indicate the direction of onshore (into the page) and negative numbers indicate the direction of the heat flux offshore (out of the page)~~and colourbar~~. Colourbar limits change per location. In each section shows a highlighted trough, in dark red, which is selected for Fig. 10 and Fig. 11. Figure 1 indicates the exact location of the trough in the tan lines.

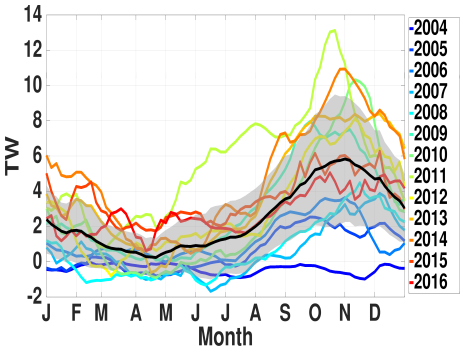

(a) Melville Bay Central Trough Heat Flux

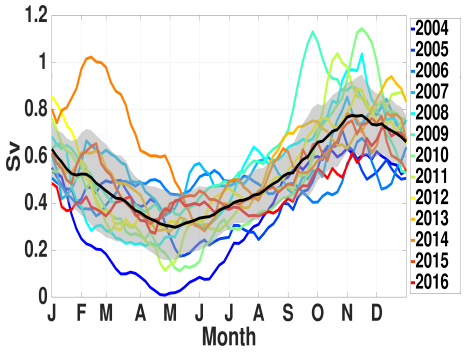

(b) Volume Flux

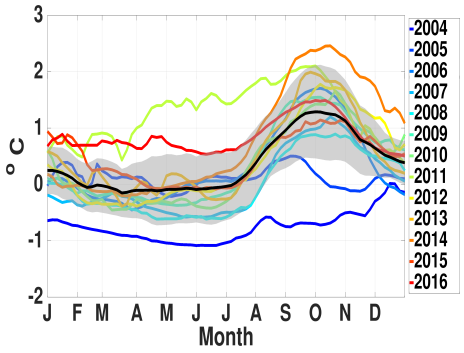

(c) Average Temperature

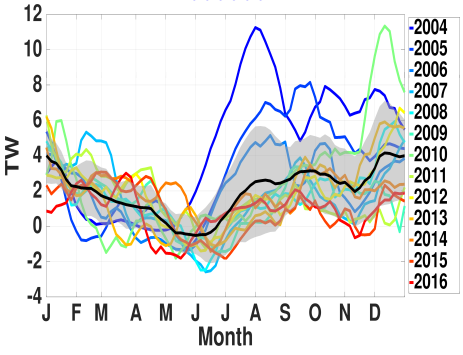

(d) Disko Bay Trough Heat Flux

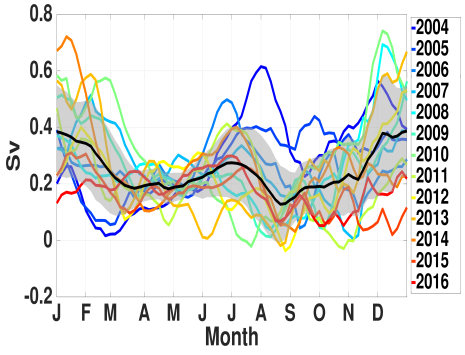

(e) Volume Flux

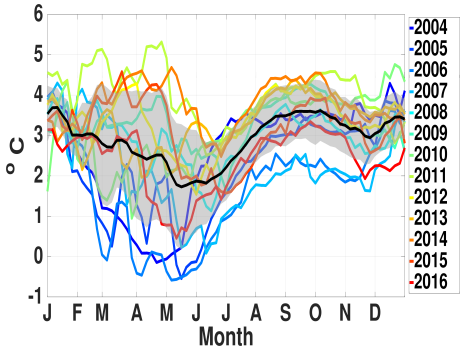

(f) Average Temperature

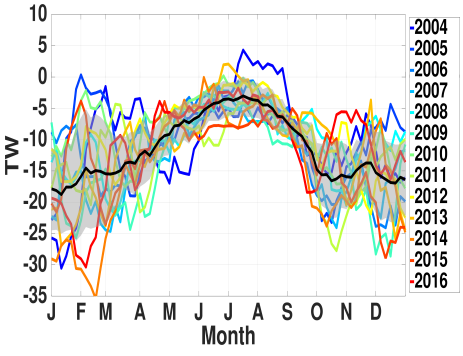

(g) Helheim ~~Trough~~ Glacier Trough 2 Heat Flux

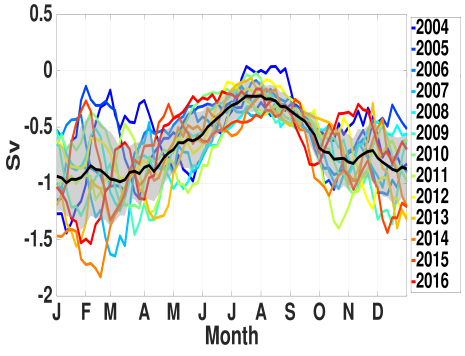

(h) Volume Flux

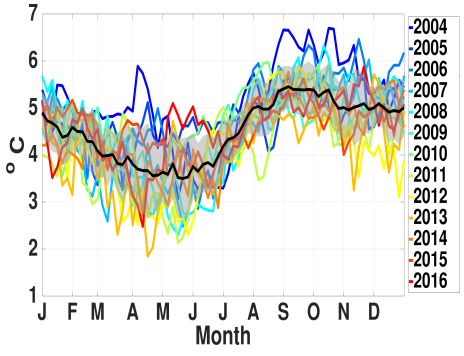

(i) Average Temperature

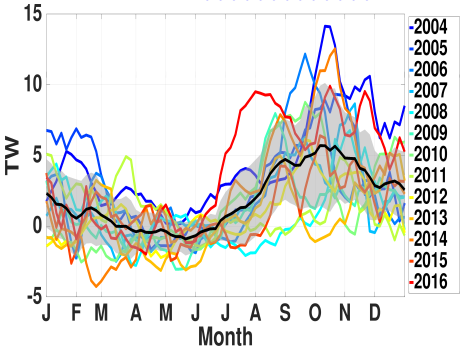

(j) Kangerdlussuaq Trough Heat Flux

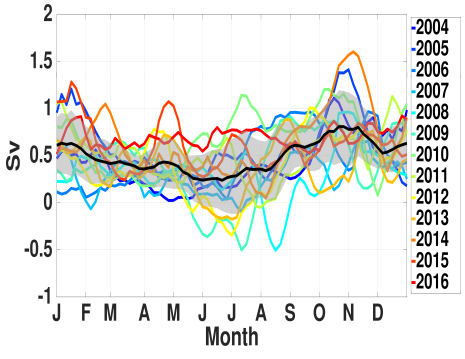

(k) Volume Flux

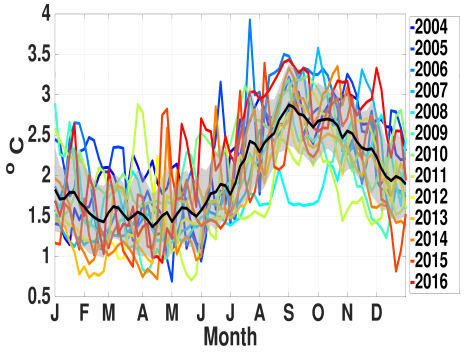

(l) Average Temperature

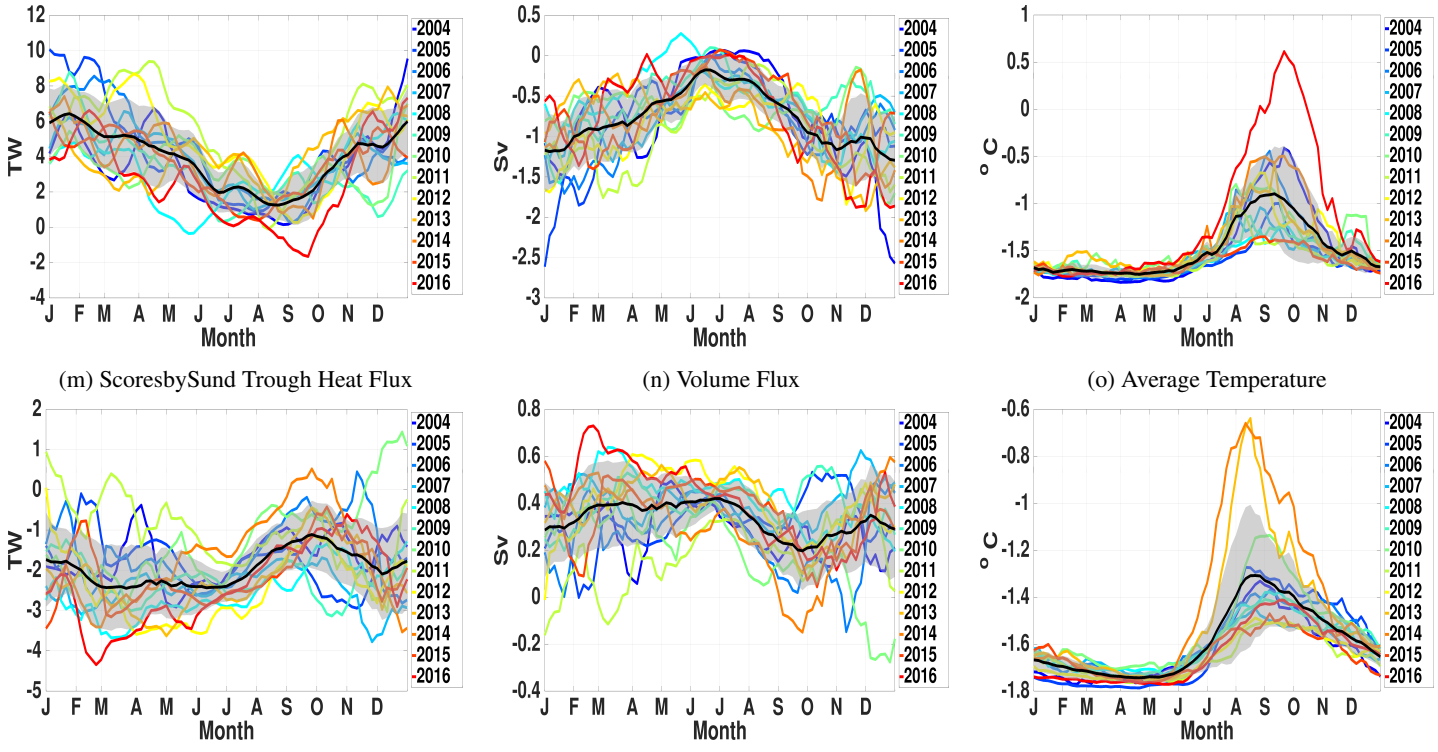

(m) ScoresbySund Trough Heat Flux (n) Volume Flux (o) Average Temperature

(p) Norkse Trough Heat Flux (q) Volume Flux (r) Average Temperature

Figure 10. ~~This figure shows the evolution and seasonality~~ Seasonality of the ~~volume and~~ heat flux (unit: TW, ~~averaged over the entire depth~~1 TW$= 10^{12}$ W), ~~through each trough~~ volume flux (unit: Sv, 1 Sv$= 10^6 m^3 s^{-1}$) and ~~average~~ section-averaged temperature ~~across the section of the trough. The six locations are~~ (unit: $^\circ C$) in MVBCT, DBT, ~~HGT2,~~ KT, SBST ~~,~~ and NT (~~indicated~~ locations shown in Fig. 1) ~~.~~ ~~The months~~ for each year from 2004 to 2016 (colour codes are ~~on~~ shown in the ~~x−axis and~~ legend). Note that the ~~values~~ black line shows the mean of ~~heat flux in , on~~ the ~~y−axis. The~~ 25-day moving ~~25 day average heat flux for 2004 to 2016~~ window averages (~~calculated using~~ (Eq. (2)) ~~is shown in black~~ over 2004 to 2016 with ~~one~~ the standard deviation ~~window in~~ shown by the grey shading. ~~The years are indicated by colour, with earlier years starting in blue to later years in red.~~

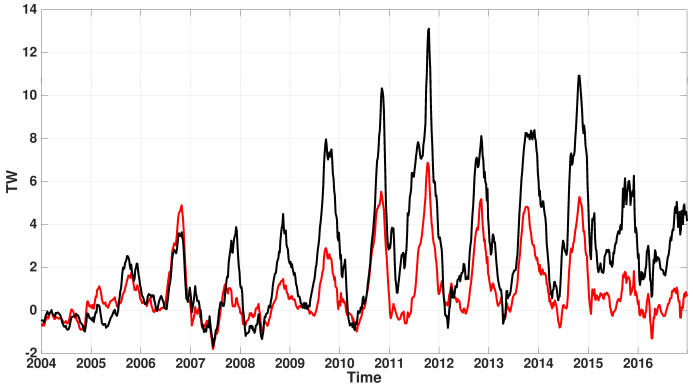

(a) MVBCT Mean

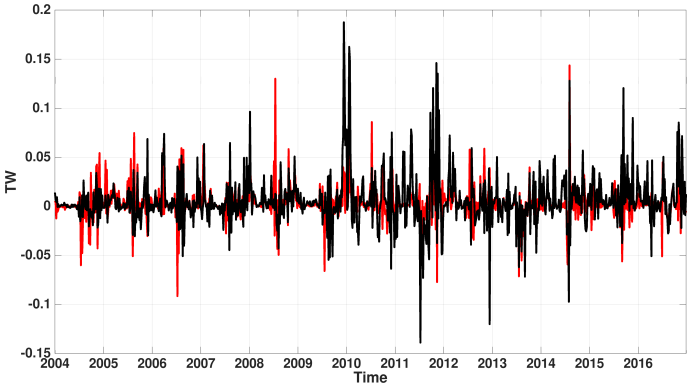

(b) MVBCT Fluctuation

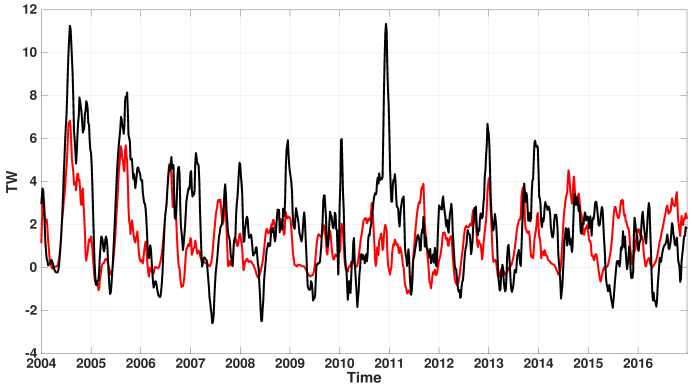

(c) DBT Mean

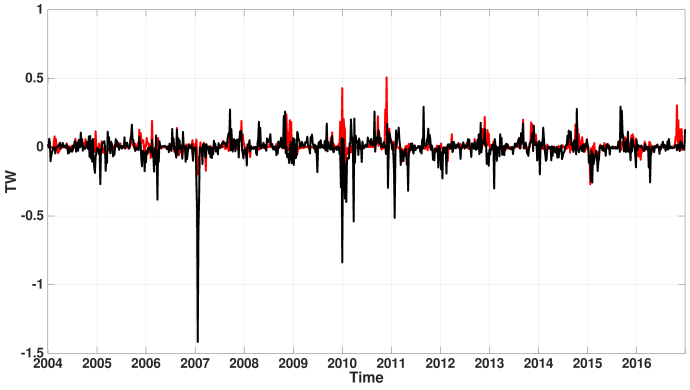

(d) DBT Fluctuation

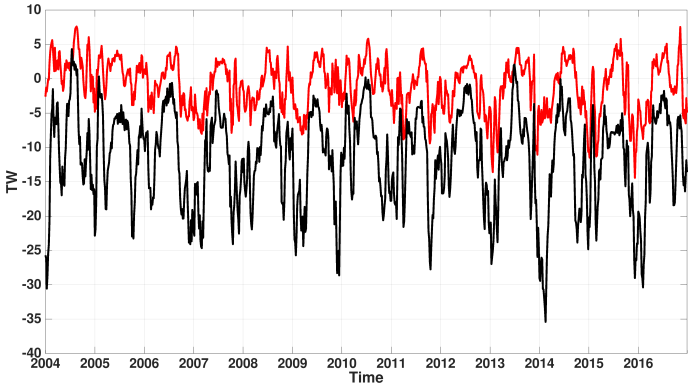

(e) HGT2 Mean

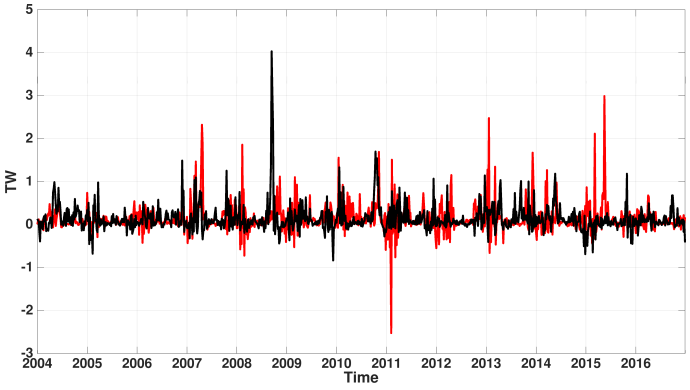

(f) HGT2 Fluctuation

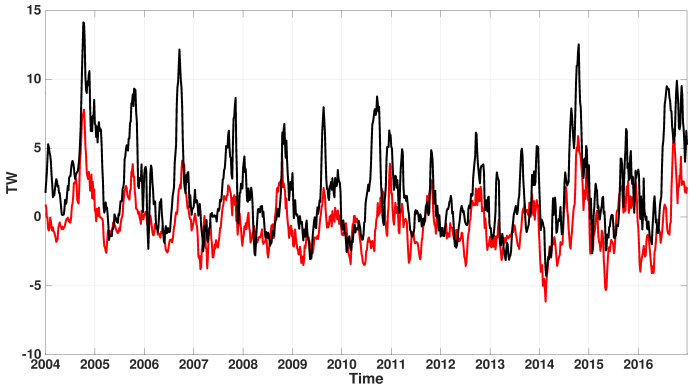

(g) KT Mean

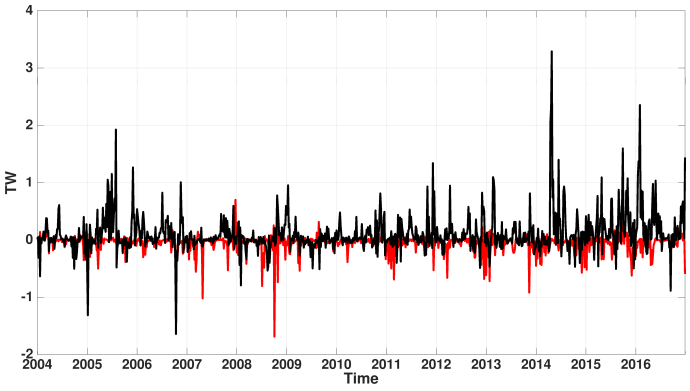

(h) KT Fluctuation

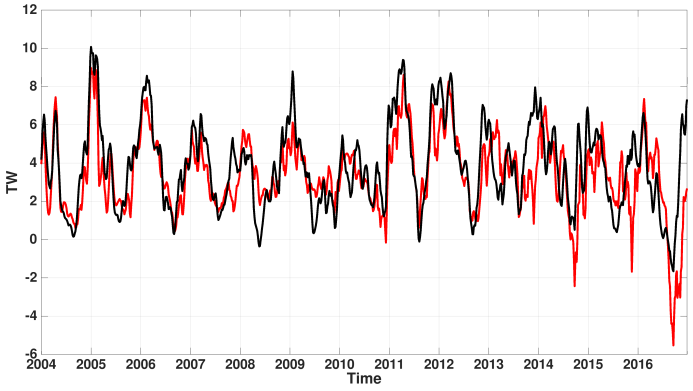

(i) SBST Mean

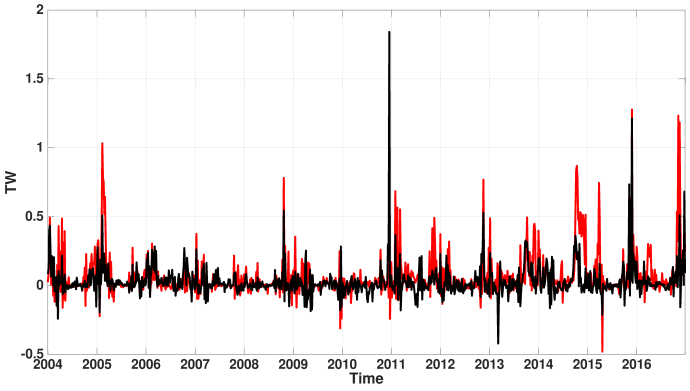

(j) SBST Fluctuation

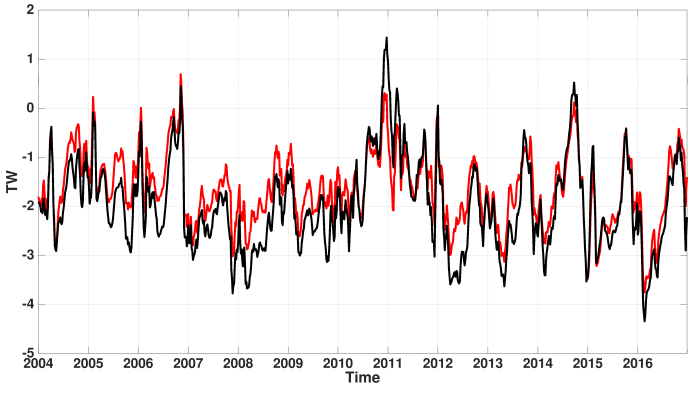

(k) NT Mean

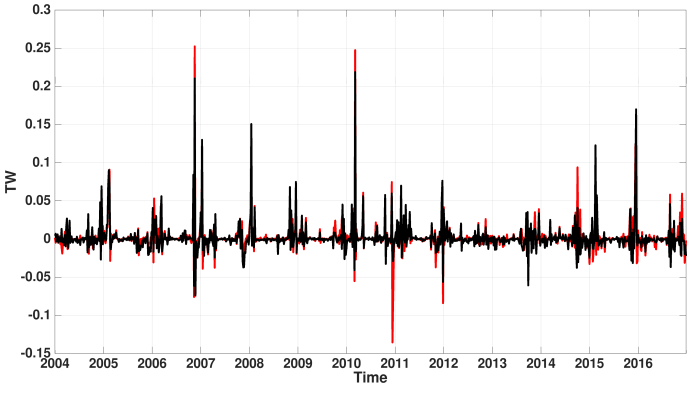

(l) NT Fluctuation

~~(m) NToff Mean (n) NToff Fluctuation~~

Figure 11. ~~This series~~ Mean (left column) and fluctuating (right column) components of ~~plots shows~~ the heat flux ~~comparison of two configurations,~~ (TW) from LowResControl (in red) and HighRes (in black). ~~Mean flow on the left column and fluctuation of the flow on the right column.~~ Plotted for the whole time series 2004 to 2016. Each row is for a different trough.

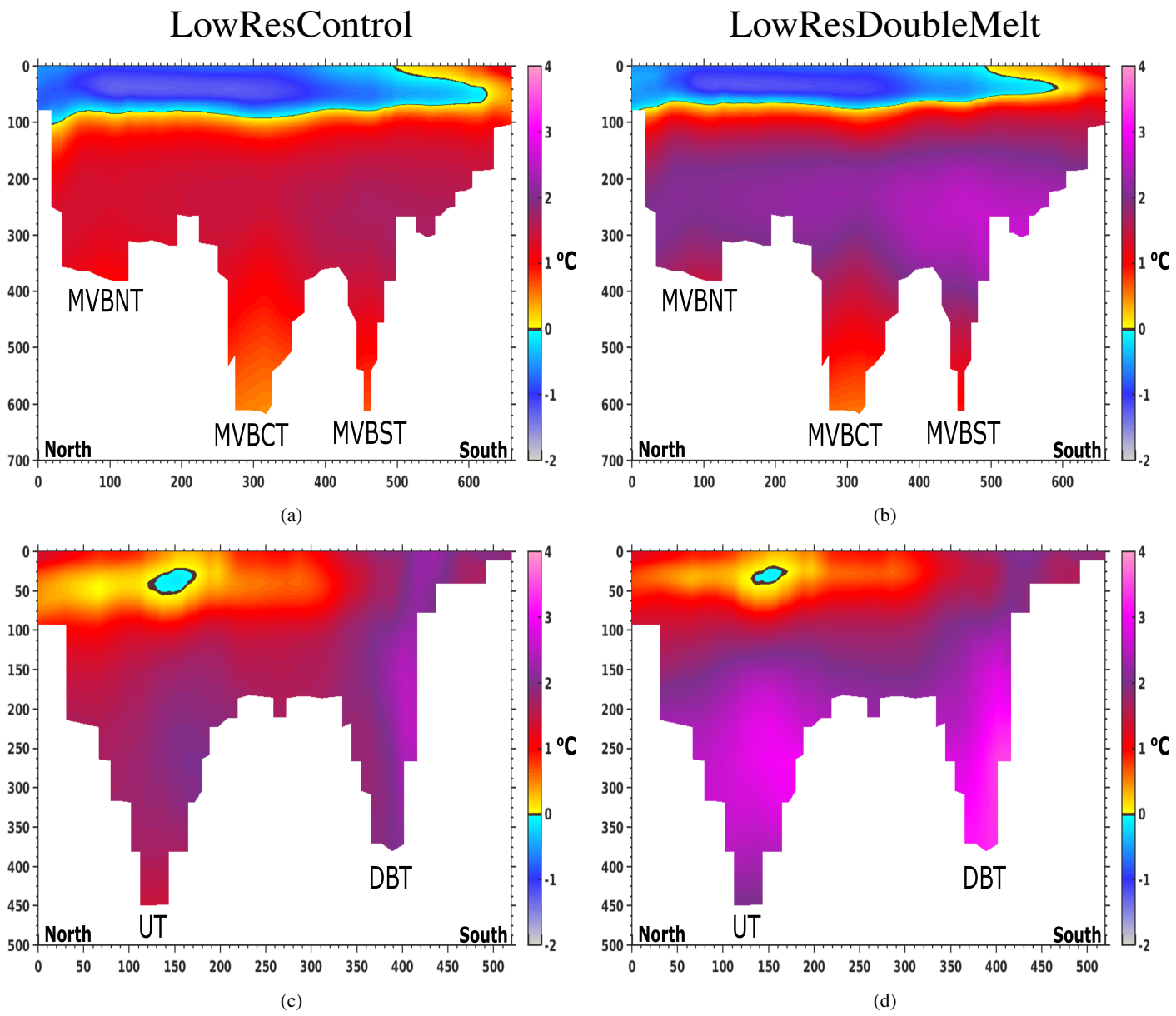

Figure 12. ~~These figures show the temperature~~ Temperature along two sections in the north-west of Greenland, Melville Bay Section and Disko Bay Section~~, for~~ . For location of the sections~~were drawn~~, see Fig. 1. ~~This shows~~ Shown is the average temperature ~~from~~ over the period of 2004 to 2016, with the model bathymetry in white (m) and the colours ~~indicate~~ indicating the temperature of the water in $^{\circ}C$. ~~Left~~ The left column shows the results for LowResControl, and the right column shows the results for LowResDoubleMelt. ~~First~~ The first row shows the section Melville Bay and the second row shows the section for Disko Bay.

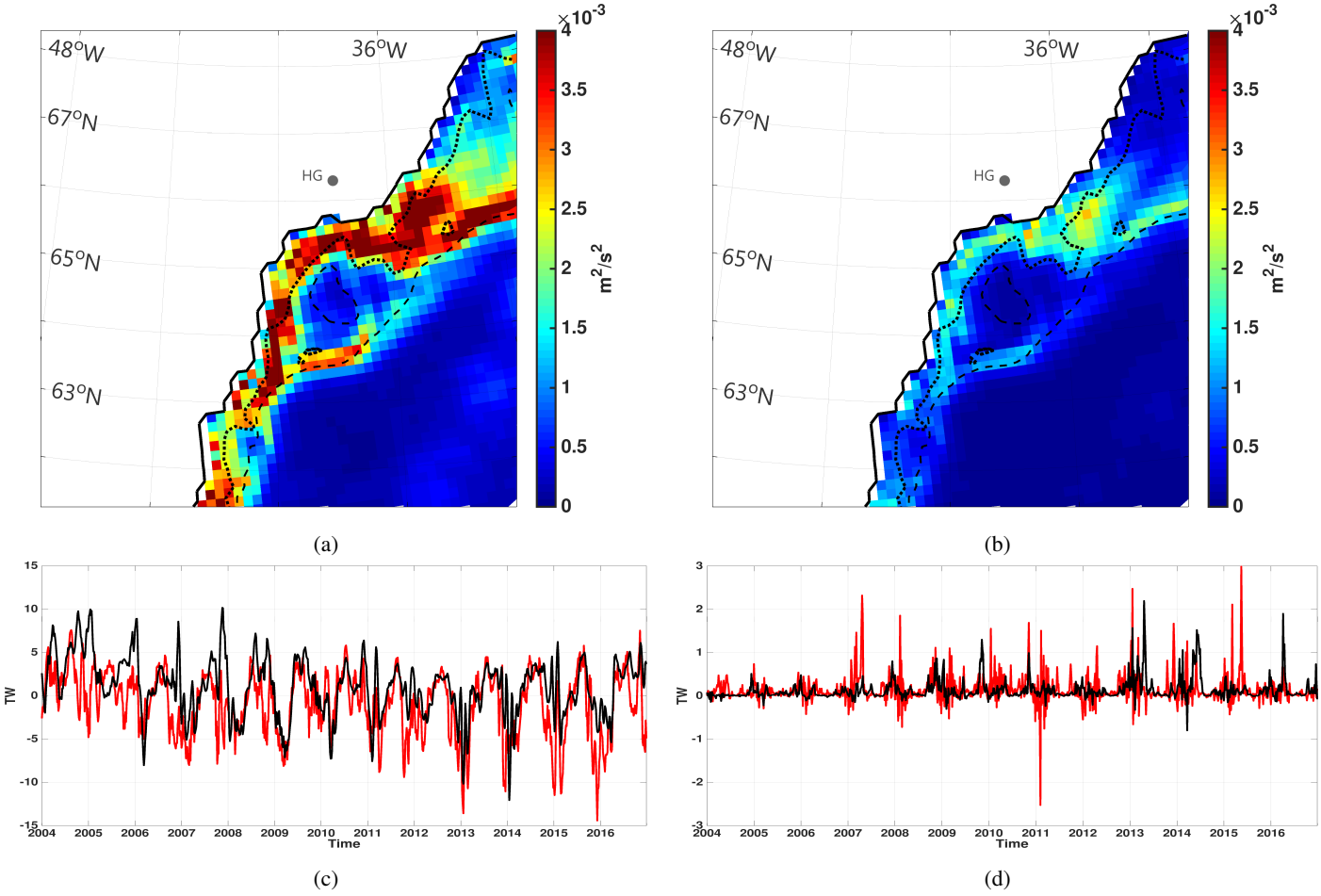

Figure 13. ~~This figure shows how~~ Comparison of filtering the atmospheric forcing in LowResNoStorms~~, affects the turbluent areas~~. (a) and (b) shows the ~~Eddy~~ Transient Kinetic Energy (TKE) integrated over the entire depth at the south-east region of Greenland for LowResControl (a) and LowResNoStorms (b). The ~~EKE~~ TKE here is the average ~~EKE~~ TKE for the period of 2004 to 2016. The thick dashed lines mark the bathymetry at 250 m and the thin dashed line marks the 500 m depth. (c) shows the mean heat flux and (d) shows the fluctuation component of heat flux through Helheim Glacier Trough 2 (~~HT~~HGT2) (location identified in Fig. 1). The LowResNoStorms configuration in black solid lines, LowResControl configuration in red solid lines.

Simulation	Resolution	Runoff	Atmospheric forcing
LowResControl	$1/4^o$	50 % Greenland FWF	CGRF
HighRes	**$1/12^o$**	50 % Greenland FWF	CGRF
LowResDoubleMelt	$1/4^o$	**100 %** Greenland FWF	CGRF
LowResNoStorms	$1/4^o$	50 % Greenland FWF	CGRF **Filtered** winds and temperature

Table 1. ANHA-NEMO simulations used in this study. All experiments include interannual river discharge from Dai et al. (2009) except for the Greenland region, which is obtained by the Greenland Freshwater Flux (FWF) provided by Bamber et al. (2012). All simulations use the same atmospheric forcing, CGRF (Smith et al., 2014), but with the winds and air temperature filtered in LowResNoStorms.

Davis Strait Water Masses	Temperature Range	Salinity Range
Polar Water	$\theta \leq 1°C$	S $\leq$ 33.7
West Greenland Irminger Water	$\theta > 2°C$	S $>$ 34.1
West Greenland Slope Water	$\theta < 7°C$	S $<$ 34.1
Transitional Water	$\theta \leq 2°C$	S $>$ 33.7

Table 2. Overview of Davis Strait's water masses. Potential temperature (θ) and salinity (S) characteristics are defined by Curry et al. (2011)

.

~~Simulation~~ **Troughs**	~~Resolution~~ **Correlations with Heat Flux** Volume Flux	~~Runoff~~ **Percent of the Heat Flux Moderated by the Fluctuations** $\overline{T}$	~~Atm~~
MVBCT	0.92	0.93	
~~HighRes~~ DBT	~~**1/12^o**~~ 0.43	~~50 % Greenland FWF~~ 0.93	
~~LowResDoubleMelt~~ HGT2	~~1/4^o~~ 0.91	~~**100 %** Greenland FWF~~ -0.25	
~~LowResNoStorms~~ KT	0.83	0.89	
SBST	-0.73	-0.76	
NT	-0.99	0.81	

Table 3. This table shows a comparison for the entire time series (2004 to 2016) of the different troughs along the shelf of the GrIS: Melville Bay Central Trough (MVBCT), Disko Bay Trough (DBT), Helheim Glacier Trough 2 (HGT2), Kangerdlussuaq Trough (KT), Scoresby Sund Trough (SBST), and Norske Trough (NT). These troughs can be identified in Fig. 1. The second and third column shows the correlation between the heat flux with the volume flux and the average temperature (T) across the section (shown in the black line in Fig. 10). The fourth, fifth and sixth columns show the average percent of the heat flux moderated by fluctuations from three configurations, HighRes, LowResControl, LowResNoStorms. Column seven shows the correlation between the total heat flux (mean and fluctuation) from two configurations, HighRes, and LowResControl.

Troughs along the GrIS	Changes in onshore heat (%)
West Coast	
HighRes vs LowResControl	96%
LowResDoubleMelt vs LowResControl	37%
South-east Coast	
HighRes vs LowResControl	4%
LowResDoubleMelt vs LowResControl	-5%
North-east Coast	
HighRes vs LowResControl	9%
LowResDoubleMelt vs LowResControl	9%

Table 4. This table shows the percentage of the difference between the onshore sum of yearly heat fluxes from three experiments, HighRes, LowResControl, LowResDoubleMelt from 2004 to 2016. ~~Troughs along the GrIS include~~ West coast includes Melville Bay Central Trough (MVBCT) ~~,~~and Disko Bay Trough (DBT), south-east coast sector includes Helheim Glacier Trough 2 (HGT2) ~~,~~and Kangerdlussuaq Trough (KT), and north-east coast includes Scoresby Sund Trough (SBST) ~~,~~and Norske Trough (NT)~~and Norske Trough Off (NToff)~~. These troughs can be identified in Fig. 1.

~~This table shows the percentage of the difference of the onshore sum of yearly heat fluxes from three configurations, HighRes, LowResControl, LowResDoubleMelt from 2004 to 2016. West coast includes Melville Bay Central Trough (MVBCT) and Disko Bay Trough (DBT), south-east coast sector includes Helheim Trough (HGT) and Kangerdlussuaq Trough (KT), and north-east coast includes Scoresby Sund Trough (SBST) and Norske Trough (NT). These troughs can be identified in Fig. 1.~~